Bio-engineering of Muscle Tissue in Culture: Influence of Neural, Cartilage or Kidney Cells and the Effect of Retinoic Acid on Muscle Cell Growth

by

Matthew Grey
B.Sc., University of Victoria, 2009

A Thesis Submitted in Partial Fulfillment
of the Requirements for the Degree of

MASTER OF SCIENCE

in the Department of Biology

Supervisory Committee

Bio-engineering of Muscle Tissue in Culture: Influence of Neural, Cartilage or Kidney Cells and the Effect of Retinoic Acid on Muscle Cell Growth

by

Matthew Grey
B.Sc., University of Victoria, 2009

Supervisory Committee

Dr. Patrick Nahirney, Division of Medical Sciences/Department of Biology
Supervisor

Dr. Brian Christie, Division of Medical Sciences/Department of Biology
Departmental Member

Dr. Perry Howard, Department of Biochemistry/Microbiology/Biology
Departmental Member

Abstract

Supervisory Committee
Dr. Patrick Nahirney, Division of Medical Sciences/Department of Biology
Supervisor
Dr. Brian Christie, Division of Medical Sciences/Department of Biology
Departmental Member
Dr. Perry Howard, Department of Biochemistry/Microbiology/Biology
Departmental Member

Skeletal muscle fibers develop from mono-nucleated myoblasts that fuse to form multinucleated myotubes. In embryonic growth, this process occurs concurrently with the formation of the early cartilaginous skeleton and innervation by migrating nerve cells. The goal of my research was to explore co-culture conditions that encourage proliferation, differentiation and maturation of myoblasts to myotubes. A variety of co-culture experiments tested the influence of three basic tissues types (murine neural, cartilage and kidney primary cells) on the formation of myotubes in the C2C12 myoblast cell line. Three plating strategies were used: 1) C2C12 myoblasts were plated first, grown for two days before the addition of a second cell type; 2) both cell types were mixed and plated simultaneously; and 3) C2C12 myoblasts were added to a pre-established, 10 day old neural, cartilage or kidney cell culture. In addition, a parallel set of experiments were treated with all-trans retinoic acid, a potent myogenic activator and embryonic patterning signaling molecule. Myotube formation was consistently highest in C2C12 and cartilage co-cultures across all three plating strategies with a 277% increase in myotube area compared to controls. These effects were further enhanced when grown in 1 µg/mL all-trans retinoic acid. Co-cultures with neural or kidney cells consistently exhibited fewer myotubes when compared to C2C12 controls. It is postulated that the enhanced muscle growth in cartilage co-cultures was due to a chondrocyte-secreted extracellular matrix that facilitated myotube attachment to the substratum.

Table of Contents

List of Tables

List of Figures

Acknowledgments

I would like to thank my friends and lab mates, Andrew and Dani Sweetnam-Holmes for their camaraderie and humour. I would like to acknowledge Dr. Bob Chow and Dr. Craig Brown for their generous donations of mice, and Dr. Stephanie Willerth for sharing her retinoic acid supplies. I would like to thank my parents for lending their ears and words of encouragement. I would also like to acknowledge my friend, Andrew Kwasnica, and my brother, Dave, for their moral support.

And finally, I would like to thank Dr. Patrick Nahirney for encouraging me to take initiative with my project and work independently. Thanks to his mentoring, I have developed a great appreciation for histology, a mastery of culturing and immunohistochemistry techniques and critical thinking. Essentially, I would like to thank Dr. Nahirney for turning me into the scientist I am today.

Dedication

To my wife.

For your patience and support throughout my Master's Program

when at times it seemed I was more married to the lab

than to you.

Introduction

Overview

As the workhorse of the body, muscle is vital to life. Whether it be used to move limbs for fun, fight, or flight, expand the thoracic cavity to draw in each breath, pump blood through arteries and veins, dilate or constrict pupils, move nutrients and wastes through the gastrointestinal tract, or contract the walls of the uterus during childbirth, it is clear this is a vital and most essential tissue of the human body. There are three types of muscle: skeletal, cardiac and smooth, with skeletal (responsible for voluntary and reflex movements) being the most abundant. The reliance on skeletal muscle for nearly every aspect of life becomes evident in severe muscle trauma and muscular diseases such as Duchenne muscular dystrophy, a debilitating disease that affects approximately 1 in every 3500 (Eagle et al., 2002).

The goal of my research was to test new methods for growing skeletal muscle tissue *in vitro*. To date, muscle restorative therapies involving the direct injection of myoblasts into the skeletal muscle of patients with Duchenne muscular dystrophy have thus far proven insufficient due to limited diffusion of the injected cells throughout the patient's muscle and immune rejection of the transplanted myoblasts (Skuk and Tremblay, 2011). Another approach to addressing the regeneration of healthy muscle may be to grow functional muscle fibers as a unit in culture and transplant the entire unit into damaged or myodegenerative sites.

My thesis presents a variety of cell culture experiments that explored the influence of three diverse cell types on myoblast growth and differentiation with the aim of developing functionally mature muscle fibers in culture. Three co-culture cell combinations included a) muscle with cartilage, b) muscle with neurons, and c) muscle with kidney epithelial cells. In addition to these three cell combinations, three co-culture plating strategies were tested: a) muscle was plated for two days prior to the addition of a second cell type, b) muscle and a second cell type were mixed and plated simultaneously, and c) muscle was plated on a pre-established, 10 day old culture of a second cell type. A parallel set of co-cultures were treated with all-trans retinoic acid. Retinoic acid acts as a signaling molecule that plays a critical role in embryonic development, control of cell growth, differentiation and death (Arnold et al., 1992; Albagli-Curiel et al., 1993; Halevy and Lerman, 1993; Froeschle et al., 1998; Blomhoff and Blomhoff, 2006; Mark et al., 2009).How Does Muscle Develop in the Embryo?

During mammalian embryonic development, mesenchymal stem cells in mesoderm aggregate and become arranged into the myotomes of the segmenting somites of the embryo (Hollway and Currie, 2005). These muscle precursor cells proliferate and migrate to specific sites in the body where they elongate and differentiate into myoblasts (Gros et al., 2004). Myoblasts align with one another, exit the cell cycle and fuse together to form large, syncytial multinucleated myotubes (Mok and Sweetman, 2011). Myotubes elongate and grow in diameter as they incorporate more myoblasts through further cell fusion. A subset of myoblasts (myosatellite cells) that fail to fuse with the growing

myotubes remain closely associated with the myotube and serve as a reserve pool of myoblasts that function in growth and repair of muscle fibers (Asakura et al., 2001). As the muscle fibers elongate, they form attachments with the developing cartilaginous skeleton. At the same time, motor and sensory neurons establish neuromuscular junctions with myotubes (Hughes et al., 2006). This innervation plays a critical role in determining the specific muscle fiber types found within mature mammalian skeletal muscles (Schiaffino and Reggiani, 2011).

Structure of Mature Skeletal Muscle Fibers

Skeletal muscle fibers are long, multinucleated cells that are organized into groups (fascicles) within a muscle. An outer encasing, epimysium, binds the fascicles together and condenses at the end of the muscle where the attachment to bone is formed. Within fascicles, a fibrous connective tissue called the perimysium provides a conduit for blood vessels and nerves. Each muscle fiber is encased by a thin, delicate connective tissue layer called the endomysium that is intimately associated with the sarcolemma (plasma membrane) of muscle fibers. Skeletal muscle fibers are filled with myofilaments that consist largely of thick (myosin-containing) and thin (actin-containing) filaments oriented in series along the length of muscle fibers. The myofilaments form alternating, overlapping bands that slide past each other during contraction (first described in the sliding filament model in 1954 by two independent research groups: Anthony F. Huxley and Rolf Niedergerke and by Hugh Huxley and Jean Hanson (Huxley and Niedergerke, 1954; Huxley and Hanson, 1954)). Myofilaments collectively form

cylindrical bundles called myofibrils that run in the longitudinal axis of the muscle fiber.

Myofilaments are organized into small linear functional units called sarcomeres (Figure 1). Each sarcomere consists of a central dark, myosin-containing A band, flanked on either side by half of a light, actin-containing, I band. Actin filaments span the I band and overlap part of the myosin filaments of the A band. Dark, transverse, Z bands, intersecting the middle of each I band, anchor the thin filaments and mark the ends of each sarcomere (Luther, 2009). The central region of the A band not overlapped with the actin filament appears lighter and is called the H zone. Located at the center of the A band is a dense cross-linking band called the M band that is rich in the protein myomesin (Clark et al., 2002). The widths of the I band and the H zone change in relation to the state of the muscle fiber contraction or relaxation due to the sliding of the actin filaments along the myosin filaments. The width of the A band, however, remains constant during contraction. As the muscle contracts, the distance between the adjacent Z bands (i.e. sarcomere length) is reduced (Figure 1).

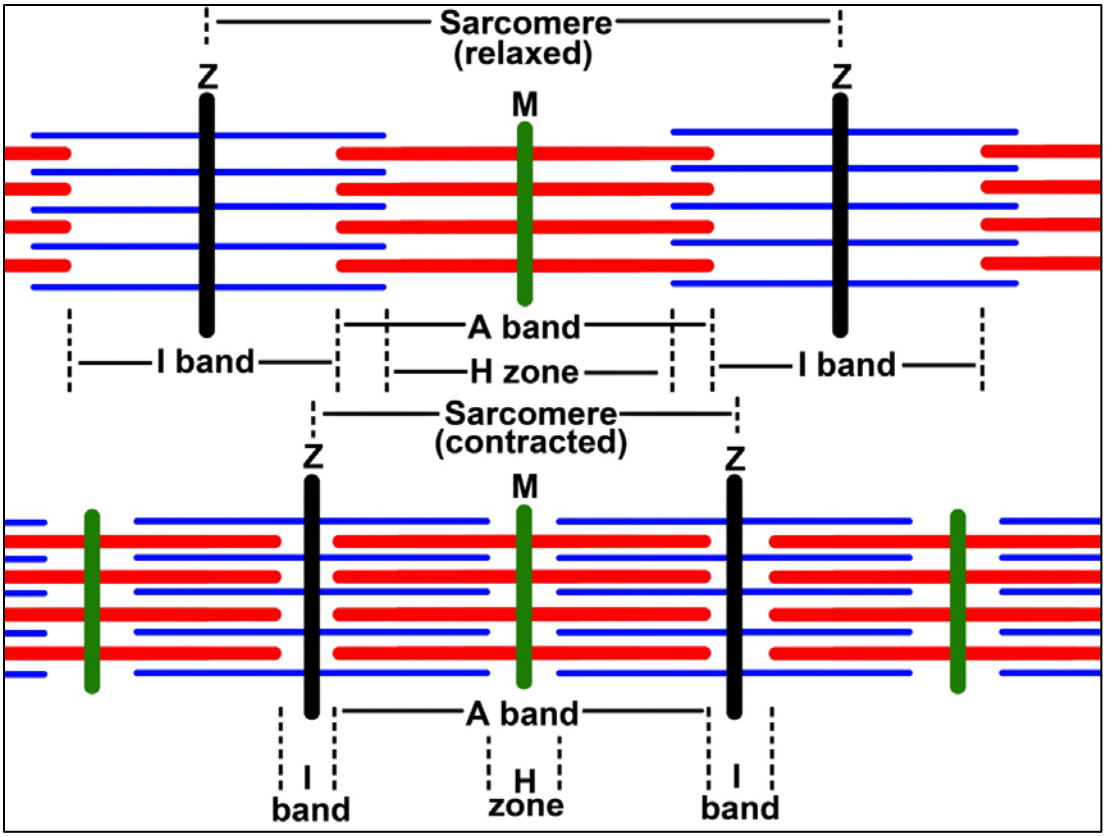

Figure 1. Schematic of a relaxed and a contractedsarcomere showing the arrangement of myofilaments. The distance between the Z bands is reduced during contraction.

In striated muscle, ~200 myosin molecules assemble into an anti-parallel arrangement in the thick filament (Clark et al., 2002). Half of the thick filament has myosin molecules oriented in one direction, and the other half contains myosin molecules oriented in the opposite direction. Each myosin molecule contains an ATPase-containing globular head and a tail region. This ATPase site facilitates the binding of the myosin head to actin, which activates the bending of the globular head of myosin (Irving et al., 2000).

Thin filaments, on the other hand, are comprised of a double helix of filamentous actin as well as two closely associated proteins, tropomyosin and the troponin complex (Kontrogianni-Konstantopoulos et al., 2009). Troponin and

tropomyosin act as a molecular switch to enable or disable the binding of the myosin heads to actin (Kontrogianni-Konstantopoulos et al., 2009).

Although the active role of muscle contraction is carried out through interactions between myosin and actin filaments, there are also other key structural proteins that are essential for the process. A third filament system in skeletal muscle is comprised of one of the largest known proteins, titin, and spans from the Z band to the M band (Wang et al., 1979). This protein contains elastic elements that contribute to the passive elasticity of muscle, helping return muscle fibers to their resting state after stretch. A fourth filament system in skeletal muscle is another giant protein called nebulin that spans the length of the thin filaments (Wang, 1982). This long, filamentous protein acts as a molecular ruler for actin filaments during development and is also believed to function as a calcium-linked regulator of actin-myosin interactions (Ottenheijm and Granzier, 2010). The Z bands of skeletal muscle are rich in α-actinin (Masaki et al., 1967), a structural protein that links actin filaments and binds to nebulin (Nave et al., 1990) and titin (Atkinson et al., 2000).

Excitation-Contraction Coupling in Muscle

Muscle is unique in that it is able to efficiently convert an excitatory electrical signal from a motor nerve terminal on a muscle fiber into rapid mechanical shortening of the muscle fiber (i.e. contraction). For most limb muscles, motor nerves arising from the ventral horn of the spinal cord or from the hindbrain form neuromuscular junctions (NMJ) with muscle fibers at a specialized region of the sarcolemma called the motor end-plate (Hughes et al., 2006). When

a motor neuron is stimulated, the depolarization travels down the axon to the presynaptic terminal of the NMJ where is causes the release of the neurotransmitter acetylcholine into the narrow space between the motor neuron and the muscle fiber called the synaptic cleft. Acetylcholine diffuses across the synaptic cleft and binds to acetylcholine receptors located in the folded postsynaptic membrane of the muscle fiber. Binding of acetylcholine to their receptors leads to an influx of cations (sodium and calcium) through acetylcholine-activated channels (Hughes et al., 2006). This rapid, acetylcholine-activated ion movement generates an endplate potential that, if sufficiently high enough, triggers the opening of voltage-gated sodium channels in the depths of the end plate folds (Hughes et al., 2006).

The resultant all-or-none action potential spreads along the entire length of the muscle fiber and radially through transverse (T) -tubules at the level of the A and I bands (Huxley and Taylor, 1958; Smith, 1966; Franzini-Armstrong, 1970; Caputo, 1978). T-tubules form associations with the sarcoplasmic reticulum (SR) cisternae at sites known as triads (Smith, 1966; Block et al., 1988) where the action potential is transferred via two receptors: the dihydropyridine receptor of the T-tubule and the ryanodine receptor of the SR to cause release of calcium ions from the SR (Franzini-Armstrong and Protasi, 1997). Dihydropyridine receptors are voltage-gated receptors that stimulate the closely associated ryanodine receptor to undergo a conformational change, which subsequently opens associated calcium channels in the SR membrane.

Calcium released from the SR diffuses to myofilaments and initiates contraction by binding to troponin C of the troponin complex (Treves et al., 2009). The troponin complex consists of three subunits: one that binds calcium (TnC), one that binds tropomyosin (TnT), and one that inhibits myosin ATPase (TnI). Once TnC has bound a calcium ion, the inhibitory effects of TnI are lifted and a conformational change in TnC occurs, shifting tropomyosin to expose the myosin binding site on actin. The myosin head then binds to actin and initiates the hydrolysis of bound ATP to ADP and P_i via the myosin ATPase located at the globular head of myosin. The myosin head then undergoes a conformational change and pulls the thin filament past the thick filament, resulting in the shortening of the sarcomere and the generation of force. ADP and P_i are then released and a new molecule of ATP binds to the myosin head which releases its attachment to actin and resets the head to its original position (Huxley, 1969; Huxley, 2000). Through this ratchet-like process, the sarcomere lengths are shortened, and, as a result, the entire muscle shortens. Myosin will continue the process of attachment, release, and reattachment as long as there are elevated calcium ion levels to bind to TnC and sufficient ATP to release myosin from actin.

Relaxation of muscle requires the removal of free calcium ions from the vicinity of the myofilaments back into the SR, a process initiated by repolarization of the sarcolemma and T-tubules and the subsequent closing of the SR calcium ion channels (Rios et al., 1991). The majority of the free calcium ions are rapidly removed from the sarcoplasm via a calcium- and magnesium-dependent ATPase pump localized within the SR membrane (de Meis and Vianna, 1979). By

coupling the hydrolysis of one ATP to the translocation of 2 calcium ions from the sarcoplasm to the lumen of the SR, free calcium surrounding the myofilaments is rapidly lowered. In addition to this, calcium-binding proteins within the SR called calsequestrin provide a calcium buffering mechanism to facilitate the continued removal of free calcium from the sarcoplasm by reducing the calcium gradient across the SR membrane (Ebashi and Ebashi, 1962; Ebashi and Lipmann, 1962; Dux et al., 1987).

Growth Regulatory Factors of Muscle

The expression of muscle specific transcription factors and proteins, and identification of where they are localized within the cell has led to the understanding of muscle-related gene expression, muscle cell fusion, and myofilament production timelines. The myogenic regulatory factors (MRFs) are transcription factors that are essential for the differentiation of skeletal muscle (Berkes and Tapscott, 2005), and along with myocyte enhancer factor-2 (Mef2) and other genetic factors coordinate the activities of co-activators and co-repressors to tightly regulate skeletal muscle gene expression during development (Berkes and Tapscott, 2005). MRFs have a conserved basic-helix-loop-helix (bHLH) structure and include a family of four transcription factors: Myf-5, MyoD, myogenin, and MRF4. Each play a crucial role in muscle cell differentiation, either in a coordinated manner or individually, by binding to consensus sites on promoters and enhancers of muscle-specific genes. An example of the influence of these factors has been demonstrated by forced expression of MyoD in non-muscle cell types (eg. fibroblasts, chondrocytes and

neurons) which causes these cells to transform and differentiate into the skeletal muscle pathway (Weintraub et al., 1989; Choi et al., 1990).

Gene knockout mice lacking specific MRFs have been shown to develop muscle abnormalities to varying degrees depending on which MRFs were absent. For example, gene knockout experiments of Myf-5 (Braun et al., 1992) or MyoD (Rudnicki et al., 1992) were shown to maintain an ability to produce muscle, but mice missing both Myf-5 and MyoD were completely devoid of myofibers and myoblasts (Rudnicki et al., 1993). Mice lacking myogenin exhibited poorly developed skeletal muscle tissue despite the presence of myoblasts, suggesting that myogenin plays a role in terminal differentiation but not in initiating the myogenic pathway (Berkes and Tapscott, 2005). MRF4 expression appears early in the establishment of the myogenic lineage and later during terminal differentiation suggesting a multifaceted role in muscle development (Berkes and Tapscott, 2005). Stem cells lacking myogenin have been shown to fully differentiate when MRF4 is over-expressed and suggest a rescuing effect of MRF4 that could not be accomplished by over-expressing MyoD (Myer et al., 2001; Sumariwalla and Klein, 2001). In summary, determination and acquisition of a myogenic fate depends on Myf5, MyoD and MRF4, while myogenin, MyoD and MRF4 are required for terminal differentiation (Buckingham, 2006).

Another group of myogenic regulators are the Pax transcription factors, Pax3 and its paralogue Pax7. During development, a population of cells that express Pax3 and Pax7 give rise to myogenic cells marked by Myf5 and MyoD

expression (Buckingham and Relaix, 2007). The absence of Pax3 and Pax7 in double mutant mice resulted in major skeletal muscle developmental deficits due to defects in myogenic specification and extensive cell death (Relaix et al., 2005; Relaix et al., 2006). The two transcription factors differ functionally; Pax7 mutant mice exhibit progressive postnatal loss of myosatellite cells due to apoptosis, an effect that cannot be saved by the presence of Pax3 and that was not seen in Pax3 mutant mice (Oustanina et al., 2004; Relaix et al., 2006). These results suggested that Pax7 has important anti-apoptotic functions in myosatellite cells, although some myosatellite cells were found in Pax7 mutants as the mice matured (Oustanina et al., 2004). Pax7 and MyoD are coexpressed after activation of quiescent satellite cells and during proliferation, but Pax7 is downregulated during differentiation (Zammit et al., 2006). Pax3, on the other hand, has been implicated in the proliferation of activated myosatellite cells (Conboy and Rando, 2002), but these cells have been shown to proliferate *in vitro* and *in vivo* without detectable Pax3, suggesting its expression is not required (Montarras et al., 2005; Relaix et al., 2006). Pax3 has also been shown to participate in the skeletal muscle determination by working in combination with Myf-5 and MRF4 to activate MyoD expression (Tajbakhsh et al., 1997; Kassar-Duchossoy et al., 2004).

Muscle Protein Expression Patterns and Myofibrillar Proteins

The expression of muscle-specific proteins begins at the postmitotic myoblast stage prior to fusion (Lin et al., 1994). After six hours of growth, myoblasts have been found to express a cohort of six muscle-specific proteins,

including desmin, myosin, titin, α-actinin, α-actin, and nebulin. The early presence of these myofibrillar proteins was irregular, but their appearance in only postmitotic myoblasts highlights the autonomous regulation of early muscle specific genes (Lin et al., 1994). With established muscle-specific expression timelines such as these, myofibrillar proteins (actin, myosin, α-actinin, titin, nebulin and myomesin) are commonly used as markers for the development of myofibrils.

Actin is a ubiquitous molecule implicated in cellular functions such as motility and cytokinesis, and is the most abundant protein in striated muscle (Clark et al., 2002). Actin first becomes incorporated into the I-Z-I complex which consists of actin filaments anchored by α-actinin. Morphologically, the I-Z-I complex is the first identifiable structural feature of myofibrils within myotubes (Holtzer et al., 1997).

Alpha (α) actinin is a major component of the Z band of skeletal and cardiac muscle and functions to cross-link the opposing actin and titin filaments of neighbouring sarcomeres. Acting as a binding hub for numerous other proteins, α-actinin and its associated proteins are thought to provide the Z band with structural support (Clark et al., 2002).

Myosin predominates in the thick filament of myofibrils and serves as a useful marker for sarcomere development. Presently, myosin is grouped into fifteen classes. The conventional myosins, which include muscle myosin, are members of class II (Clark et al., 2002). While the entire myosin molecule can be grouped into two functional regions, the head and the tail, these can be further

divided into two heavy chains and four light chains. The N-terminal of each heavy chain and two light chains make up the myosin head, while the C-terminal regions of each heavy chain make the tail (Clark et al., 2002).

Titin is the largest protein identified to date and is the third most abundant protein after actin and myosin in skeletal muscle (Clark et al., 2002). Containing elastic elements which contribute to the passive elasticity of muscle, titin helps return muscle fibers to their relaxed state after stretch. Reaching across half the length of the sarcomere, titin forms a continuous filament system in myofibrils, with its N-terminal end anchoring to the Z band and its C terminal inserting into the M band (Clark et al., 2002).

Myomesin is localized to the M band of sarcomeres and is one of the last myofibrillar proteins to be expressed (Lin et al., 1994; Reddy et al., 2008). Although the physiological role of myomesin is still being elucidated, its association with myosin and titin molecules suggests a linking role at the M band (Blanco-Bose and Blau, 2001; Reddy et al., 2008).

Cell Culture Models of Muscle Development

Much has been learned about muscle development *in vitro* (cell culture) with dissociated primary cells or with immortalized myoblast cell lines. A number of myoblast cell lines are available, including the L6, MM14, G8 and, one of the most commonly used for studying early events in myogenesis, the C2 myoblast cell line. In 1977, Yaffe and Saxel produced the C2 myoblast cell line by serial passage of cultured satellite cells 70 hours after a crush injury to the thigh muscles of C3H mice (Yaffe and Saxel, 1977). From the C2 line, the C2C12 line

was subcloned by Blau and coworkers in 1983 (Blau et al., 1983) and has served as a reliable, tractable and consistent model for muscle cell growth and differentiation. When grown in culture, the C2C12 myoblasts will proliferate and fuse to form myotubes significantly faster than the original C2 line (Blau et al., 1983; Sharples et al., 2010).

Although bio-engineering of skeletal muscle has made advancements over the last decade, several hindrances to the development of functional skeletal tissue *in vitro* remain. These challenges include low contractile force and an inability to control myoblast adhesion and myotube formation spatially (Molnar et al., 2007). Many researchers have modified the surface on which the myoblasts were plated. Molnar and coworkers found C2C12 myotube formation significantly increased when substrates were coated with laminin or vitronectin, and were able to organize patterns of myotubes by laying parallel 30 μm wide strips of vitronectin onto the substrate (Molnar et al., 2007). Using oriented poly ε-caprolactone/collagen based nanofibers, Choi and coworkers found they could induce muscle cell alignment and myotube formation (Choi et al., 2008). Lan and coworkers approached myoblast culturing from a biochemical approach and demonstrated that myotube formation could be influenced by chemical modification of a fibronectin-coated substrate (Lan et al., 2005). Other studies using three dimensional matrices, such as Matrigel, Vitrogen and fibrin gels, have been used with some success (Jay and Barald, 1985; Barbero et al., 2001; Matsumoto et al., 2007; Sato et al., 2011). In addition, applying cyclic strain application to cells has been shown to promote matrix production from cells and

can enhance the mechanical properties of 3D cell and matrix constructs (Matsumoto et al., 2007). While these techniques have advanced our understanding of conditions required for enhancing muscle growth in culture, and could prove beneficial in combination with the approaches of my research, I did not employ any exogenously added substrate coatings. Instead, I was interested in the effect of the active secretion of matrices by specific cells, such as chondrocytes, and how this affects myoblast proliferation, adhesion and myotube formation.

Another approach to bioengineering muscle is to encourage the growth of myoblasts to form ‘myoballs’ as a model for studying the electrophysiological properties of muscle (Boldin et al., 1987; Hume and Thomas, 1989; Zebedin et al., 2004; Zebedin et al., 2007). In this case, a lower degree of muscle cell substrate adhesion encourages a spherical morphology. While useful for electrophysiology, others view myoball formation as a divergence from normal differentiation into the elongated morphology of myotubes (Daniels and Sandra, 1990; Dalkilic et al., 2006). In 1990, Daniels and Sandra showed myoballs to have cytoskeletal proteins that were morphologically and biochemically distinct from myotubes (Daniels and Sandra, 1990). Their studies showed that myoballs possessed altered ratios of actin and tubulin isoforms and of phosphorylated and nonphosphorylated vimentin compared to myotubes. Due to these inherent differences reported by others, myoballs were excluded from morphometric analyses in my studies.

A depletion of fetal bovine serum (FBS) within the growth media has been commonly used for triggering myogenic differentiation (Sugiyama et al., 2000; Kim et al., 2006; Martinez-Marmol et al., 2007). The standard method involves a reduction of the serum concentration from 10% to 2%, or a complete replacement of FBS with horse or calf serum. The inhibitory effects of FBS on muscle differentiation are thought to be caused by serum mitogens (eg. fibroblast growth factor and transforming growth factor) that down-regulate the bHLH myogenic regulatory factors (Li et al., 1992). In contrast, Yoshiko and coworkers showed that differentiation of C2C12 myoblasts did not depend on the serum depletion in the media (Yoshiko et al., 2002). Specifically, this group demonstrated that an autocrine/paracrine loop of IGFs, bFGF, and TGF-β_1 was active in proliferating and differentiating C2C12 cells without a depletion of serum and endogenous IGFs actively overrode the negative control of differentiation by serum mitogens in FBS. Similarly, it was also determined in my studies that culture media containing 10% FBS was sufficient for normal differentiation and fusion of C2C12 myoblasts into myotubes despite the presence of the mitogen-rich FBS. This concentration of FBS (10%) was also advantageous since it promoted the proliferation of the neural, cartilage and kidney cells that were cultured in combination with the C2C12 cells.

Co-cultures of Muscle with Other Basic Tissue Types

Co-culture experiments provide an opportunity to study the effects of cell populations on each other and to examine how they can potentially modify growth and differentiation of each cell type. While myoblast fusion has been

observed between some closely related species (eg. between rabbit and rat myoblasts), fusion appears to be cell-specific as myoblasts will not fuse with another cell type, such as heart or kidney cells (Bischoff, 1978). Muscle co-cultures have been tested by a number of researchers who explored an array of cell types including nerve cells (Guo et al., 2011), adipose cells (Kovalik et al., 2011), epicardium-derived cells, mesenchymal stromal cells and endothelium (Gentile et al., 2011), mesenchymal stem cells (Beier et al., 2011), adipose-derived stem cells (Mizuno, 2010), cartilage (Cairns et al., 2010a), tenocytes (Kostrominova et al., 2009) and bone marrow mesenchymal stem cells (Carvalho et al., 2008). In a study conducted by Cooper and coworkers, a fibroblast feeder layer (a technique commonly applied in stem cell maintenance) was used as a substrate to produce highly differentiated C2C12 myotubes. They proposed that a fibroblast feeder layer provided an elastic substratum to support contractile activity and likely secreted growth factors and extracellular matrix proteins that assisted myotube development (Cooper et al., 2004).

My research aims were to attempt to re-create *in vitro* muscle growth conditions that were reflective of those found in the developing embryo. In light of this, cartilage and nervous tissue cells were chosen for co-culture with myoblasts as they are both closely associated with muscle during development in the embryo (muscle fibers attach to the embryonic cartilaginous skeleton and are then innervated by developing neurons).

Neural and Muscle Co-Culture

Many researchers have explored muscle and neural tissue co-cultures and focussed on the association between the two cell types and the formation of NMJs (Das et al., 2007; Kubo et al., 2009; Das et al., 2010; Guo et al., 2011). For example, Guo and coworkers reported a novel human-based system to produce NMJs from neural and skeletal muscle stem cells in a serum-free culture condition (Guo et al., 2011). Das and coworkers found they were able to increase survival of cultures from 10-12 days up to 7 weeks when NMJs were formed between motoneurons and skeletal muscle cells (Das et al., 2010). Dutton and coworkers plated ventral spinal cord neurons onto prepared primary myotube cultures and found neurons to induce a redistribution of myotube acetylcholine receptors (Dutton et al., 1995). In a study by Jiang and coworkers, the presence of muscle induced nerve cells to increase production of acetylcholinesterase (Jiang et al., 2003). When dissociated whole muscle fibers were added to cultures of spinal cord complex, muscle fibers in contact with neural processes regenerated much more quickly than those more distal from the neural contact point (Peterson, 1978).

Others have reported that cholinergic neurons formed NMJs with C2C12 myotubes and upregulated GDNF production by myotubes (Vianney and Spitsbergen, 2011). Additionally, muscle has been shown to alter dorsal root ganglion neurofilament phenotype and type of tyrosine kinase receptor expression (Wang et al 2009).

Based on these observations, it has become clear that the presence of nervous tissue can influence the growth of muscle *in vitro,* as well as muscle affecting the protein expression and phenotype of neurons.

Cartilage and Muscle Co-culture

The combination of muscle and cartilage in culture has been recently studied by Cairns and coworkers who demonstrated that muscle can increase cartilage matrix production (Cairns et al., 2010a). This group examined the secreted factors that muscle cells released into the media and their influence on chondrocytes. By co-culturing chondrocytes and C2C12 cells, a marked increase in alcian blue staining and elevated collagen II and IX expression was measured. It was also found that by removing the potential influence of the physical presence between the cell types, and plating chondrocytes in muscle cell-conditioned medium, an increase in cartilage production was also observed, indicating muscle cells were secreting pro-chondrogenic factors (Cairns et al., 2010a). In addition, muscle cells appeared to impart cytokine resistance to cartilage by modulating pro-inflammatory molecules (Cairns et al., 2010b). However, these studies did not analyze the development of the C2C12 myoblasts and how cartilage could potentially regulate muscle cell growth.

Kidney Epithelium and Muscle Co-culture

Kidney epithelial cells were used in co-culture experiments to provide a control cell type for comparison with nerve and cartilage co-culture combinations. Although kidneys are similar to muscle embryonically, in that the two cell types

are both derived from mesoderm, they are not otherwise developmentally or functionally related tissues. Kidneys consist predominantly of compound tubular glands, and therefore develop as invaginations of the surface epithelium that penetrate into the underlying matrix (Kreidberg et al., 1993). Kidney epithelial cells were selected as a control co-culture in an attempt to provide evidence for the hypothesis that growth conditions more similar to that found in the embryo benefit muscle development, and that it is not merely the presence of another basic tissue cell type.

Co-Culture Strategies and Myoblast Fusion Conditions

My project attempted to ascertain the cellular influences on myoblast growth and differentiation by three basic cell types. In addition, three co-culture strategies were developed to elucidate the optimal growth conditions for myoblasts to proliferate, fuse and form differentiated, functional myotubes.

In total there were three co-culture strategies that combined neural, cartilage, or kidney epithelial cells with myoblasts. The first strategy was to plate the myoblasts on the glass coverslip first, allow the cells to proliferate for two days, and then add the second cell type. A proliferation time of two days was chosen as myoblasts divide rapidly within that time but will not form myotubes, making this strategy ideal for studying the effects of another cell type on well established and numerous myoblasts. The second strategy was to mix the two cell types and add them to a glass coverslip simultaneously. The third strategy was to plate neural, cartilage, or kidney epithelial cells first and allow 10 days to proliferate before adding myoblasts. A timeline of 10 days was allotted for the

establishment of neural, cartilage, and kidney epithelial cultures prior to the addition of myoblasts as these cell types typically required longer time periods to attain the same levels of growth as the myoblasts. In addition to these three strategies and their pure myoblast control dishes, a parallel set of experiments was conducted with the addition of a powerful mitotic agent, retinoic acid. Its biological action will be discussed in the following section.

Retinoic Acid and Development

Retinoic acid (RA), an active metabolite of vitamin A, plays a role in a wide range of biological processes, such as cell growth and apoptosis, directing cell migration and cell differentiation (Arnold et al., 1992; Albagli-Curiel et al., 1993; Halevy and Lerman, 1993; Froeschle et al., 1998; Blomhoff and Blomhoff, 2006; Mark et al., 2009). RA acts at the level of transcription and, being a lipophilic molecule, diffuses through the nuclear envelope and binds to the heterodimeric RA receptors (RAR) and retinoid X receptors (RXR) (Mark et al., 2009). It is through these two classes of RA receptors and their isoforms that retinoic acid is able to exert such a wide range of effects within the nucleus. In addition to a variety of RA receptors, several forms of the metabolite itself exist as well, generating a level of complexity unmatched in other vertebrate nuclear receptor signaling systems (Chambon, 1996). For my study, the all-trans isoform of RA was used as it has been shown to influence cell proliferation, differentiation, apoptosis and tissue patterning in the developing embryo (Kennedy et al., 2009; Le May et al., 2011; Ryan et al., 2011).

A wide range of RA concentrations have been found to promote or inhibit muscle, cartilage or neural development. While Ryan and coworkers found 3 nM RA promoted myogenesis in the form of a significant increase in myogenin and MyoD transcription factor expressions, Arnold and coworkers, found 1 µM of RA alleviated the inhibition of myogenic differentiation in a similar manner (Arnold et al., 1992; Ryan et al., 2011). Kennedy and coworkers used the addition of 25 nM all-trans RA to their growth media, which lead to an increase in myoblasts in their experiment (Kennedy et al., 2009). However, not all experiments found RA addition led to promotion of myogenesis. For example, by applying concentrations of RA ranging from 0.1 µM to 10 µM, Xiao and coworkers found muscle cultured in the presence of RA developed significantly fewer myotubes than those cultured with standard growth media (Xiao et al., 1995). Overall, myogenesis has been found to be increased within a dose range of 1 nM to 1 µM all-trans RA (Arnold et al., 1992; Le May et al., 2011).

With regards to neural differentiation, Bain and coworkers found 0.5 µM of RA to promote neuron growth while at the same time repressed mesodermal tissue growth (Bain et al., 1996). At the lower end of the spectrum, Henion and Weston found a range of 1-100 nM RA promoted neurogenic precursor proliferation and survival (Henion and Weston, 1994). Another study found the addition of 10 nM RA to stimulate accelerated neural specification (Lu et al., 2009). Overall, the range of RA concentrations that promote neural development was found to be from 1 nM to 1 µM all-trans RA (Henion and Weston, 1994; Canon et al., 2004).

The effects of RA on cartilage development have also been studied extensively, but again, concentrations varied widely from study to study. While Biddulph and coworkers found concentrations as low as 0.17 nM RA to inhibit chondrogenesis, Enomoto and coworkers found low concentrations (0.1 nM to 10 nM) of RA would promote proliferation of chondrocytes, and higher concentrations would inhibit the secretion of their extracellular matrix and convert the cells into a more fibroblast-like phenotype (Biddulph et al., 1988; Enomoto et al., 1990). In contrast, other research has shown much higher concentrations to effectively promote chondrogenesis. For example, Sekiya and coworkers applied 1 µM RA to their chondrocyte cultures and found the dose to increase the expression of extracellular matrix component genes, such as aggrecan and type II procollagen (Sekiya et al., 2000). Overall, the concentrations that have been shown to promote cartilage development range from 0.1 nM to 1 µM all-trans RA (Enomoto et al., 1990; Sekiya et al., 2000).

Based on the wide range of all-trans RA concentrations found within the literature, a range of concentrations were tested in the growth media in my experiments, with the lowest concentration being 10 ng/mL (30 nM) and the highest being 0.1 mg/mL (0.3 mM).

Diseases of Muscle and Potential Therapies

The questions addressed in this thesis are directed towards the ultimate goal of developing strategies for bio-engineering muscle tissue. This may be applied to conditions of muscle disease and trauma. For example, one group of

myopathies, identified as muscular dystrophies, is characterized by progressive conditions in which the patient experiences increasing muscle wasting and weakness (Campbell, 1995). Patients with Duchenne and Becker muscular dystrophy either lack the structural protein dystrophin or contain abnormal types of this protein (Hoffman et al., 1987). The absence of dystrophin leads to a disruption in the linkage between the sarcolemmal cytoskeleton and a glycoprotein complex in the sarcolemma membrane which can lead to muscle cell necrosis (Campbell, 1995). In addition, muscle trauma is another condition which could benefit from the transplantation of new, healthy and fully functioning muscle. The ability to introduce whole muscle transplants and understand how this tissue interacts with the neighbouring tissues will be a large step towards having a method to supplement muscle activity in these patients.

Methods

A) Myoblast culture – C2C12 cell line

The immortalized C2C12 cell line was obtained from Developmental Studies Hybridoma Bank at the University of Iowa. Cultures were grown in a standard growth media, consisting of 10% fetal bovine serum (FBS), 1% penicillin:streptomycin and 0.01% gentamicin, in high glucose Dulbecco's Modified Eagle Medium (DMEM) (Invitrogen)**.** Cells were maintained at 5% CO_2 in a humidified 37˚C incubator. Myoblasts were expanded in 60 x 15 mm Falcon Standard plastic Petri dishes (Fisher Scientific) and excess cells were frozen for future experiments and stored in liquid N_2. During media changes, cultures were gently rinsed with sterile Dulbecco's phosphate buffered saline (DPBS) (Invitrogen) and fresh growth media replaced to a volume of 4 mL per 60 mm dish. Media was replaced every two to three days. Once enough cells were available for co-culture, or the dish reached a state of near confluence, the cells were split and replated (see section C). C2C12 cultures were split up to a maximum of 7 times to maintain the characteristics of the cell line, at which point a new batch was removed from its storage in liquid N_2.

B) Chondrocyte, neuronal and kidney primary cell culture

C57 Black mouse pups, ranging from post-natal day zero to post-natal day three, were generously donated by Dr. Craig Brown and Dr. Bob Chow of the University of Victoria. Mice were sacrificed by cervical dislocation according to

standard the policies of the Canadian Council of Animal Care. The skin was carefully removed and all four limbs were removed and placed into a Petri dish containing DPBS. The rib cage was then gently opened, making sure not to rupture any internal organs to avoid excess bacteria. Once the rib cage was separated from the inner organs, the ribs were cut free of the spinal cord and placed in PBS. Kidneys and brain were also removed and placed in PBS. Isolation of hyaline cartilage was much more tedious and required the very thorough and meticulous removal of all muscle and tendon tissue from the articular joints, ball and socket joints, and ribs. If all the muscle could not be removed from a particular piece of cartilage, that piece was discarded. Once all the required tissue types were acquired, they were washed twice with DPBS, and transferred to separate 1.5 mL eppendorf. Each tissue was then minced with small scissors into fine pieces of approximately 1 mm or smaller.

The minced tissues were then enzymatically dissociated for one hour at 37ºC with 1% collagenase type II (Invitrogen) in trypsin (0.25%) with ethylenediaminetetraacetic acid (EDTA) (Invitrogen) on an Orbit Environ Shaker. The dissociated cells were centrifuged at 500 RPM for 10 minutes, the supernatant was removed and the pellet of cells was resuspended in standard growth media. Cells dissociated from the brain and kidneys were plated in separate 60 x 15 mm plastic Petri dishes, and incubated overnight at 37 ºC and 5% CO_2. Minced pieces of cartilage and the dissociated chondrocytes were plated in flat bottom, 24 well tissue culture plates and incubated overnight. After the overnight incubation, non-adhered cells were decanted and replated in

growth medium in separate 60 x 15 mm Petri dishes (for brain and kidney), or flat bottom, 24 well, tissue culture plates (for cartilage), for a second overnight incubation. Dishes containing brain and kidney cells were washed thoroughly after the overnight incubation with DPBS (x3) to remove tissue debris remaining from the dissection. Cartilage pieces that failed to adhere to the dish were removed and plated in a 60 x 15 mm plastic Petri dish. Adhered cartilage pieces and dissociated cells were washed thoroughly after the overnight incubation with DPBS (x3) to remove tissue debris remaining from the dissection. Each cell type was allowed to proliferate until enough cells were available for the desired co-culture experiments at which point they were split (see section C). If any primary cultures contained visible impurities (for example, myotube formation within a cartilage dish) or unhealthy looking cells (for example, poor growth rate or excess lysosome formation), these dishes were not used for co-culture experiments.

C) Colony Splitting

Cells were washed with DPBS for one minute before being treated with trypsin-EDTA for 15-20 minutes to release the cells from the plastic Petri dish. Gentle pipette stirring helped remove the cells from the dish and mechanically disrupted any cells which remained in clusters. Once all cells were released from the dish and mechanically broken apart, they were transferred to a Falcon tube containing standard growth media and were centrifuged at 500 RPM for 10 minutes. The supernatant was aspirated away and the pellet of cells was resuspended in standard growth media and replated either on glass coverslips for co-culture experiments, or plastic Petri dishes to proliferate again. Cell counts

(section D) were performed to standardize the number of cells plated within, and between, co-culture experiments.

D) Cell counts for Co-culture Experiments

After cultures were released from the plastic Petri dish and centrifuged, the cells were diluted with 2-4 mL depending on the size of the pellet. Cell counts for all cell types were performed using a Neubauer hemocytometer. Dilutions were increased until a total cell count of 50-60 cells was obtained by counting 5 large squares (the four corners and the center), each of which measured 0.1 mm^3. The total cell count of 50-60 cells per 0.5 mm^3 (100-120 cells per mm^3) was multiplied by 1000 to determine the cell count per mL. The final cell count per mL was determined by multiplying with the initial dilution factor, which was dependent on the pellet size and often differed for each cell type, to bring the final cell concentration to ~200,000-240,000 cells/mL. One drop (approximately 50 µL) of each cell type was added to their respective 22 x 22 mm coverslip, which plated ~1.2 x 10^4 cells. The manner in which the cells were added to coverslips was dependent on the co-culture strategies explained in section E.

E) Co-culture experiments

Three strategies for co-culture experiments between C2C12 myoblasts and cartilage cells, C2C12 myoblasts and neuronal cells, and C2C12 myoblasts and kidney cells were employed:

i) C2C12 myoblasts were plated first and allowed two days to proliferate before cartilaginous, neuronal or kidney cells were added.

ii) Two cell types (C2C12 myoblasts and neural, C2C12 myoblasts and cartilage, or C2C12 myoblasts and kidney) were mixed in growth media in an eppendorf and plated simultaneously as a mixture on the same coverslip.

iii) Cartilaginous, neuronal or kidney cells were plated first and allowed 10 days to proliferate on the coverslip before C2C12 myoblasts were added.

A parallel set of experiments were conducted which included the addition of all-trans retinoic acid (10 ng/mL – 0.1 mg/mL) (generously donated by Dr. Stephanie Willerth, Division of Medical Sciences, University of Victoria) to the growth medium. These cultures were grown in the one concentration of retinoic acid per experiment, which was replenished with new growth media every two to three days. Retinoic acid concentrations tested included 10 ng/mL, 0.1 µg/mL, 0.5 µg/mL, 1 µg/mL, 1.5 µg/mL, 10 µg/mL, and 0.1 mg/mL.

Glass coverslips were etched overnight in 10N sodium hydroxide at room temperature and rinsed thoroughly before the plating of cell cultures. Each experiment consisted of 16 etched glass coverslips (4 for each co-culture and 4 for the controls) fixed to the bottoms of plastic Petri dishes. All dishes were grown in 5 % CO_2 at 37 ˚C and were gently rinsed with sterile DPBS before given fresh growth media every two to three days.

F) Alcian Blue Staining of Cartilage Extracellular matrix glycoproteins

Sulphated mucosubstances (chondroitin, dermatan, and keratin sulphate) found within the extracellular matrices surrounding chondrocytes were labelled using a 1.0 g/100 mL alcian blue stain with 0.1 M hydrochloric acid (HCl) solvent. Cartilage-containing cultures were fixed for approximately one hour at 5˚C with 2 % paraformaldehyde in PBS (pH 7.4). The coverslips were then washed three times with DPBS (10 minutes per wash). Alcian blue solution was added to coverslips in square weigh boats within a hydrated chamber and left overnight at RT. The alcian blue solution was gently aspirated away and the coverslips were rinsed with 0.1 HCl (the solvent for the stain), followed by three washes with DPBS. These coverslips then followed the steps laid out in section G, beginning with permeabilization.

G) Immunocytochemistry

Co-cultures were fixed for approximately one hour at 4˚C with 2% paraformaldehyde in DPBS (pH 7.4). The coverslips were then washed three times with 0.1 M PBS (10 minutes per wash). The cells were then permeabilized with 0.1% Triton X-100 in PBS for 10 minutes. Triton X-100 was then removed, and cells were blocked with 1% bovine serum albumin (BSA) and 0.05% sodium azide in PBS (PBS BSA) for thirty minutes. Coverslips were treated with a cocktail of primary antibodies (monoclonal and polyclonal) for the two cell types

of each particular co-culture, and left overnight at room temperature (RT) in a hydrated chamber.

Myoblasts, chondrocytes, neurons and kidney cells were labelled with the following cell or tissue specific antibodies:

1. Anti-skeletal muscle myosin monoclonal antibody (F59 clone from Developmental Studies Hybridoma Bank (DSHB), unconjugated or biotinylated) was used either simply as a supernatant or in a purified, biotinylated form diluted 1:20. F59 is a highly specific antibody that binds to the hinge region of skeletal muscle myosin and was used to identify differentiated muscle cells.
2. Anti alpha actinin, a monoclonal antibody (Cat # A7811, Sigma) was used at a dilution of 1:10 to label α-skeletal muscle alpha actinin found at Z lines of sarcomeres of differentiated myotubes.
3. Anti-myomesin, a monoclonal antibody (Cat # mMaC myomesin B4-s DSHB) was used at a dilution of 1:10 to label M lines of sarcomeres of differentiated myotubes.
4. Anti-myogenin, a polyclonal antibody (Cat # SC-576, Santa Cruz Biotech Co.) was used at a dilution of 1:100 to label the transcription factor involved in skeletal muscle development and repair. Myogenin is part of the MRF transcription factor family, a muscle-specific basic-helix-loop-helix (bHLH) transcription factor most active in early stages of muscle development.

5. A type II collagen polyclonal antibody (Cat # CL50251AP, Cedarlane Labs) was used at a dilution of 1:200. Type II collagen is the most predominant isoform of collagen in the chondrocyte extracellular matrix and provides it with tensile strength.
6. A neurofilament protein monoclonal antibody (Cat # 2H3-s, DSHB) was diluted 1:6 and used to detect differentiated neuronal cells.
7. A cytokeratin monoclonal antibody (Cat # Z0622, Cedarlane Labs) was used to label epithelial cells from kidneys.
8. Phalloidin (Cat # A12381, Invitrogen), a high affinity probe for filamentous actin, was diluted 1:40 and used to label C2C12 and kidney epithelial cells.
9. A β tubulin monoclonal antibody (Cat # E7-s, DSHB) was diluted 1:10 and used to label microtubules in C2C12 and kidney epithelial cells.

After overnight incubation with primary antibodies at RT, the coverslips were washed three times with PBS BSA and treated with a cocktail of secondary antibodies – goat anti-mouse (GAM) for monoclonal antibodies, goat anti-rabbit (GAR) for the rabbit polyclonal antibodies, and streptavidin (strep) for biotinylated antibodies (Alexa Fluor GAM 488, Cat # A11017; Alexa Fluor GAM 594, Cat # A11032; Alexa Fluor GAR 488, Cat # A11070; Alexa Fluor GAR 594, Cat # A11012; Alexa Fluor strep 488, Cat # A32360; Alexa Fluor strep 594, Cat # A-24927. Invitrogen) diluted at 1:200 and incubated for two hours in a hydrated chamber at RT. The secondary antibodies were gently aspirated off and 1 µg/ml

DAPI in PBS (~0.5 mL of solution) was added to each coverslip for 10 minutes to label nuclei of all cells.

Biotinylated primary antibodies followed a modified procedure before the DAPI nuclear stain was conducted. For biotinylated antibodies, the secondary antibody was washed off thoroughly (3 x 10 min) before incubation with the biotinylated primary antibody (1-2 hr incubation at RT). The coverslips were washed with PBS BSA, and treated with streptavidin (either Strep-488 or Strep 594) (2 hr incubation at RT). The fluorochrome-conjugated streptavidin was gently aspirated off and 1 µg/ml DAPI nuclear stain (0.5 ml) was added for 10 minutes.

At the end of the immunolabeling procedures, coverslips were washed with PBS BSA (3 x10 min), and mounted on Thermo Scientific Superfrost Plus 25 x 75 x 1 mm glass microscope slides with ~1 drop of fluoromount-G and then sealed with clear nail polish enamel at the edges.

All observations were made on an Olympus IX81 inverted epifluorescence microscope. Images were captured with a Photometrics CoolSNAP HQ^2 camera using Metamorph Automation and Image Analysis Software. Images were saved as tif files and edited in Adobe Photoshop CS4 by adjusting levels and creating merged images.

H) Analysis of co-culture experiments

Four low magnification fields each measuring 0.90 x 0.67 mm (0.61 mm^2) were captured from each coverslip. All fields were analyzed using the Java-based image processing program, Image J (NIH). Fluorescent images were

thresholded to reveal the myosin positive myotubes and a combined area of all myotubes in each image was measured using the wand tool. The number of myosin-positive cells per image was quantified (only myosin positive cells with two or more nuclei were included) and the complexity of each myotube was determined, wherein each myotube was either identified as being straight or branched. Each myotube was also measured with the straight line selection tool for an overall length and an average width. Using a merged image in Adobe photoshop CS4, the number of nuclei found within each myotube was quantified and totalled to give the number of nuclei found within all myotubes in the field; if a nucleus was seen to be in contact with a myotube, it was added to the nuclear count of that syncytium, even if the entire nucleus was not within the myosin stained region (Figure 2).

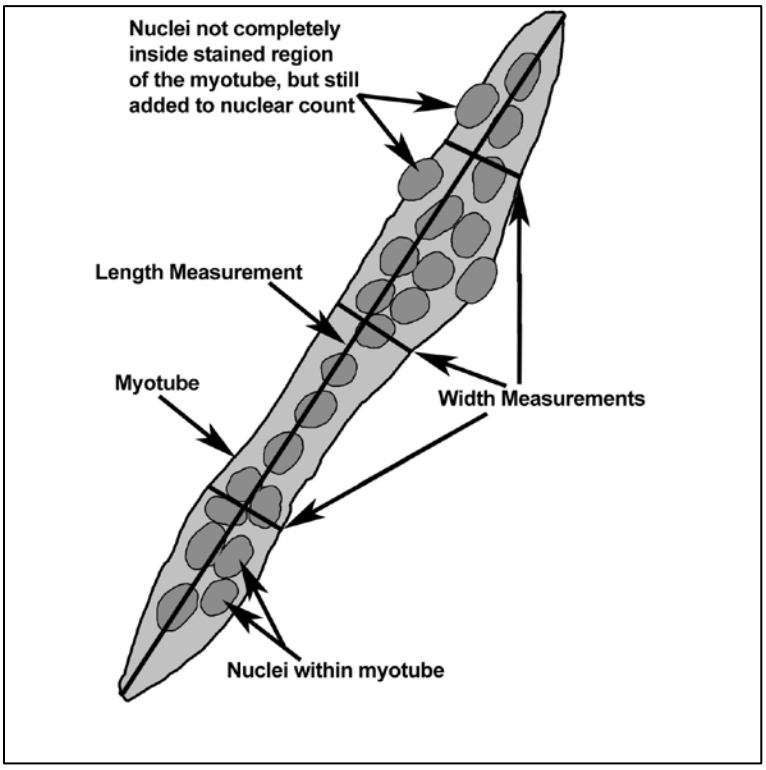

Figure 2. Schematic of a myotube showing examples of the measurement techniques which included length and width, as well as nuclear counts.

I) Statistical Analysis

Statistical analysis was conducted using Microsoft Excel. Within each field, the minimum, maximum, and average values with standard deviations were calculated for: myotube length and width, the total number of nuclei within myotubes, the number of nuclei per myotube, the proportion of straight and branched myotubes, and overall number of myotubes. The total area covered by myotubes in each field was calculated and expressed as a percentage of the field. The average myotube size (in μm^2) was determined from the total area occupied by all myotubes in the field of view. Averages for each coverslip from the four field analysis were collated, and then averages and standard deviations for all coverslips within a specific condition (eg. Cartilage-C2C12) per experiment were determined. One-way ANOVAs were conducted to compare variance across the four growth conditions (i.e. control, neural-C2C12, cartilage-C2C12, and kidney-C2C12). Two-way ANOVAs with repetition were conducted to compare interactions between the four growth conditions and differences in media (i.e. standard growth media and growth media with all-trans RA). An unpaired t-test was used to determine significance between two samples of interest. All significance was based on an alpha value of 0.1. R-squared values were determined to confirm goodness of fit.

Results

Myoblast and Myotube Morphology

As muscle cell fusion was the main focus of this research, muscle cells were analyzed at both the myoblast and myotube stages. Early after plating the cells, myoblast growth was marked by mitotic figures (cell divisions), cytoplasmic extensions, and proliferation. After three days of growth, the majority of myoblasts were spindle shaped with a smaller proportion exhibiting long cytoplasmic extensions at the slender tips (Figure 3). Dividing cells were round and had a faint glow around them when viewed with phase contrast. Myoblasts would typically continue to divide as long as there was open space around them. At five days of growth, the number of cells increased, space between groups of myoblasts decreased and as a result, cell-cell contact increased and the number of dividing cells decreased compared to the cultures at three days of growth (Figures 3&4). Myoblasts maintained the spindle shape at five days of growth, but few exhibited the cytoplasmic extensions seen at earlier stages of growth (Figure 4). At this point of growth, myoblasts formed swirls of staggered, parallel-arranged cells. Initial signs of myoblast fusion were observed at approximately seven days of growth, which was marked by the presence of small, newly formed myotubes (Figure 5).

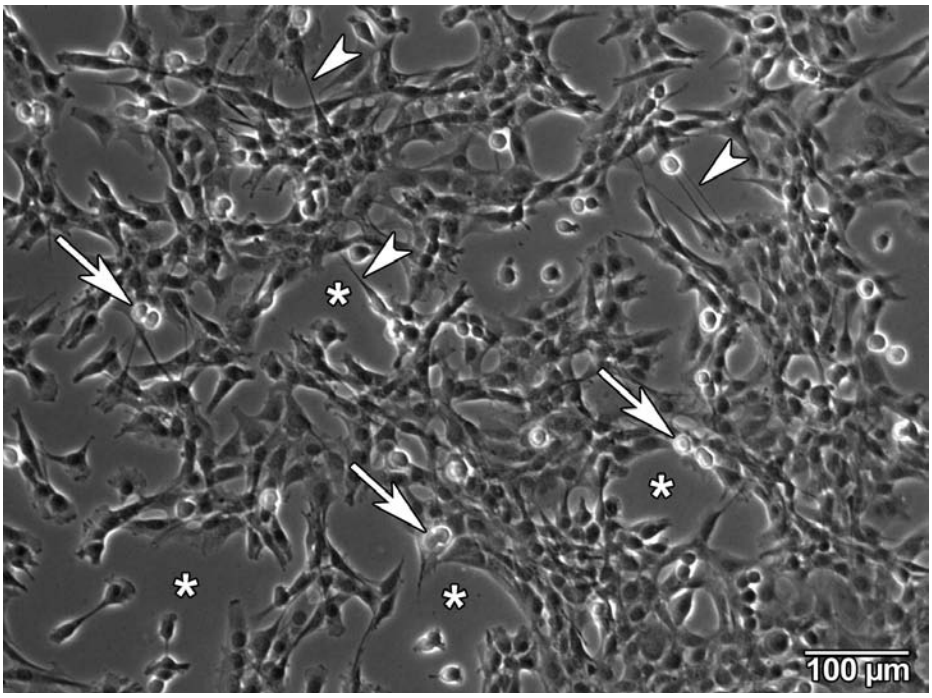

Figure 3. C2C12 myoblasts grown for three days on an NaOH-etched glass coverslip. Myoblasts were spindle shaped, some of which had long cytoplasmic extensions (arrowheads), and were undergoing division at ~12 hour intervals. The bright rounded cells were undergoing mitosis (arrows). Open space between cells is identified with *. Phase contrast, 190x.

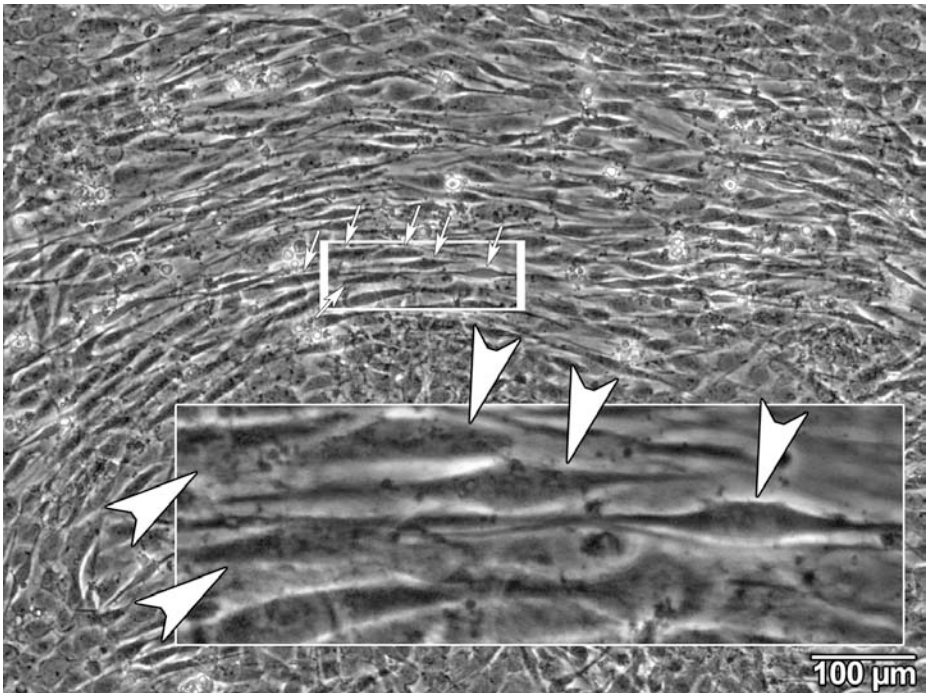

Figure 4. C2C12 monolayer grown for 5 days on a glass coverslip. Myoblast cell-cell contact increased and myoblasts began to form swirls wherein they aligned end to end (arrows). The long axis alignment was shown in the inset, with individual, spindle-shaped myoblasts marked with arrowheads. Phase contrast, main image 190x.

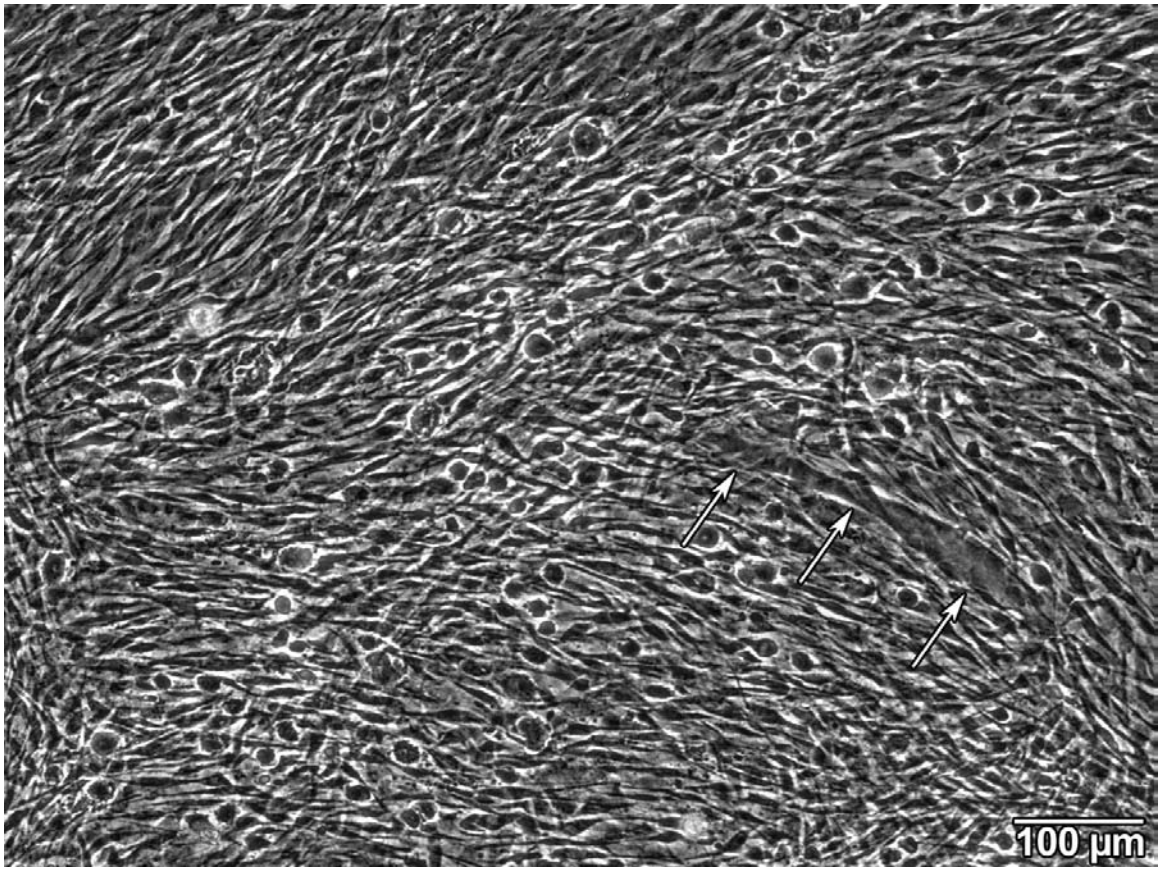

Figure 5. C2C12 myoblasts grown on a glass coverslip for seven days. Cells reached a state of confluency and were aligning into rows. Little to no space can be seen between cells. One newly formed myotube was indicated by the arrows. Phase contrast, 170x.

After initial fusion at seven days of growth, myotubes continued to grow by incorporating additional free myoblasts or by fusing together with other myotubes. The number of nuclei found within myotubes ranged from two to over one thousand. As the cells continued to fuse, myotubes increased in length and width, and sometimes took on a branched morphology. Myotubes were consistently found after eleven days of growth and were the endpoint for the majority of the experiments within my project (Figure 6).

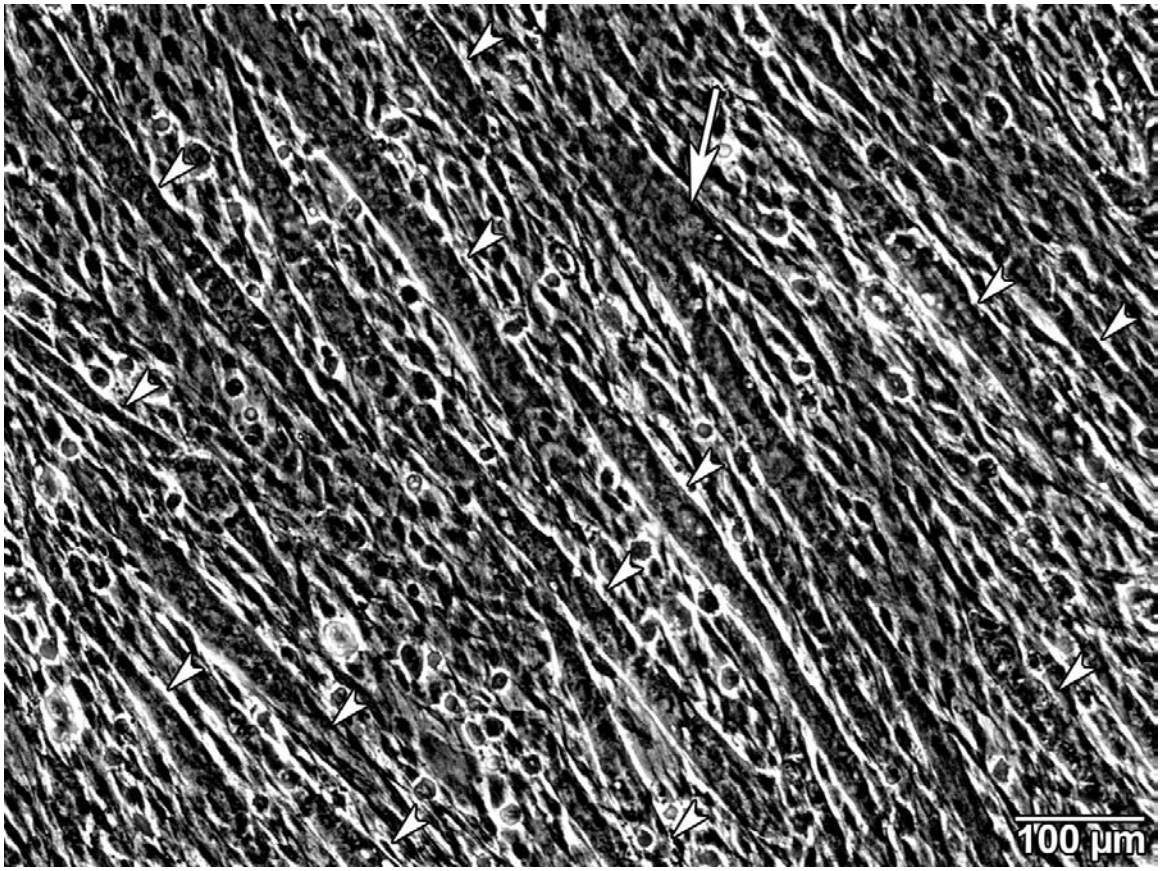

Figure 6. C2C12 myoblasts grown on a glass coverslip for 11 days. Myotubes (arrowheads) were multinucleated and arranged in parallel. Unfused cells were seen between the myotubes. Most myotubes were straight, but occasional branched myotubes were observed (arrow). Phase contrast, 170x.

Immunocytochemistry of Muscle Specific Proteins in Myotubes

To determine the stage of myotube development and myofibril assembly, immunocytochemical procedures were performed on the muscle cultures. Anti α-actinin was employed for observations of muscle cell differentiation and localized to the Z lines of sarcomeres. Using anti α-actinin to immunolabel myotubes highlighted the striated appearance of the skeletal muscle and enabled visualization of myofilament maturation (Figure 7).

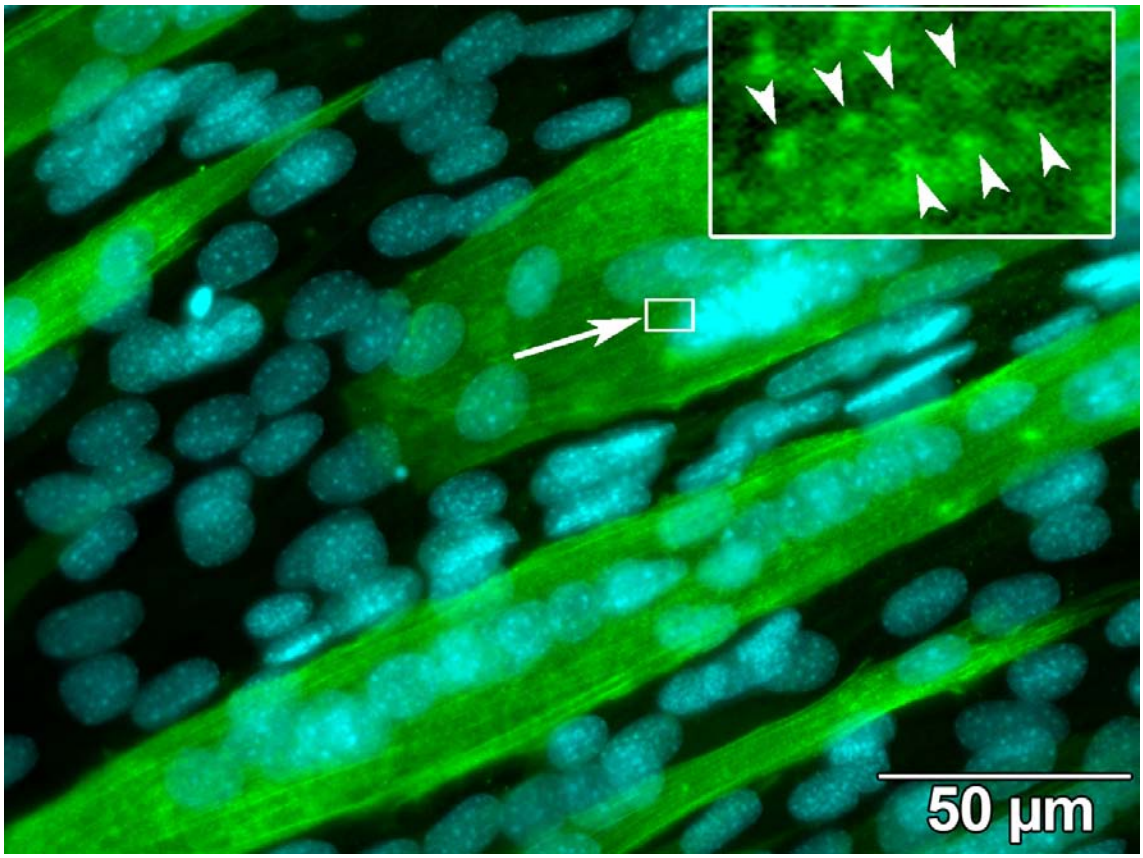

Figure 7. Myotubes grown on glass coverslips for 11 days and immunolabelled with anti-α-actinin (green). Myotubes exhibited a diffuse sarcoplasmic distribution of α-actinin and some visible Z lines (arrow). Arrowheads indicate individual Z lines in inset. Nuclei were stained with DAPI (blue). Main image 660x.

Another monoclonal antibody used in my experiments was anti-myomesin, an antibody that localizes to the M line of sarcomeres. Myomesin enabled the visual observation of myofilament maturation by highlighting the striated appearance of differentiated skeletal muscle (Figure 8).

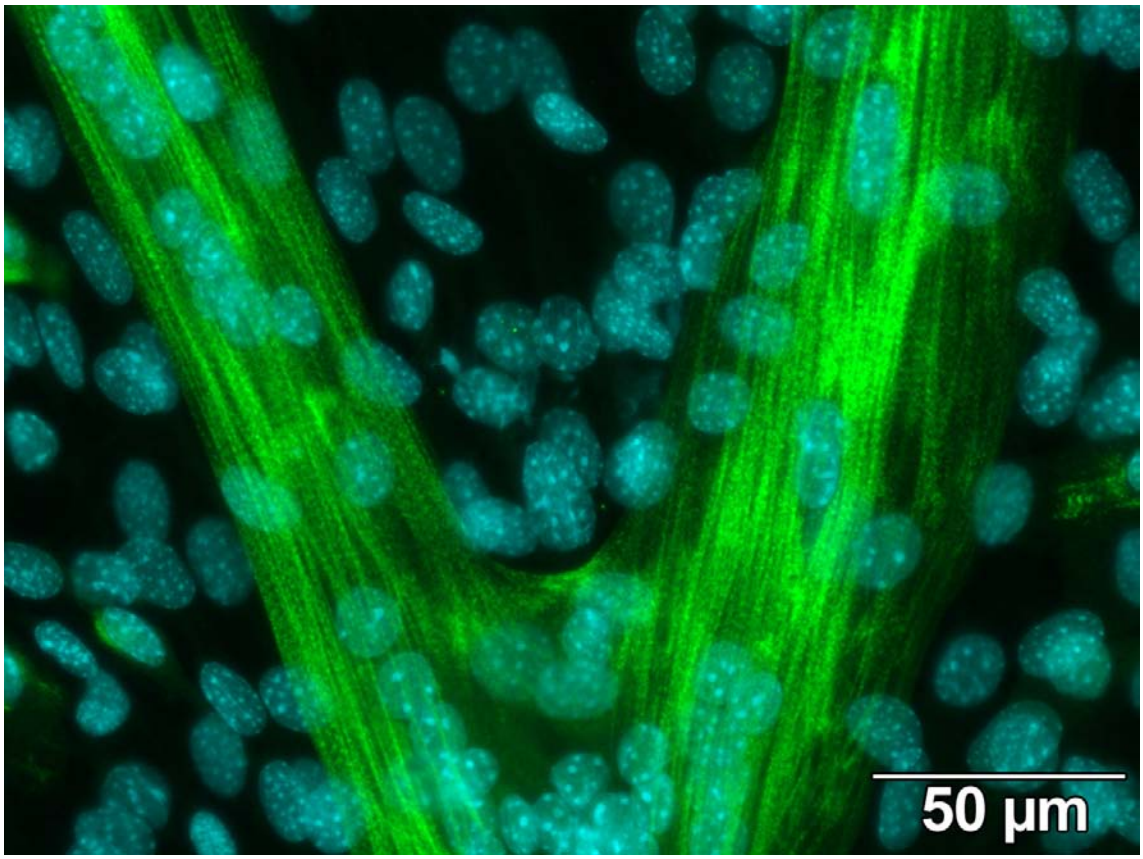

Figure 8. Example of a branched myotube labelled with anti-myomesin (green) after 10 days of growth on a glass coverslip. M lines were visible throughout the myotube and denoted maturation and alignment of developing myofibrils. Nuclei were stained with DAPI (blue). 660x.

A third monoclonal antibody used to identify differentiated myoblasts and myotubes was an anti-myosin antibody (F59). F59 was found to effectively label myosin expression within the sarcoplasm of myotubes and provided information on the state of myofilament maturation (Figure 9). The reliable staining of myotubes using F59 led to the use of this antibody and its biotinylated form (F59 biot) for the majority of my experiments. F59 biot was used in conjunction with other monoclonal antibodies for dual labelling purposes and stained myotubes as effectively as F59.

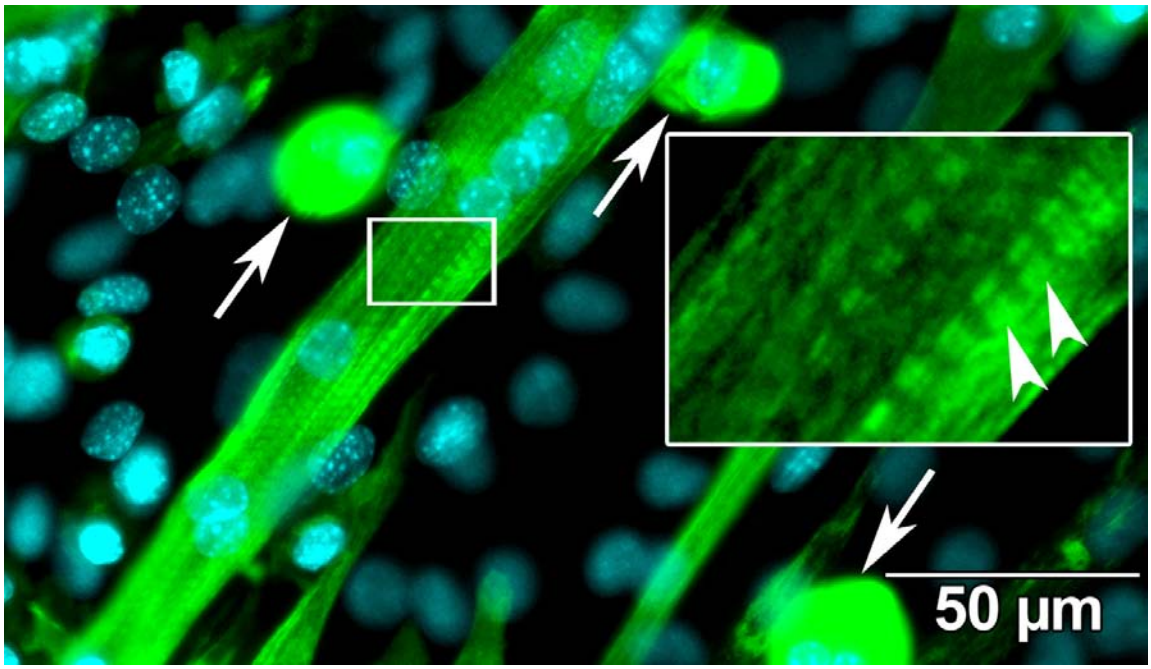

Figure 9. Myotubes grown for 14 days on glass coverslips and labelled with anti-myosin (F59). Myosin expression (green) was positive and showed prominent striations in the large elongated myotubes. Arrowheads in the inset denote A bands. Some myotubes detached due to spontaneous contraction and formed myoballs (arrows). Nuclei were stained with DAPI (blue). Main image 680x.

C2C12 Control Experiments

A control group of C2C12 myoblasts were plated on eight glass coverslips and immunolabelled with F59 to determine myotube development in monocultures. Four fields measuring 0.90 x 0.67 mm (0.61 mm^2) per coverslip were captured, and analyzed to quantify average myotube development after approximately 1.2 x 10^4 myoblasts were plated and cultured for 11 days. The total area covered by myotubes as a percentage of the total field of view ranged from 13.21% to 45.07%, with an average area covered of 29.36 ± 4.78%. The average area per myotube ranged from 672 μm^2 to 1977 μm^2, with an average myotube area of 1290.8 ± 285.2 μm^2. The average myotube length was found to be 69.3 ± 9.6 µm, with the shortest and longest myotubes being recorded as 8.3

μm and 1074.1 μm, respectively. The average myotube width was found to be 18.4 ± 1.3 μm, with the thinnest and widest myotubes being recorded as 4.8 μm and 85.8 μm, respectively. The number of nuclei found within each myotube ranged from 2 to 1018 nuclei, with an average of 15.9 ± 2.9 nuclei. The proportion of branched myotubes ranged from 0.6% to 7.7%, with an average of 3.9 ± 1.0%. Overall, the number of myotubes per field ranged from 95 to 207 myotubes, with an average of 143.6 ± 14.6 myotubes. The total nuclear count within all myotubes per field ranged from 1354 to 3148 nuclei, with an average of 2226.5 ± 344.5 nuclei. The compiled results from the morphometric analysis of control C2C12 monocultures are shown in Table 1.

Table 1. Morphometric analysis of myotube formation in 11 day old C2C12 control cultures grown on glass coverslips. Myotubes (myosin positive and containing at least two nuclei) were counted in four separate fields (0.90 x 0.67 mm (0.61 mm^2) on eight coverslips and then averaged. MT, myotube.

Slide #	MT Area (%)	Area/ MT (μm^2)	Length (μm)	Width (μm)	Nuclei per MT	Branched (%)	Number of MT	Total # of Nuclei
1	33.6	1509.9	78.4	20.0	15.3	5.4	135	2065.3
2	25.2	1110.5	75.9	17.6	12.5	2.6	149.5	1786.3
3	36.5	1747.9	78.8	19.2	17	4.6	128.3	2133.8
4	32.9	1276.0	69.4	17.6	17	4.1	163.5	2691
5	22.6	888.6	49.1	18.3	12.1	3.3	158	1846
6	29.7	1518.4	73.5	18.1	20.5	3.7	121.3	2475
7	28.9	1235.8	67.4	17.3	18.7	4.9	142.3	2647
8	25.5	1039.2	63.7	17.7	14.4	2.9	150.8	2167.8
Ave.	29.4	1290.8	69.5	18.2	15.9	3.9	143.6	2226.5
SD	4.8	285.2	9.8	0.9	2.9	1.0	14.6	344.5
Min	13.2	672.0	8.3	4.8	2.0	0.6	95	1354
Max	45.1	1977.0	1074.1	85.8	1018	7.7	207	3148

Primary Cultures of Kidney Epithelial Cell

Kidney epithelial cells obtained from newborn mice were easily cultured and proliferated rapidly when plated in plastic Petri dishes with standard growth media (10% FBS). The kidney cells started small, displaying either a stellate or

elongated morphology. As the cells matured they continued to divide and adopted a flattened, squamous morphology. The epithelial cell morphology was successfully visualized using antibodies for kidney specific elements (cytokeratin) or general cell cytoskeletal elements (β-tubulin). A phalloidin stain was used to label filamentous actin, and anti-β-tubulin was used to label the microtubule network (Figure 10). An anti-cytokeratin antibody was used as an epithelial-specific antibody that labelled the keratin-containing intermediate filaments and typically localized to the perinuclear cytoplasm of kidney cells.

Kidney Epithelial and C2C12 Muscle Cellular Interaction in Co-cultures

While myoblasts were still able to proliferate and fuse to form myotubes when in co-culture with kidney epithelial cells, there was little to no physical colocalization of the two cell types. Myotubes were seen next to epithelial cells, but did not appear to make contact (Figure 11). Myotube number and size was greatly reduced with kidney epithelial cells in comparison to C2C12 control coverslips (Figure 12).

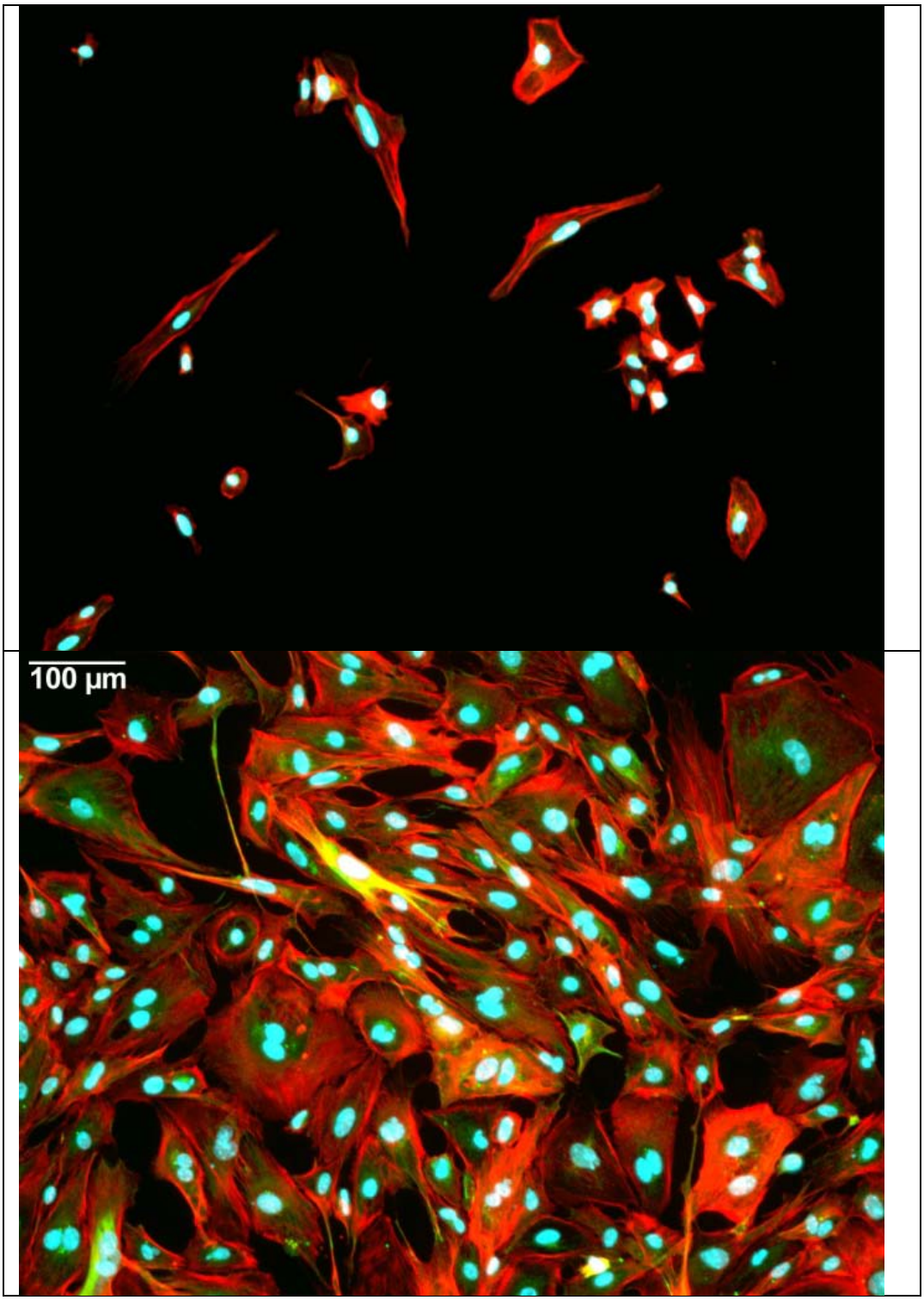

Figure 10. Kidney epithelial cells grown for 6 days (top) and 14 days (bottom) on glass coverslips. Cells were labelled with phalloidin (red) and α-tubulin (green). Nuclei were stained with DAPI (blue). At 6 days kidney cells were small with either a stellate or elongated morphology. At 14 days, the cells increased in number and size, and adopted a flattened, squamous morphology with some cells measuring over 150 µm across. 150x.

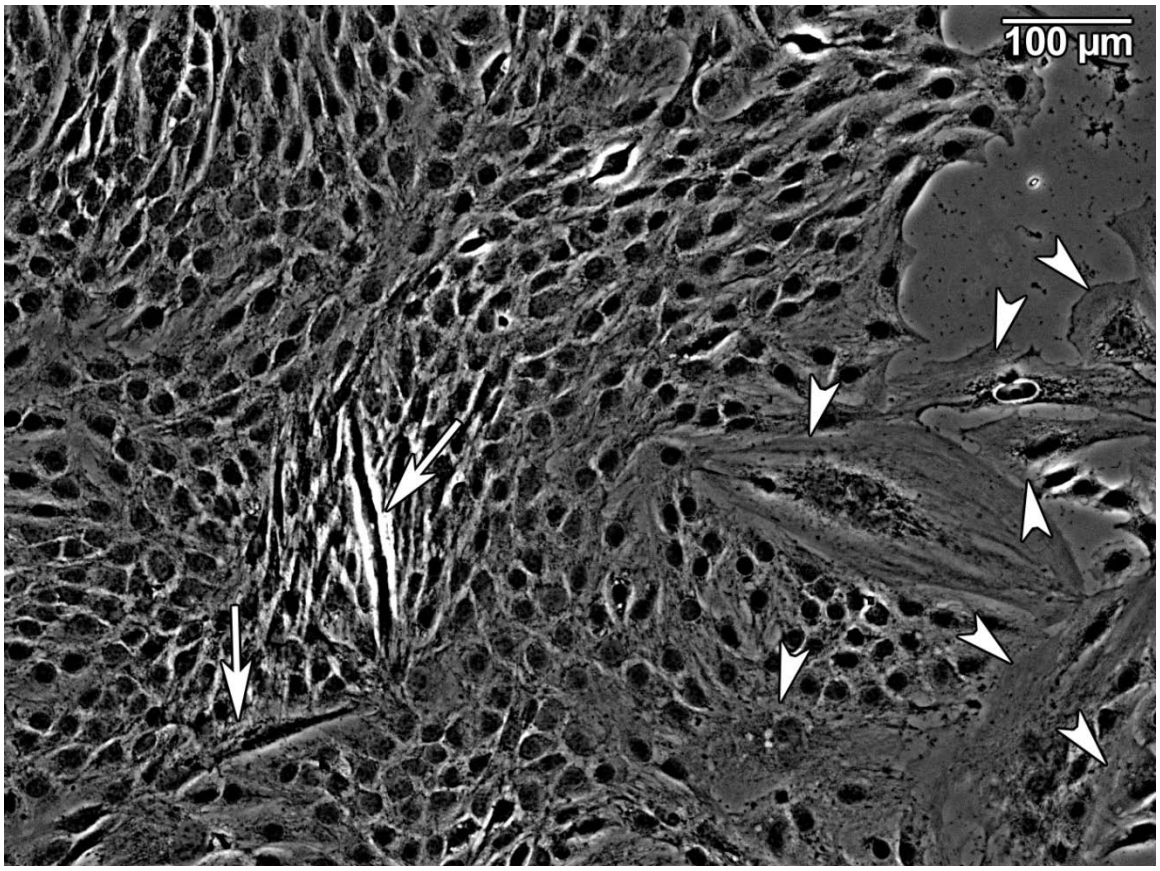

Figure 11. Mixed and simultaneously plated kidney-C2C12 myoblasts culture grown for 11 days on a glass coverslip. Two myotubes (arrows) were next to large, squamous epithelial cells (arrowheads). Myotubes were smaller and few in number and did not appear to make contact with epithelial cells. Phase contrast. 170x.

Although there were fewer myotubes per field in the mixed C2C12 and kidney epithelial cell co-cultures, closer inspection of myotubes revealed that myotube maturation (ie. myofibrillogenesis) was not affected by the presence of kidney epithelial cells. Occasional striated myotubes were observed after 10 days of growth (Figure 13).

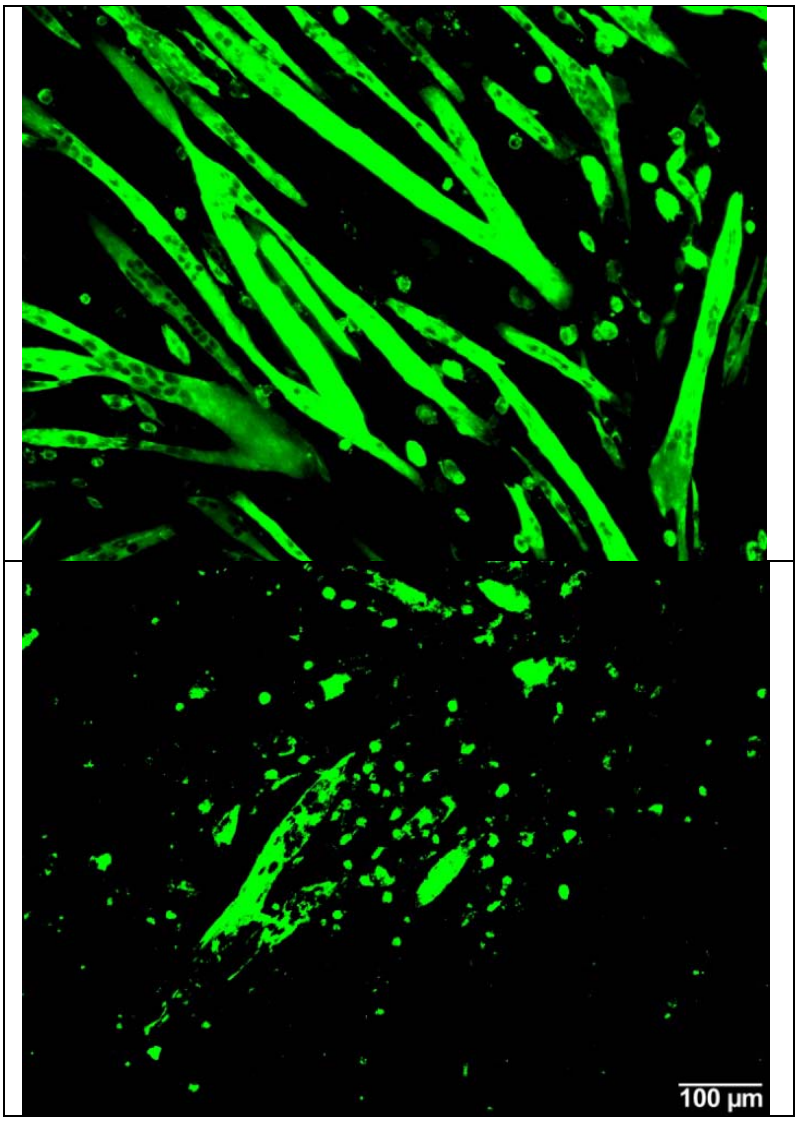

Figure 12. Comparison of C2C12 myoblast control (top) and a mixed kidney-C2C12 myoblast culture (bottom) grown for 11 days on glass coverslips. Myotubes were immunolabelled with F59. A dramatic reduction in myotube formation was observed when C2C12 cells were grown with kidney epithelial cells. 110x.

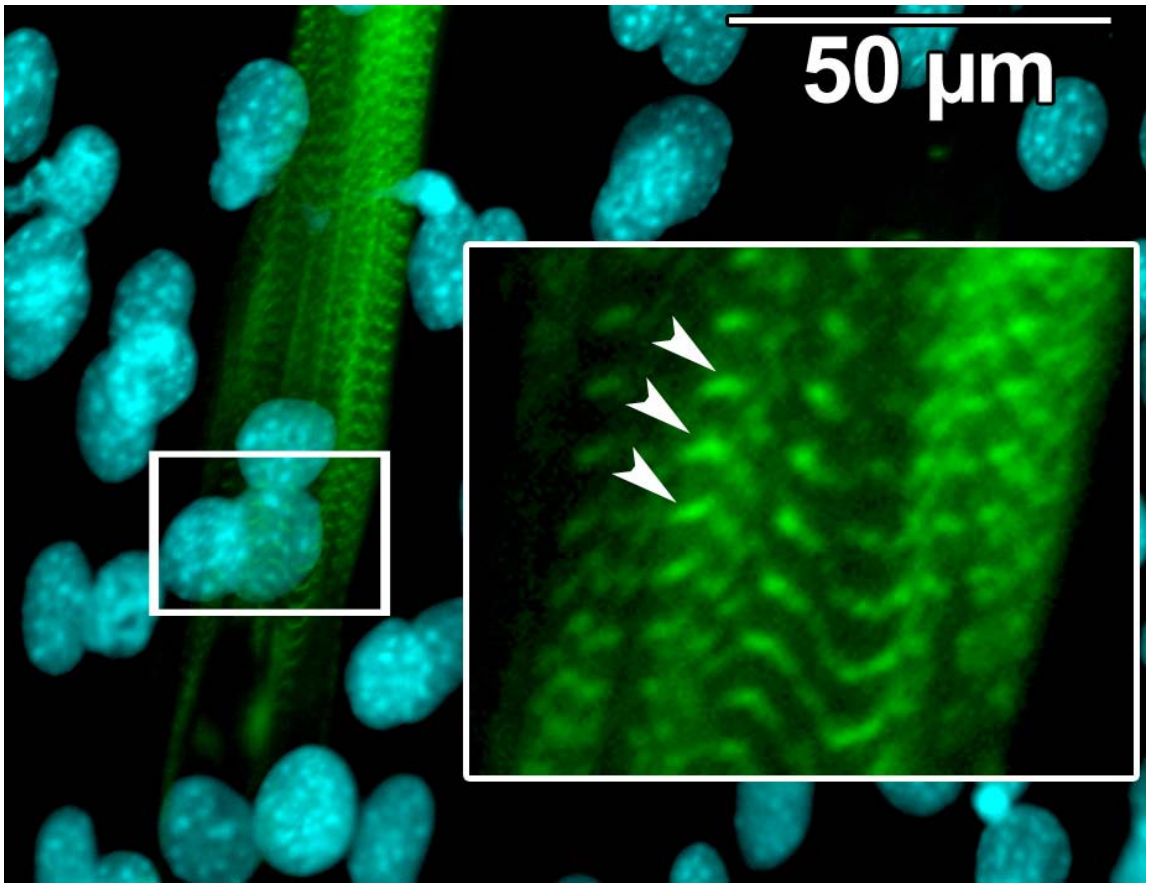

Figure 13. Myotube (10 days old) immunolabelled with myomesin (green) in a mixed kidney-C2C12 myoblast culture. Aligned myomesin-positive M bands of myofibrils were evident within the sarcoplasm (arrowheads in inset). Nuclei were stained with DAPI (blue). Main image 1000x.

Neural Cell and C2C12 Myotube Cellular Interaction in Co-cultures

Murine primary neural cells were cultured, and proliferated rapidly when plated in a plastic Petri dish with standard growth media. Neurons exhibiting cell-typical morphology with cell bodies extending long axonal cytoplasmic processes were observed after approximately 14 days of growth. An example of neural cells plated at low density and grown for 30 days can be seen in Figure 14.

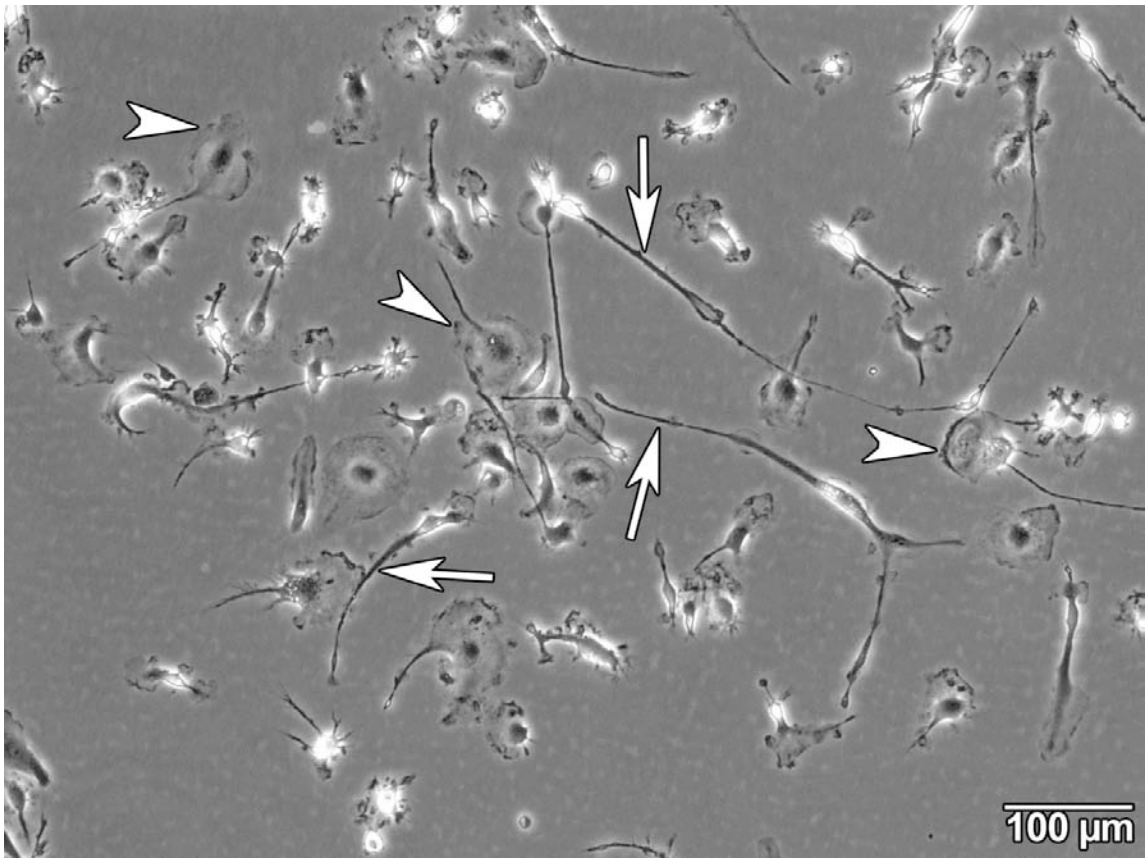

Figure 14. Primary neural cells seeded at low density on a plastic Petri dish and incubated for 30 days demonstrating axonal processes (arrows) growing from their cell bodies (arrowheads). Phase contrast, 170x.

Using a neuron-specific monoclonal antibody which labelled neurofilament protein, neural cells were observed to closely associate with myoblasts and myotubes (Figure 15). Surprisingly, the number and size of myotubes was reduced in neural-C2C12 myoblasts cultures when compared to C2C12 myoblast control dishes (Figure 16).

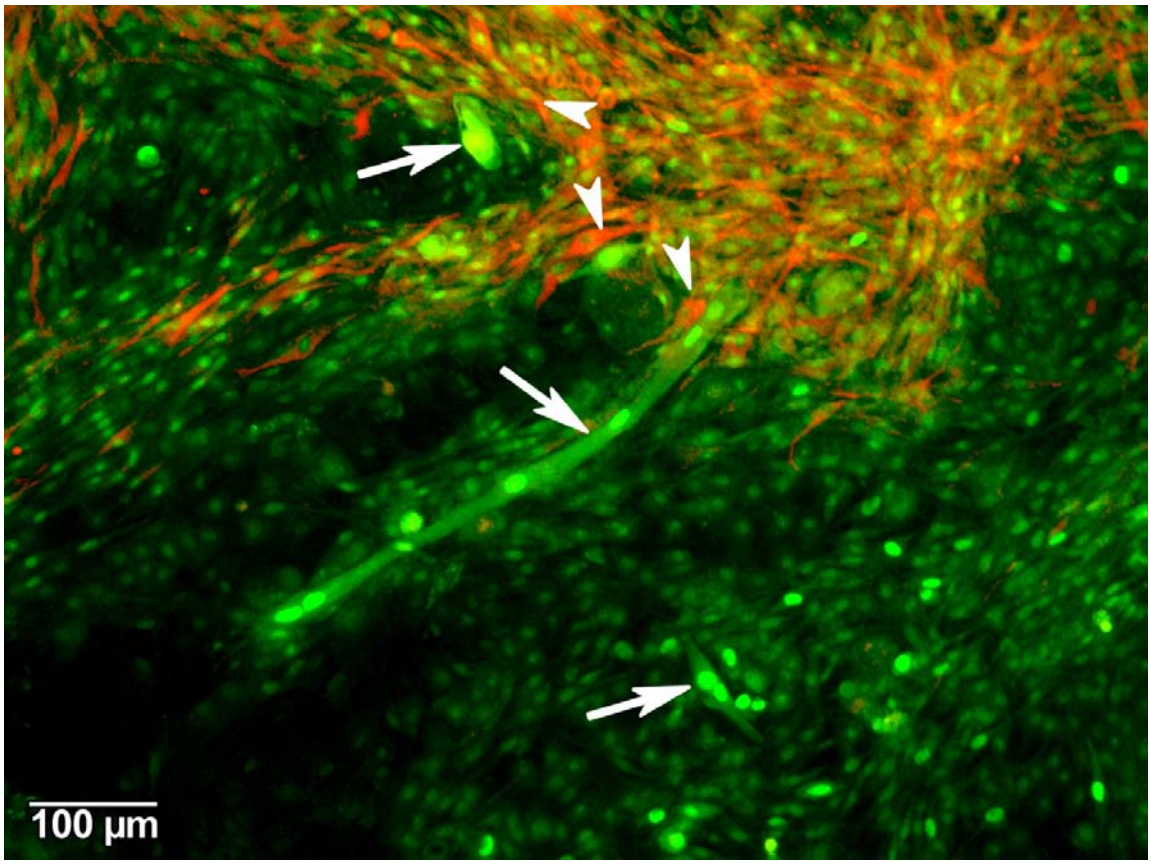

Figure 15. Mixed neuronal-C2C12 myoblast culture grown for 13 days on a glass coverslip. Myotubes were labelled with myogenin (green) which labeled nuclei brightly, and neurons were immunopositive for neurofilament protein (red). Neurons (arrowheads) were closely associated with myotubes (arrows). 170x.

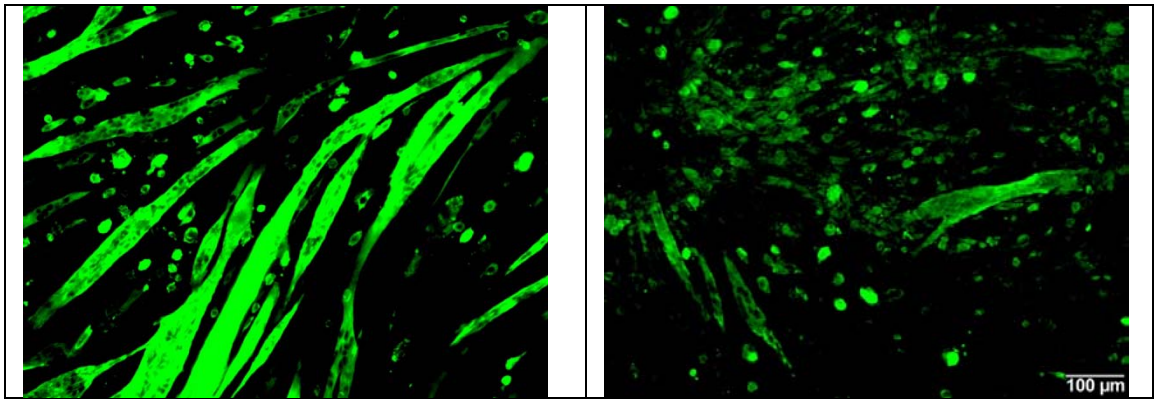

Figure 16. Comparison of a C2C12 control (left) and mixed neural-C2C12 myoblast culture (right). Both cultures were grown for 11 days on glass coverslips and immunolabelled with F59. A reduction in myotube formation was observed when C2C12 myoblasts were grown with neural cells. 80x.

Cartilage Morphology and Immunocytochemistry

Chondrocytes appeared to prefer a higher cell density culture condition and were, therefore, cultured in smaller dishes (1 cm diameter). Additionally, to obtain sufficient chondrocyte numbers, both the dissociated cells and microdissected (< 1 mm) pieces of cartilage were cultured together. If the cartilage pieces adhered to the bottom of the dish, rapidly migrating and dividing chondrocytes spread outwards from that point and aggregated into closely associated islands (Figure 17). At later time points (eg. 11 days in culture), the cells were round and embedded within a delicate extracellular matrix. To confirm the composition of the extracellular matrix, an alcian blue staining produced intense blue staining in the established cultures of chondrocytes and within the small pieces of cartilage. Cartilage cultures were also immunolabelled with anti-type II collagen polyclonal antibody, which is a main constituent of the normal cartilage extracellular matrix. Type II collagen expression was observed in both intracellular or extracellular regions where it covered and surrounded chondrocytes.

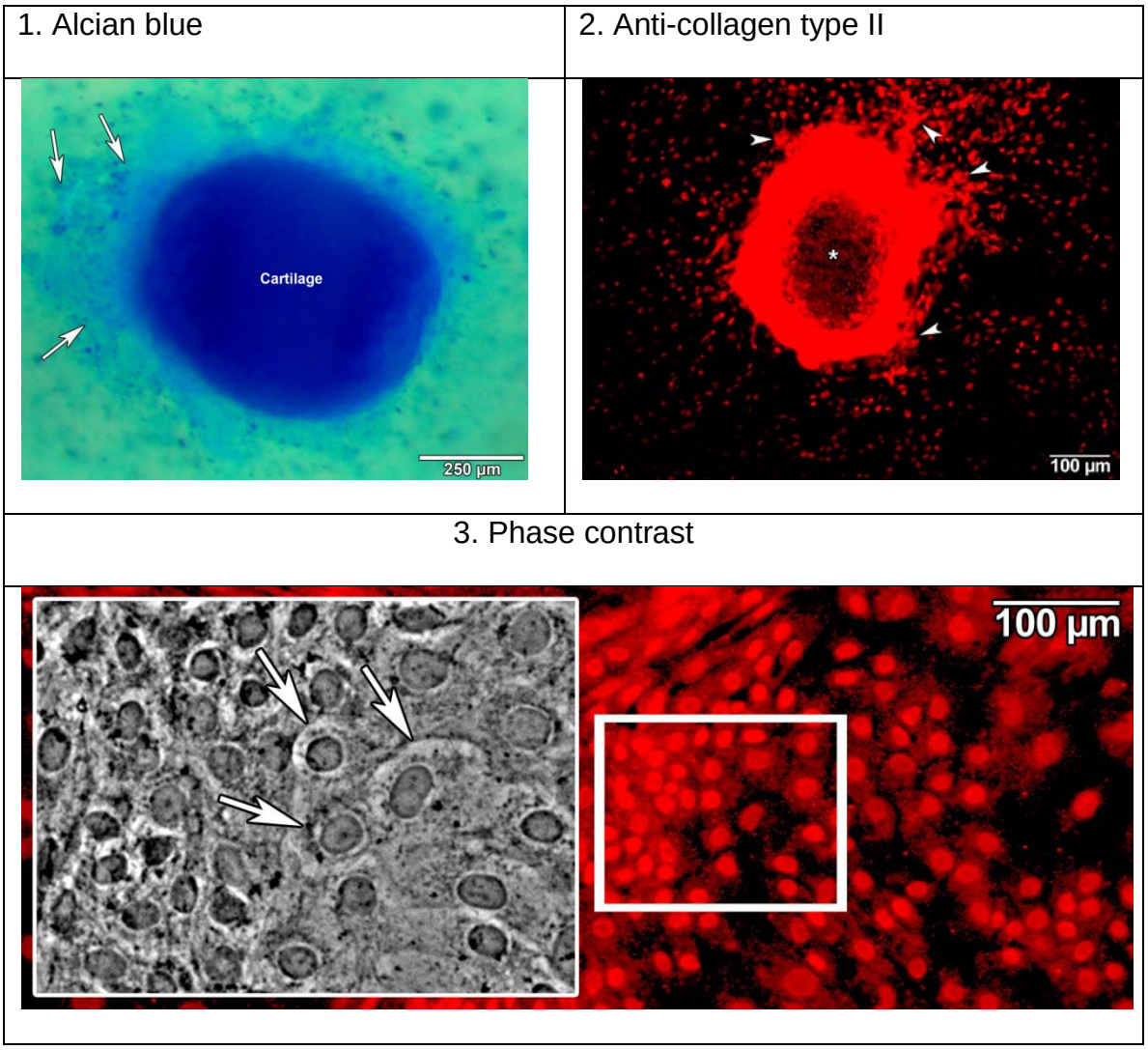

Figure 17. 1) Alcian blue stain of the extracellular matrix surrounding a piece of cartilage and proliferating chondrocytes (arrows) grown for 11 days on a glass coverslip. 76x. 2) A 21 day old adhered piece of cartilage (*) immunolabeled with anti-type II collagen (red) showing chondrocytes proliferating radially from the cartilage (arrowheads). 80x. 3) Higher magnification view of 21 day old chondrocytes immunolabelled with anti-type II collagen (red). Inexplicably, both nuclei and cytoplasm of chondrocytes are positive for type II collagen. Inset shows the phase contrast image of the enclosed area to the right and illustrating the rounded and tightly-packed nature of chondrocytes (arrows). Main image 170x.

Cartilage and C2C12 Myotube Interactions in Co-cultures

Cartilage and C2C12 myotubes exhibited high co-culture compatibility and contained numerous myotubes in close proximity to chondrocytes as well as to attached cartilage pieces. When whole pieces of cartilage (< 1 mm) were present in a co-culture with C2C12 myoblasts, myotubes were routinely found in close proximity or attached to the cartilage piece (Figure 18). Myotubes that made contact with adhered cartilage pieces exhibited a greatly increased longevity (up to 74 days) compared to myotubes grown in any other co-culture condition. These myotubes exhibited advanced sarcomere development to the point of spontaneous contraction and were observed contracting without pulling free of the substrate. Myotubes in control mono-culture conditions were also capable of developing sarcomeres to the point of spontaneous contraction, but would often pull themselves off of the Petri dish and form myoballs at ~16 days. In addition to enhanced longevity, myotubes in the cartilage co-culture condition were larger when compared to C2C12 mono-culture controls (Figure 19).

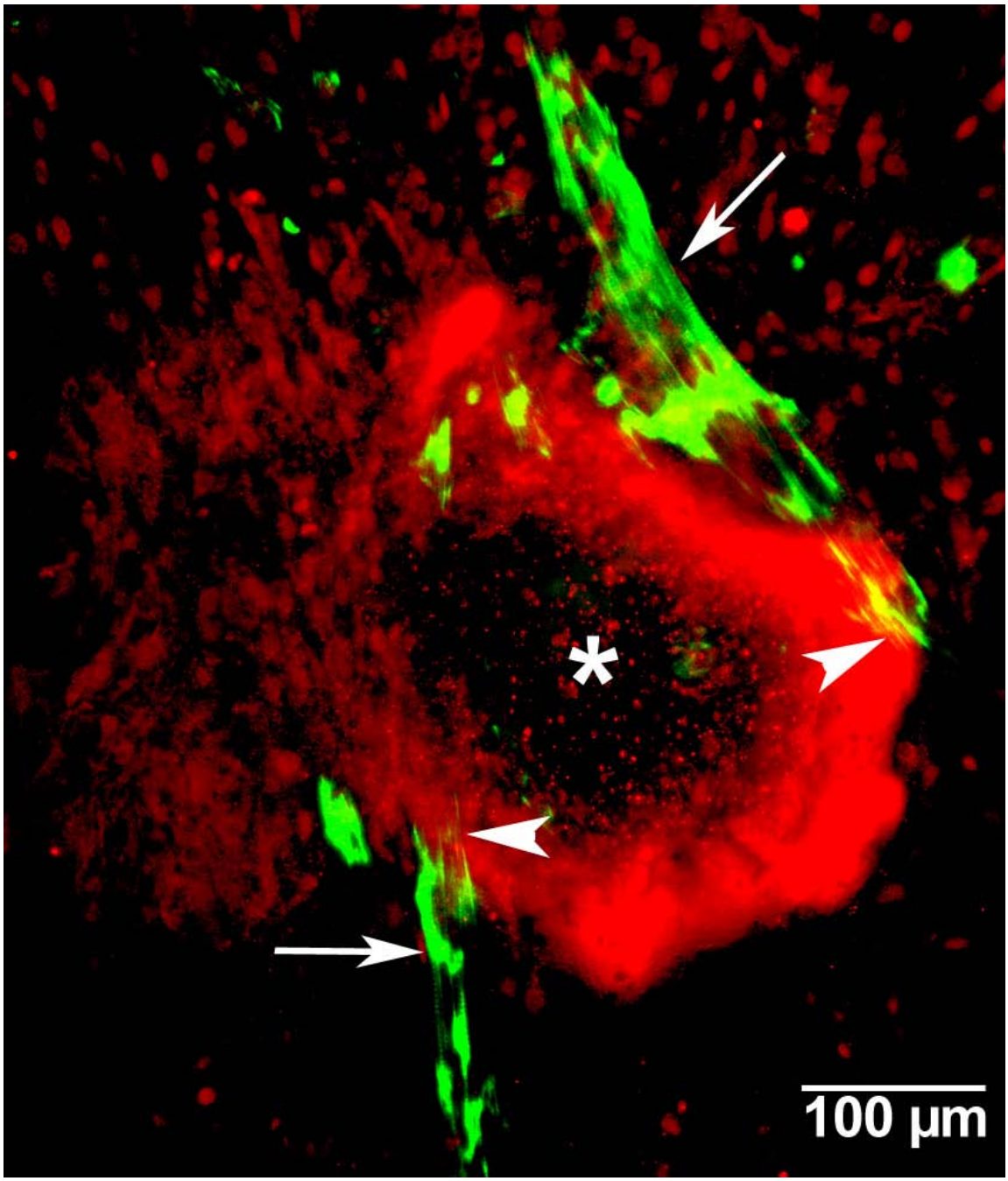

Figure 18. C2C12 myotubes (11 days) grown in a pre-established, 10 day old cartilage culture. Myotubes were immunolabelled with F59 (green) and cartilage was labelled with anti-collagen type II antibody. A small piece of cartilage (*) is in close proximity with two mature myotubes (arrows). Myotube appear to attach to the cartilage (arrowheads). 230x.

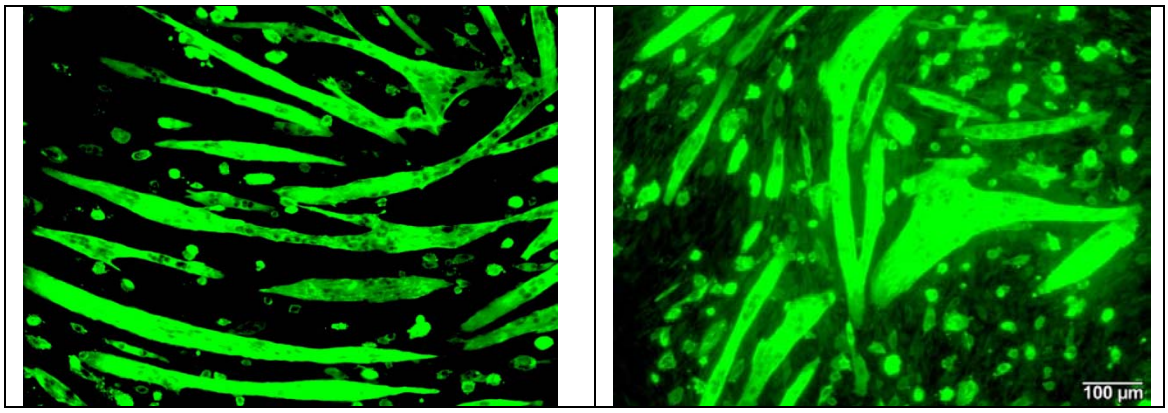

Figure 19. Myotube development in C2C12 control (left) and cartilage-C2C12 myoblast culture (right) grown for 11 days on glass coverslips. Myotubes were immunolabelled with F59 (green). Although more myotubes were seen in the C2C12 control dish, myotubes in the C2C12 and cartilage co-culture were increased width and area. 80x.

Upon closer inspection, myotubes co-cultured with cartilage had some of the most advanced sarcomere development when compared to C2C12 control dishes and to any other co-culture conditions attempted in my research. The myofibrils observed in these co-cultures had a high level of alignment and uniformity across the width of the myotube, as opposed to myofibrils in other co-culture conditions in which they appeared less aligned or merely lined the edges of the myotubes. Myofibrillogenesis appeared to be increased when myotubes were in contact with individual chondrocytes (Figure 20) and when in contact with a piece of cartilage (Figure 21).

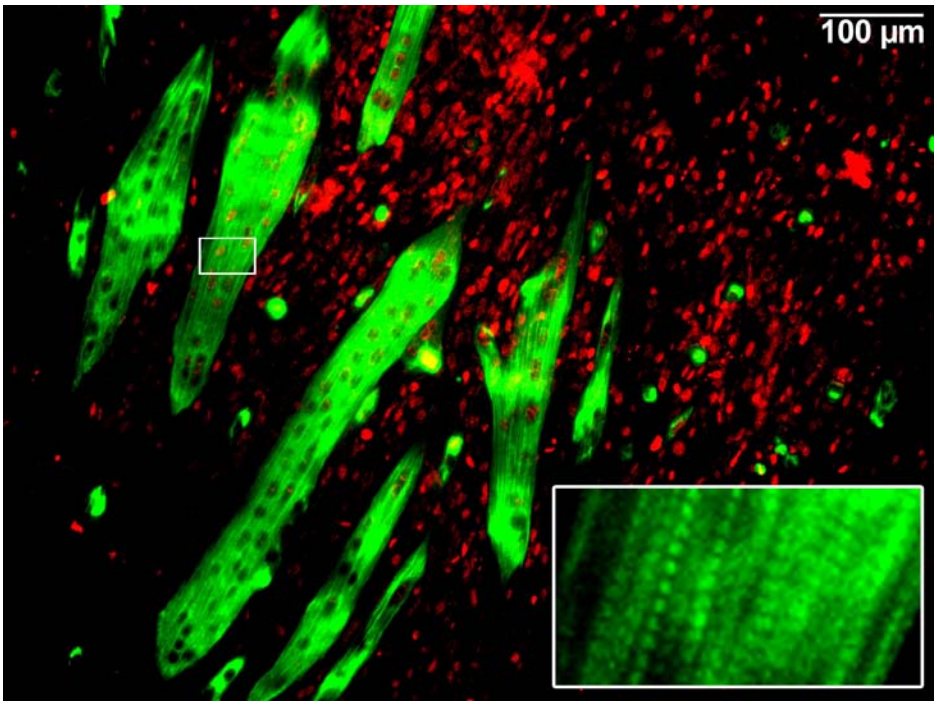

Figure 20. Mature (11 day) myotubes grown on a pre-established 10 day old culture of cartilage. Myotubes were labelled with F59 (green) and chondrocytes were labelled with collagen type II antibody (red). Myofibrils are aligned and distributed uniformly across the myotubes. Main image, 190x.

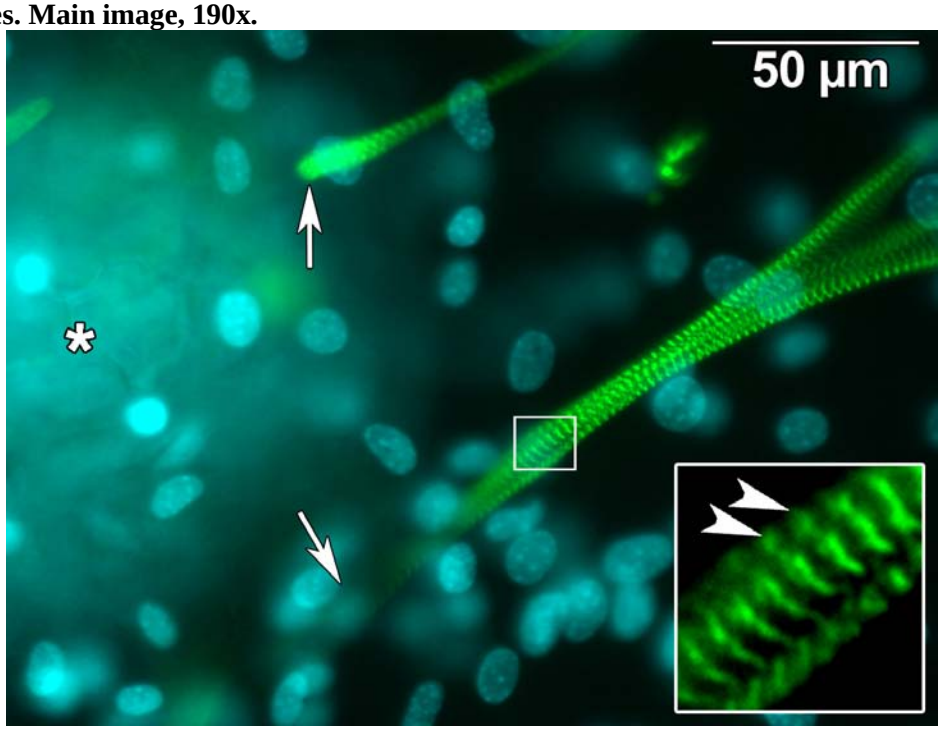

Figure 21. Mature (11 day) myotubes grown on a pre-established 10 day old culture of cartilage. A small piece of cartilage occupies the left of the field (*, pale blue region). Myotubes were immunolabelled with anti-myomesin (green). Myofibrils spanned the length of the myotubes and exhibit a well aligned banding pattern. Contact sites with the cartilage are indicated (arrows). M bands of myofibrils are indicated in the inset (arrowheads). Main image, 540x.

C2C12 Myoblasts Grown for Two Days before addition of Neural, Cartilage or Kidney Epithelial Cells

Myoblasts were found to successfully proliferate and form myotubes in all three co-culture conditions (C2C12 first, mixed simultaneous, and neural, cartilage or kidney first), however some combinations of cell types produced more robust myotubes than others. In the co-culture condition where C2C12 myoblasts were grown for two days prior to the addition of a second cell type (n = 7), the largest myotubes were found within the cartilage-C2C12 myoblast cultures (Figure 22). Neural-C2C12 myoblast cultures produced smaller and less numerous myotubes when compared to all other co-culture combinations.

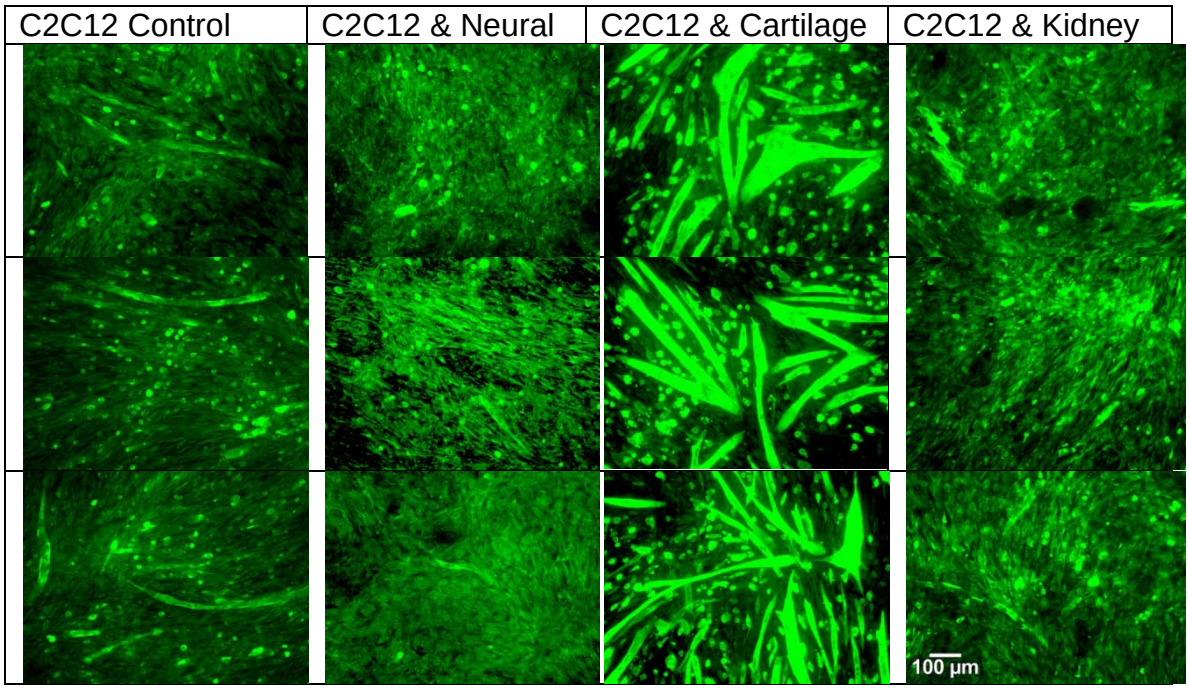

Figure 22. C2C12 cultures initially grown for two days prior to addition of neural, cartilage, or kidney epithelial cells. Cultures were grown for a total of 11 days and then immunolabelled with F59. Three examples from each growth condition were shown from top to bottom. Neural-C2C12 myobalst and kidney-C2C12 myoblast cultures showed a dramatic reduction in myotube formation, whereas cartilage-C2C12 cultures showed enhanced myotube growth when compared to C2C12 controls. 40x.

Analysis of the co-culture condition where C2C12 myoblasts were grown for two days prior to the addition of a second cell type revealed myotubes grown with cartilage covered a higher total area as a percentage of the total field of view area (30.9 ± 3.2%), as well as a higher average area covered per myotube (973.2 ± 52.4 μm^2) when compared to other growth conditions (C2C12 control: 10.4 ± 6.2% of total area, 350.8 ± 124.0 μm^2 per myotube; C2C12 and neural: 1.1 ± 1.1% of total area, 186.0 ± 161.4 μm^2 per myotube; C2C12 and kidney: 4.0 ± 1.3% of total area, 233.1 ± 16.4 μm^2 per myotube) (see Table 2). A one-way ANOVA was used to test for total myotube area and average area per myotube in the four growth conditions and both total and average area differed significantly across the culture conditions, $F(3,4) = 31.19$, $p = 0.003$ (total area), $F(3,4) = 60.33$, $p = 0.0009$ (average area). The increase in total myotube area and area per myotube in cartilage co-cultures compared to controls were statistically significant using unpaired t-tests, $p = 0.09$ (total area), and $p = 0.06$ (area per myotube). In addition to this, myotubes grown with cartilage were found to contain a higher average of nuclei within each myotube (12 ± 0.6 nuclei), a higher total number of nuclei found within myotubes (2307.5 ± 57.3 nuclei), a larger width (19.25 ± 0.8 μm), and a higher percent of branched myotubes (2.05 ± 0.8 % branched) compared to all other co-culture combinations (C2C12 control: 9.7 ± 0.6 nuclei per myotube, 1657.5 ± 556.5 total nuclei within myotubes, 16.5 ± 1.1 μm wide, 0.35 ± 0.5 % branched; C2C12 and neural: 3.7 ± 0.5 nuclei per myotube, 117 ± 43.8 total nuclei within myotubes, 10.5 ± 7.1 μm wide, 0 ± 0.0 % branched; C2C12 and kidney: 5.0 ± 0.7 nuclei per myotube, 529 ± 190.9 total

nuclei within myotubes, 16.7 ± 0.2 μm wide, 0.5 ± 0.7 % branched) (Figure 23). A one-way ANOVA was used to test for the average number of nuclei within each myotube, total number of nuclei found within myotubes, width and percentage of branched myotubes in the four culture conditions. All of these tests revealed significant differences across the culture conditions with the following results: $F(3,4) = 94.9$, $p = 0.0004$ (nuclei per myotube), $F(3,4) = 23.15$, $p = 0.005$ (total number of nuclei), $F(3,4) = 6.5$, $p = 0.05$ (width), and $F(3,4) = 5.8$, $p = 0.06$ (branched). Using an unpaired t-test, the increases in the number of nuclei per myotube and the myotube width of myotubes grown with cartilage compared to C2C12 controls were statistically significant, $p = 0.007$ (nuclei per myotube) and $p = 0.1$ (width). Neural-C2C12 myoblast cultures exhibited a reduction in the number of myotubes, total number of nuclei found within myotubes, average nuclei per myotube, total myotube area, and average length when compared to all other co-culture combinations. Myotubes found within kidney-C2C12 myoblast cultures exhibited a reduction in length, the number of nuclei per myotube and to the total number of nuclei found within myotubes when compared to C2C12 controls and cartilage-C2C12 myoblast cultures.

Table 2. Data for co-cultures wherein C2C12 myoblasts were plated first and allowed two days of growth before the addition of neural, cartilage, or kidney epithelial cells. Averages (± SD) of total myotube area per field (Area), area per myotube (Area/MT), myotube length and width, number of nuclei per myotube (Nu/MT), the percentage of branched myotubes, the total number of myotubes (total MT), and the total number of nuclei found within myotubes (total Nu within MT) are listed.

C2C12 myoblasts plated 1st	C2C12 Control	C2C12 with Neural	C2C12 with Cartilage	C2C12 with Kidney
	Average	Average	Average	Average
Area (%)	10.4 ± 6.2	1.1 ± 1.1	30.9 ± 2.3	4.0 ± 1.3
Area/MT ($\mu m^{2)}$	350.8 ± 124.0	236.0 ± 90.7	973.2 ± 52.4	233.1 ± 16.4
Length (µm)	50.0 ± 2.8	17.9 ± 11.5	48.9 ± 1.8	36.4 ± 3.3
Width (µm)	16.5 ± 1.1	10.5 ± 7.1	19.3 ± 0.9	16.7 ± 0.2
Nu/MT	9.7 ± 0.6	3.7 ± 0.5	12.0 ± 0.6	5.0 ± 0.7
Branched (%)	0.4 ± 0.5	0.0 ± 0.0	2.1 ± 0.8	0.5 ± 0.7
Total MT	171.0 ± 46.7	31.5 ± 7.8	192.5 ± 3.5	104.0 ± 25.5
Total Nu within MT	1657.5 ± 556.5	117.0 ± 43.8	2307.5 ± 57.3	529.0 ± 190.9

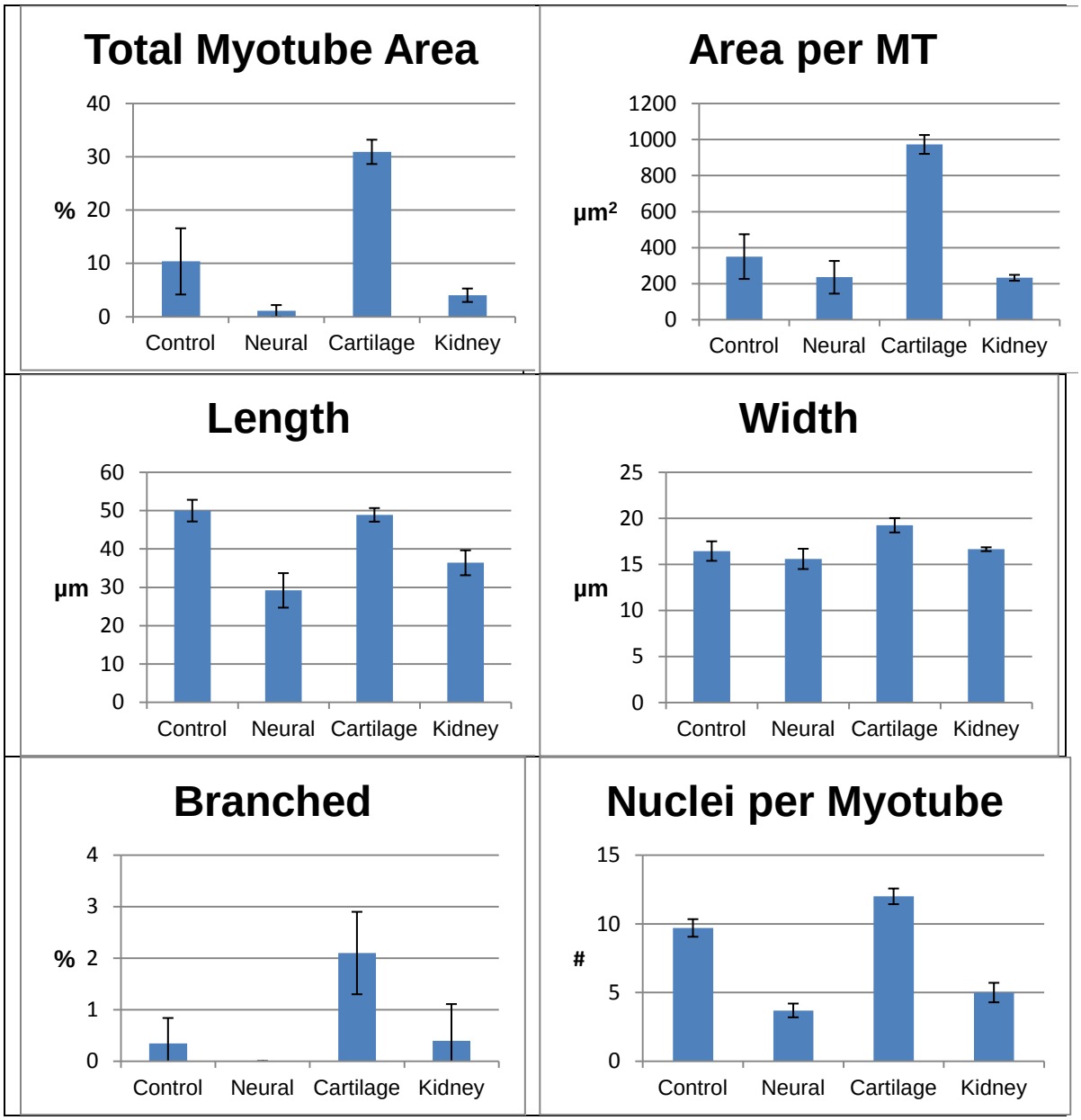

Figure 23. Graphic representation of the C2C12 first co-culture condition analysis.

Mixed C2C12 Co-culture with either Neural, Cartilage or Kidney Cell Types

In my second co-culture strategy, C2C12 myoblasts were first mixed together with either neural, cartilage, or kidney cells and then plated on NaOH-etched glass coverslips (n = 16). This represented the mixed co-culture condition. Mixed cultures produced similar results to growth conditions in which C2C12

myoblasts were plated first. Between the three cell types used in co-culture, the cartilage co-culture produced the largest myotubes. However, while the second most successful myotube development conditions were found in the C2C12 controls (as was the case in the growth conditions where C2C12 myoblasts were plated first), pre-mixed C2C12 myoblasts and neural cell co-cultures produced far more developed myotubes when compared to the C2C12 myoblasts plated first conditions. Pre-mixed conditions with neural cells or kidney epithelial cells with C2C12s produced larger and more numerous myotubes than those found within the C2C12 plated first conditions with each cell type, but were still smaller and less numerous than the control C2C12 cultures (Figure 24).

Analysis of mixed co-culture conditions revealed that the total area covered by myotubes was similar between mixed C2C12 and cartilage conditions (21.2 ± 2.3 %) and C2C12 controls (23.72 ± 2 %), both of which were higher than the mixed neural-C2C12 myoblast (9.33 ± 3.0 %) and kidney-C2C12 myoblast (7.74 ± 0.9 %) cultures (see Table 3). A one-way ANOVA was used to test total area covered by myotubes across the four growth conditions and the total area differed significantly across the culture conditions, $F(3,4) = 27.29$, $p = 0.004$. However, when the average area per myotube was calculated, myotubes grown with cartilage (1074.7 ± 303.8 μm^2) were found to have the highest area per myotube when compared to all other mixed co-culture conditions (Contol = 675.5 ± 55.0 μm^2; Neural = 310.3 ± 52.4 μm^2; Kidney = 379.5 ± 4.4 μm^2) (Figure 25). A one-way ANOVA was used to test the average area per myotube across the four average myotube area observed in cartilage co-cultures was statistically

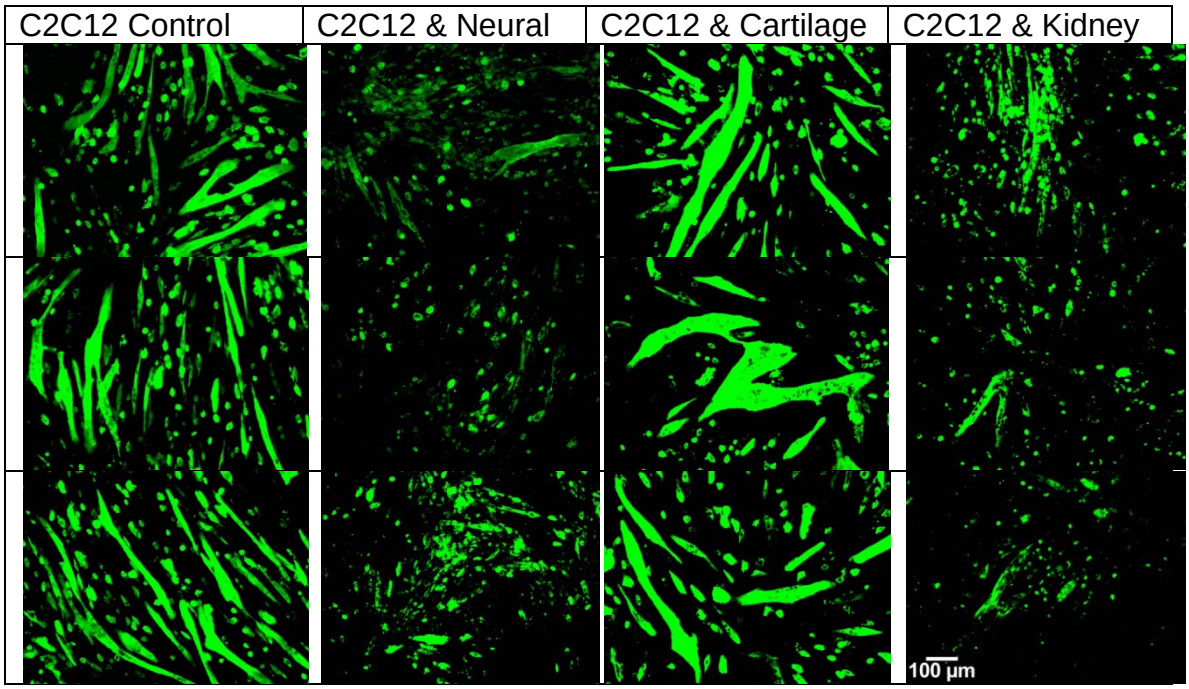

Figure 24. C2C12 myoblasts mixed and plated simultaneously with neural, cartilage, and kidney epithelial cells. Cultures were grown for 11 days total on glass coverslips before myotubes were immunolabelled with F59. Three examples from each growth condition were shown from top to bottom. Neural and kidney co-cultures showed a dramatic reduction in myotube formation, whereas cartilage co-cultures showed an increased myotube width and area when compared to C2C12 controls. 40x.

significant when compared to the next highest average myotube area found in controls, $p = 0.1$. In addition to this, myotubes grown with cartilage also exhibited the highest average number of nuclei per myotube (10.9 ± 0.6 nuclei) when compared to all other mixed co-culture conditions (Contol = 8.2 ± 0.6 nuclei; Neural = 5.7 ± 2.0 nuclei; Kidney = 5.3 ± 0.6 nuclei). A one-way ANOVA was used to test the average number of nuclei per myotube across the four growth conditions and the number of nuclei per myotube differed significantly across the culture conditions, $F(3,4) = 10.78$, $p = 0.02$. Using an unpaired t-test, the increase in average number of nuclei per myotube observed in cartilage co-cultures was statistically significant when compared to the next highest average

myotube area found in controls, p = 0.006. While C2C12 control conditions displayed a similar average length to mixed cartilage-C2C12 myoblast cultures, both values were above those found in mixed neural-C2C12 myoblast and kidney-C2C12 myoblast cultures. Mixed cartilage-C2C12 myoblast cultures also exhibited a larger average myotube width (18 ± 0.3 µm) when compared to all other mixed co-culture conditions (Contol = 15.8 ± 0.8 µm; Neural = 13.8 ± 0.8 µm; Kidney = 15.1 ± 0.6 µm). A one-way ANOVA was used to test the average length and width of myotubes across the four growth conditions and both the length and width differed significantly across the culture conditions, F(3,4) = 18.2, p = 0.009 (length), F(3,4) = 14.62, p = 0.01 (width).

Table 3. Data for pre-mixed co-cultures of C2C12 myoblasts and either neural, cartilage or kindey epithelial cells. Averages (± SD) for total myotube area (Area), area per myotube (Area/MT), myotube length and width, number of nuclei per myotube (Nu/MT), the percentage of branched myotubes, the total number of myotubes (Total MT), and the total number of nuclei found within all myotubes (total Nu within MT) are shown.

Mixed and simultaneously plated	C2C12 Control	C2C12 with Neural	C2C12 with Cartilage	C2C12 with Kidney
	Average	Average	Average	Average
Area (%)	23.7 ± 2.0	9.3 ± 3.0	21.2 ± 2.3	7.7 ± 0.9
Area/MT ($\mu m^{2)}$	675.5 ± 55.0	310.3 ± 52.4	1074.7 ± 303.8	379.5 ± 4.4
Length (µm)	49.4 ± 3.3	35.6 ± 0.7	52.7 ± 5.2	32.8 ± 2.1
Width (µm)	15.8 ± 0.8	13.8 ± 0.8	18.0 ± 0.3	15.1 ± 0.6
Nu/MT	8.2 ± 0.6	5.7 ± 2.0	10.9 ± 0.6	5.3 ± 0.6
Branched (%)	1.4 ± 1.3	0.3 ± 0.4	1.4 ± 1.1	0.8 ± 0.1
Total MT	212.5 ± 0.7	179.5 ± 29	126.5 ± 48.8	123.5 ± 16.3
Total Nu within MT	1760.0 ± 173.9	995.5 ± 181.7	1366.5 ± 467.4	660.0 ± 151.3

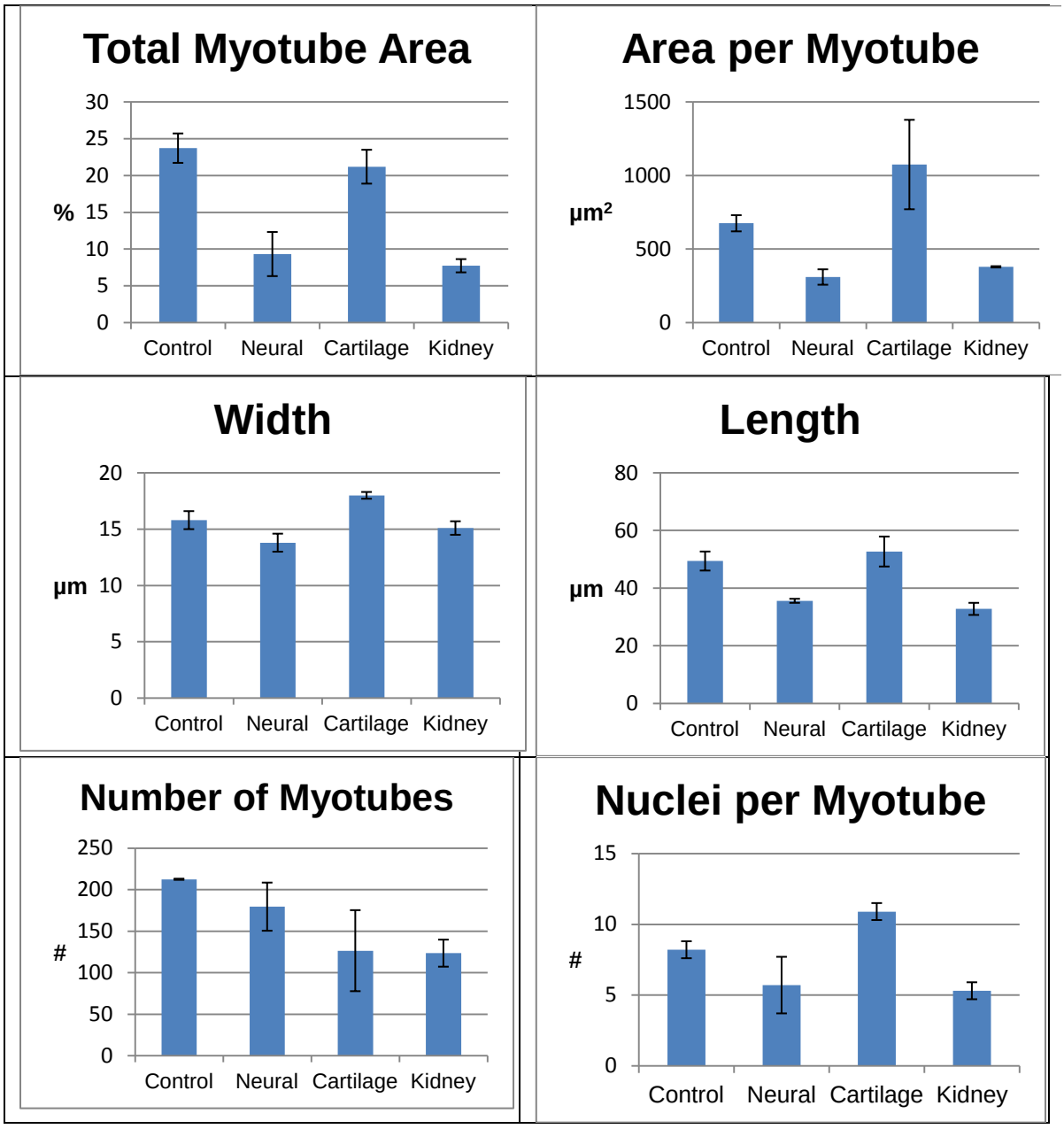

Figure 25. Graphic representation of data obtained from the pre-mixed co-culture conditions.

C2C12 Myoblasts on Established Neural, Cartilage or Kidney Cultures

My third co-culture strategy consisted of myoblasts plated on pre-established (10 day old) neural, cartilage or kidney cultures (n = 10), and followed similar trends as its two counterparts (i.e. C2C12 first and mixed co-

culture experiments). C2C12 plated on pre-established cartilage cultures produced the most robust myotubes (Figure 26). Plating myoblasts on pre-established neural or kidney cultures produced increased myotube development compared to C2C12 first and mixed co-culture strategies. Myotubes grown on pre-established cartilage cultures exhibited the largest average area per myotube (1973.9 ± 390.2 $\mu m^{2)}$ as well as the highest percent of branched myotubes (12.3 ± 0.3 %) when compared to all other growth conditions (Control: 620.2 ± 51.4 μm^2, branched = 2.1 ± 1.2 %; Neural: area = 624.9 ± 47.8 μm^2, branched = 0.9 ± 1.3 %; Kidney: area = 300.5 ± 80.9 μm^2, branched = 0.5 ± 0.8 %) (see Table 4). A one-way ANOVA was used to test the average area per myotube and the percentage of branched myotubes across the four growth conditions and the area per myotube and percentage of branched myotubes differed significantly across the culture conditions, $F(3,4) = 27.07$, $p = 0.004$ (area per myotube), $F(3,4) = 63.37$, $p = 0.0008$ (branched). Using an unpaired t-test, the increase in average area per myotube and percentage of branched myotubes observed in cartilage co-cultures when compared to the next highest values for each found in controls was statistically significant, $p = 0.07$ (area per myotube), $p = 0.02$ (branched). All cell-type combinations produced myotubes of approximately the same average width, while cartilage-C2C12 myoblast and neural-C2C12 myoblast cultures produced myotubes with a greater average length (Cartilage = 90.1 ± 18 μm; Neural = 76.9 ± 9.3 μm) compared to C2C12 control (57.3 ± 3.9 μm) and kidney-C2C12 myoblast (43.4 ± 8.0 μm) culture conditions (Figure 27). A one-way ANOVA was used to test the average length and width of myotubes

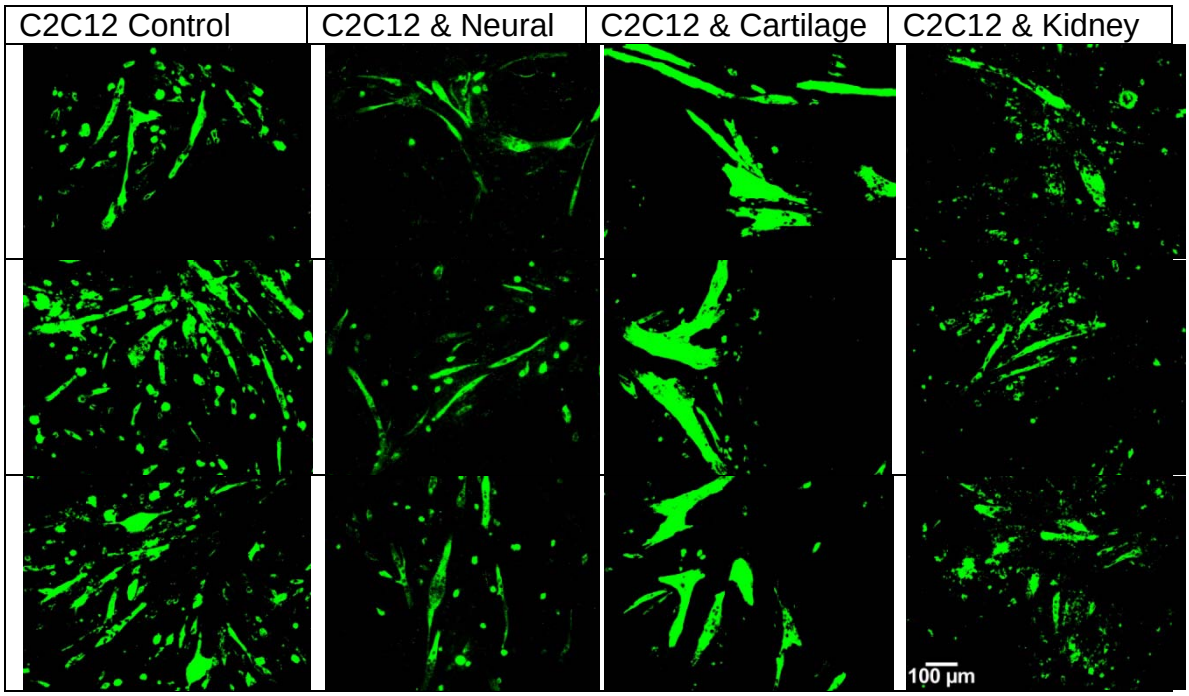

Figure 26. Eleven day old myotubes grown on pre-established (10 day) neural, cartilage or kidney epithelial cultures. Myotubes were immunolabelled with F59 and three examples from each growth condition are shown from top to bottom. Neural co-cultures and kidney co-cultures myotube formation was similar to that found in the C2C12 controls, whereas cartilage co-cultures showed increased myotube width and area when compared to C2C12 controls. 40x.

across the four growth conditions and while the length differed significantly, $F(3,4) = 855,76$, $p = 0.05$, the difference in width was not significant, $F(3,4) = 1.23$, $p = 0.4$. The DAPI nuclear stain was unsuccessful for the C2C12 and cartilage co-cultures, but comparisons between the remaining cell-type combinations revealed that myotubes in neural-C2C12 myoblast cultures had a higher average number of nuclei per myotube (12.5 ± 4.7 nuclei) than kidney-C2C12 myoblast (5.4 ± 1.6 nuclei) cultures and approximately the same as C2C12 controls (6.8 ± 2.7 nuclei). A one-way ANOVA was used to test the average number of nuclei per myotube across the four growth conditions and the

number of nuclei per myotube did not differ significantly across the culture conditions, $F(3,4) = 2.61$, $p = 0.2$.

Table 4. Data for co-cultures of C2C12 myoblasts plated on pre-established (10 day) neural, cartilage or kidney epithelial cell cultures. Averages (± SD) for total myotube area (Area), area per myotube (Area/MT), myotube length and width, number of nuclei per myotube (Nu/MT), the percentage of branched myotubes, the total number of myotubes (total MT), and the number of nuclei found within all myotubes (total Nu within MT) are shown.

Neural, Cart and Kidney plated 1st	C2C12 Control	C2C12 with Neural	C2C12 with Cartilage	C2C12 with Kidney
	Average	Average	Average	Average
Area (%)	9.2 ± 5.0	6.2 ± 1.4	10.5 ± 1.9	5.8 ± 0.8
Area/MT ($\mu m^{2)}$	620.2 ± 51.4	624.9 ± 47.8	1973.9 ± 390.2	300.5 ± 80.9
Length (µm)	57.3 ± 3.9	76.9 ± 9.3	90.1 ± 18	43.4 ± 8.0
Width (µm)	19.0 ± 1.7	19.4 ± 2.4	18.7 ± 2.1	16.3 ± 0.5
Nu/MT	6.8 ± 2.7	12.5 ± 4.7	NA	5.4 ± 1.6
Branched (%)	2.1 ± 1.2	0.9 ± 1.3	12.3 ± 0.3	0.5 ± 0.8
Total MT	93.0 ± 56.6	60.0 ± 8.5	32.5 ± 0.7	125 ± 49.5
Total Nu within MT	710.5 ± 635.7	773.0 ± 401.6	NA	637.5 ± 77.1

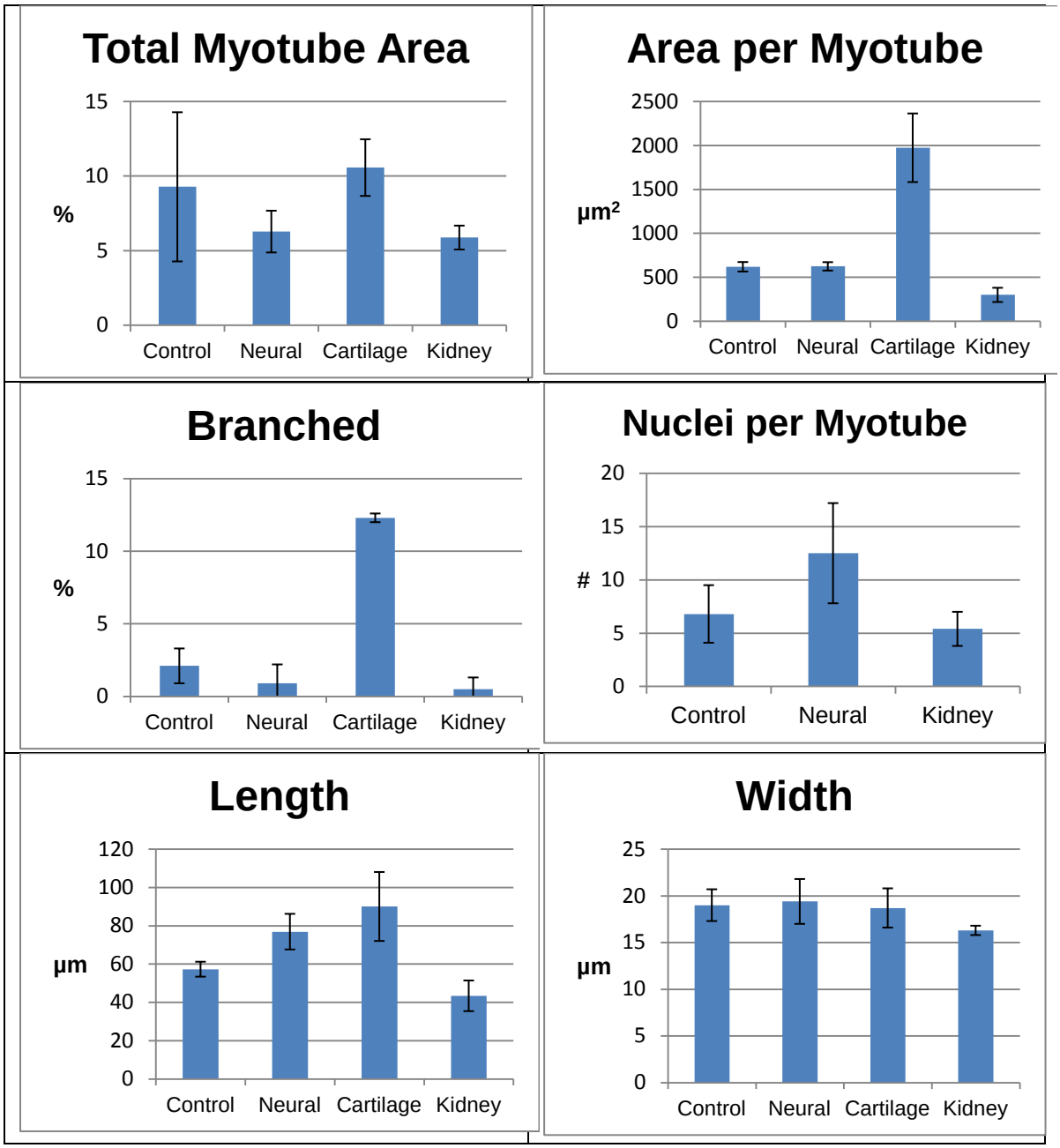

Figure 27. Graphic representation of co-culture conditions with myoblasts added to pre-established (10 day) neural, cartilage or kidney epithelial cell cultures.

Summary of Co-culture Plating Strategies

In co-cultures where C2C12 myoblasts were plated first and allowed two days of growth prior to the addition of a second cell type, C2C12 and cartilage

cells consistently produced the largest myotubes. This was followed by C2C12 control cultures, while neural-C2C12 myoblast and kidney-C2C12 myoblast cultures displayed a similar low density count of myotubes.

Mixed simultaneous plating co-cultures produced the same order and cartilage-C2C12 myoblast cultures produced the largest myotubes, followed by C2C12 controls, followed by neural-C2C12 myoblast and kidney-C2C12 myoblast cultures.

When comparing muscle growth in the last co-culture plating strategy (i.e. C2C12 myoblasts grown on established neural, cartilage or kidney epithelial cultures), the C2C12 myoblasts grown with cartilage cells consistently produced the largest myotubes, followed by similar development observed in C2C12 control cultures and neural-C2C12 myoblast cultures, which were, in turn, followed by kidney-C2C12 myoblast cultures (see Table 5).

Table 5. Ranking of co-culture cell type combinations (C2C12 control, neural-C2C12, cartilage-C2C12, and kidney-C2C12) within the three plating strategies based on total myotube area per field, average area per myotube and the average number of nuclei per myotube.

	C2C12 Plated First	Mixed Simultaneous Plating	Neural, Cartilage and Kidney plated First
C2C12 Control	2	2	2
C2C12 and Neural	4	4	2
C2C12 and Cartilage	1	1	1
C2C12 and Kidney Epithelial	3	3	3

When comparing plating strategies of neural-C2C12 myoblast cultures, the most effective plating strategy that produced the largest and most developed myotubes for that cell type combination was C2C12 myoblasts plated on established 10 day old neural cell cultures. The second most effective co-culture plating strategy for C2C12 and neural co-cultures was mixed simultaneous plating, followed by plating C2C12 myoblasts first and allowing two days of growth before the addition of neurons.

When comparing C2C12 and cartilage cell co-cultures, the most effective co-culture plating strategy that produced the largest and most developed myotubes overall, was to plate C2C12 myoblasts on an established, 10 day old cartilage culture. The second most consistent plating strategy for C2C12 and cartilage was to plate C2C12 myoblasts for two days before the addition of cartilage cells, followed by mixing and plating C2C12 myoblasts and cartilage cells simultaneously.

Kidney-C2C12 myoblast cultures revealed that the most successful co-cultures were of pre-mixed simultaneous plating or addition of C2C12 myoblasts on established, 10 day old kidney epithelial cells. The least consistent co-culture plating strategy for C2C12 and kidney was plating C2C12 myoblasts first and allowing two days of growth prior to the addition of kidney epithelial cells (see Table 6).

Table 6. Ranking of co-culture plating strategies (C2C12 plated first; mixed simultaneous plating; neural, cartilage and kidney cell types plated first for 10 days) across the co-culture cell type combinations based on total myotube area per field, average area per myotube and the average number of nuclei per myotube.

	C2C12 and Neural	C2C12 and Cartilage	C2C12 and Kidney Epithelial
C2C12 Plated First	3	2	3
Mixed Simultaneous Plating	2	3	1
Neural, Cartilage and Kidney Plated First	1	1	2

Effects of Retinoic Acid on Myotube Development in Co-culture Conditions

A range of all-trans retinoic acid (RA) concentrations (10 ng/mL to 0.1 mg/mL) were tested in an attempt to determine a concentration most complimentary to muscle growth and development. RA concentrations of 10 µg/mL (33 µM) and higher were detrimental to myotube growth, with no myotube formation found within these concentrations (data not shown). Once the upper limits of RA concentrations had been determined, experiments using a range of lower RA concentrations were tested in the mixed co-culture conditions (Figure 28). Myotubes formed in the C2C12 controls exhibited a reduction in size with 10 ng/mL and 0.1 µg/mL all-trans RA when compared to those grown in standard growth media controls. Myotubes in mixed neural-C2C12 myoblast cultures did not exhibit any obvious change when grown in the presence of these lower concentrations of RA compared to standard growth media. In contrast, myotubes in mixed cartilage-C2C12 myoblast cultures displayed greatly increased myotube

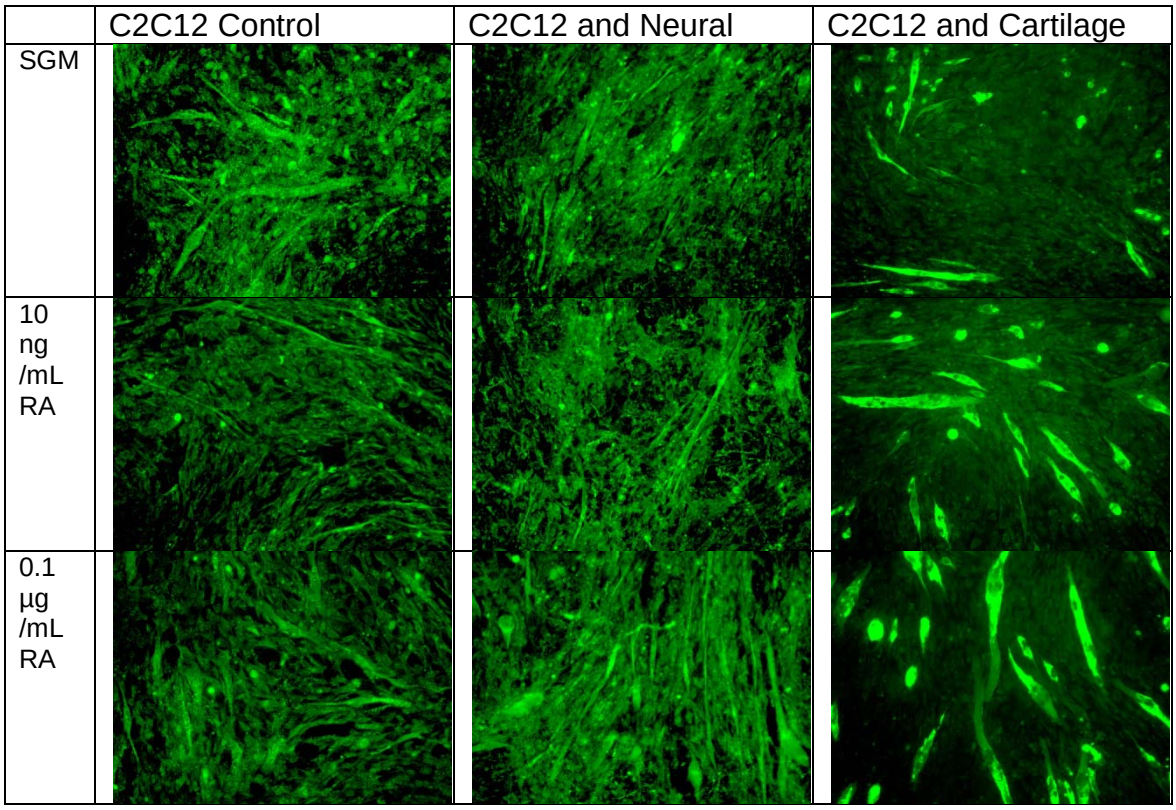

Figure 28. Effects of a range of all-trans retinoic acid (RA) on mixed neural-C2C12 myoblast and cartilage-C2C12 myoblast cultures. Cultures were grown for 11 days on glass coverslips in standard growth media (SGM), 10 ng/mL RA, and 0.1 µg/mL RA. Myotubes were labelled with F59. Cartilage co-cultures exhibited increased myotube development when grown in RA. 40x.

development in the presence of retinoic acid compared to standard growth media controls.

Adding 1 µg/mL (3.3 µM) all-trans RA to C2C12 first co-culture conditions caused an increase in myotube size and branching when compared to the standard growth media controls for each condition (Figure 29). C2C12 controls exhibited a noticeable increase in the number of large myotubes and the overall size of these myotubes. Myotubes in the neural co-cultures displayed the largest increase in size and number when compared to the standard growth media control, however, the total number of myotubes was lower compared to controls

and cartilage co-cultures. Cartilage-C2C12 myoblast cultures exhibited a large increase in branched myotubes and a reduction in the number of smaller myotubes. Finally, although the effects on C2C12 and kidney were not as pronounced as those in the other C2C12 first co-culture conditions, an increase in the number and size of myotubes was also observed.

(Figure 29 is continued on the next page)

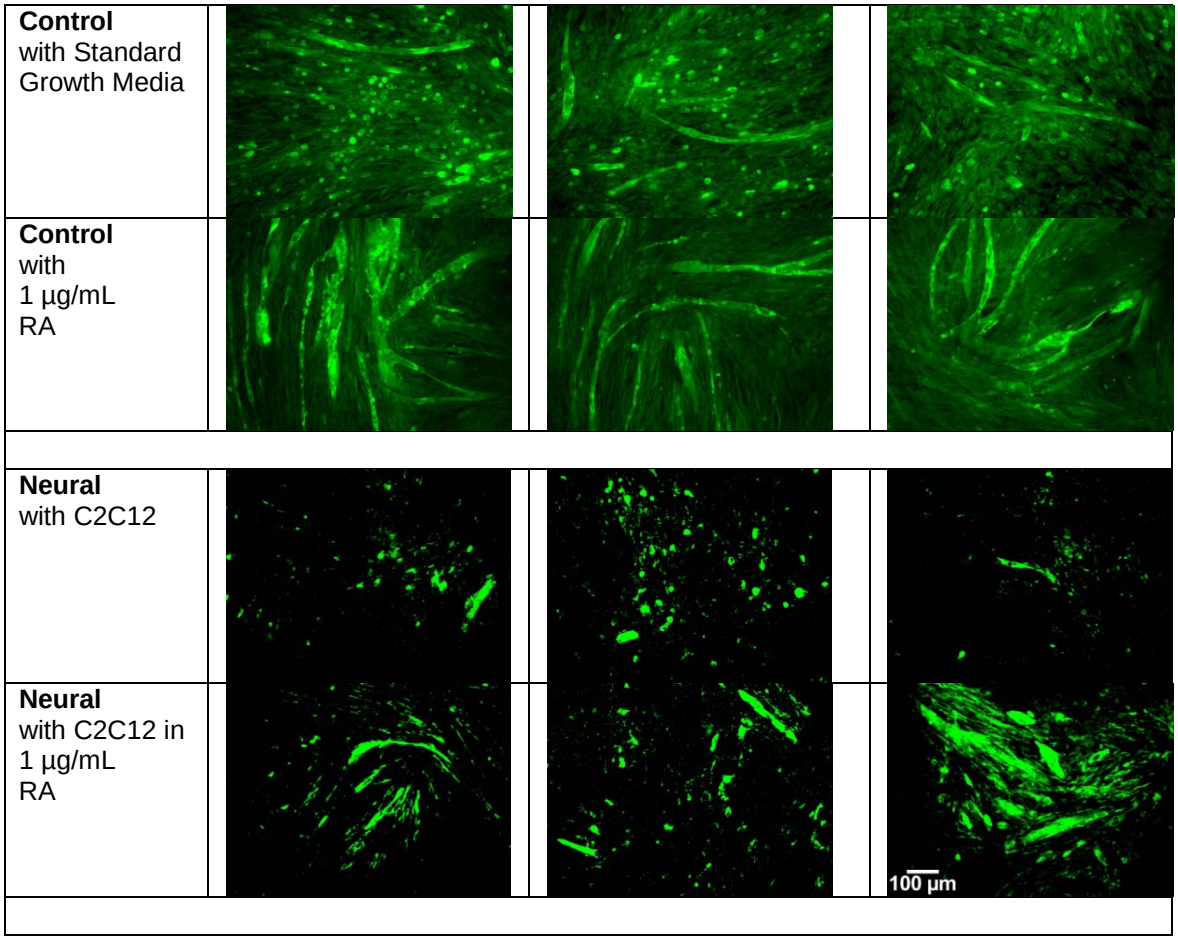

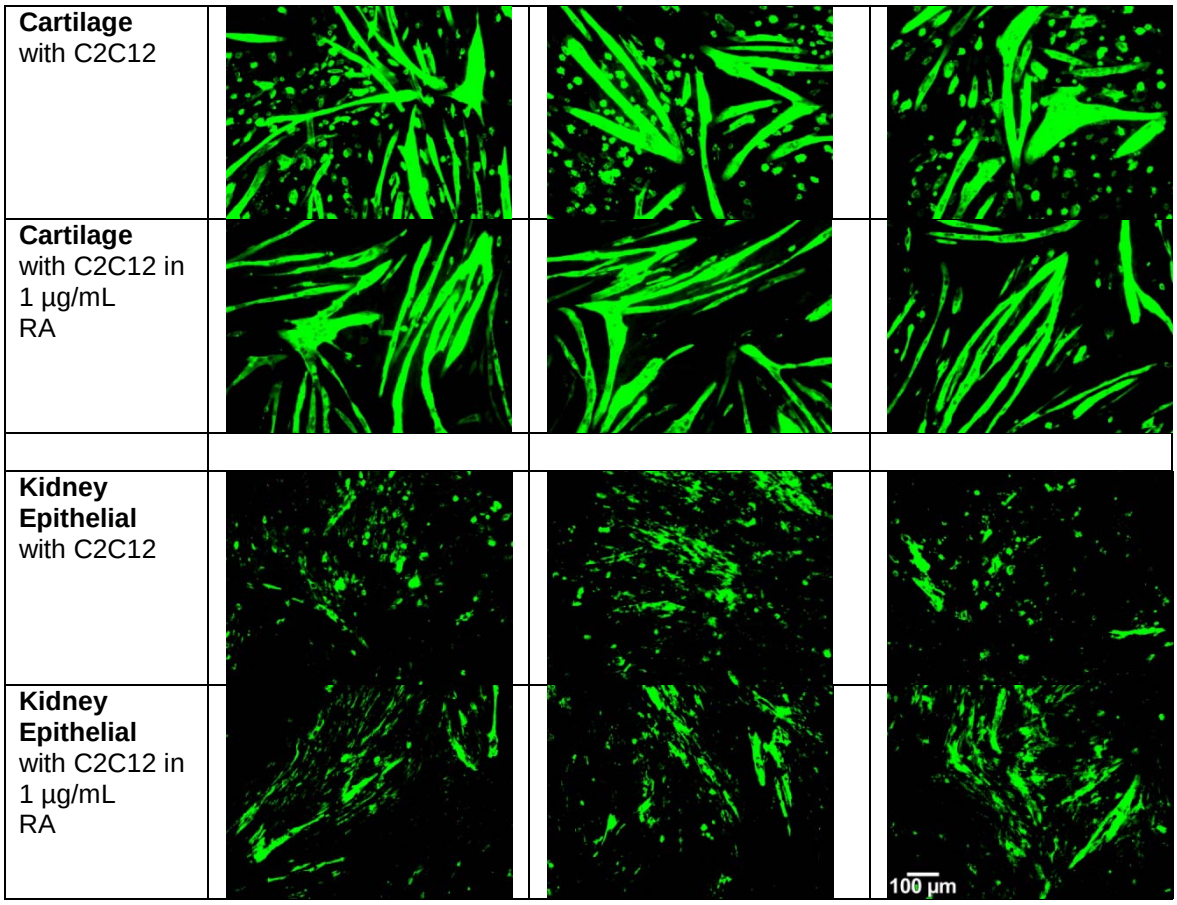

Figure 29. The effects of 1 µg/mL all-trans retinoic acid (RA) on muscle growth compared to standard growth media. Myotubes were grown for 11 days; neural, cartilage, and kidney epithelial cells were added after C2C12 myoblasts had been plated for two days. Myotubes were immunolabelled with F59. Three examples from each growth condition were presented from left to right. An increase in number and size of myotubes was observed in all co-culture conditions when grown in RA compared to standard growth media. A reduction in smaller myotubes was noted in the RA treated control and cartilage co-cultures. 40x.

Analysis of the co-cultures of C2C12 myoblasts grown for two days prior to the addition of a second cell type (neural, cartilage or kidney epithelial) in the presence of 1 µg/mL all-trans RA (RA) revealed co-cultures with cartilage grown in standard growth media (30.94 ± 2.3 %) and in RA (24.64 ± 2.6 %) had the largest total myotube areas compared to all other growth conditions. A two-way ANOVA was used to test the total myotube area across the four growth conditions in standard growth media and in RA and the total area did not differ

significantly across media conditions (p = 0.3), but differed significantly between cell types (p = 0.00002) and when cell type and media condition were considered (p = 0.08). Using an unpaired t-test revealed a statistically significant increase when total myotube area grown with cartilage was compared to the next highest area found in the controls (p = 0.04) (see Table 7). In addition to this, cartilage co-cultures grown in the presence of RA exhibited a drastic increase in the average area per myotube (277.4 ± 598.7 μm^2) when compared to all other co-culture conditions, a value that was 214% of the next highest average area per myotube which was found in the C2C12 control grown in RA (1292.8 ± 498.8 μm^2), a statistically significant increase (p = 0.05). A two-way ANOVA was used to test the average myotube area across the four growth conditions in standard growth media and in RA and the average area did not differ significantly across media conditions (p = 0.2), differed significantly between cell types (p = 0.00009) and did not differ significantly when cell type and media condition were considered (p = 0.6). Cartilage co-cultures grown in RA also exhibited the highest percent of branched myotubes (11.0 ± 3.5 %) when compared to all other growth conditions, a statistically significant increase when compared to the next highest percentage of branched myotubes, found in controls with RA (p = 0.1) (Figure 30). A two-way ANOVA was used to test the percentage of branched myotubes across the four growth conditions in standard growth media and in RA and the branching differed significantly across media conditions (p = 0.002), between cell types (p = 0.001) as well as when cell type and media condition were considered (p = 0.01). A statistically significant increase in both myotube length (p = 0.1)

and the number of nuclei per myotube (p = 0.07) was found in cartilage co-cultures grown in the presence of RA when compared to controls grown in RA (Cartilage co-cultures in RA: 130.9 ± 1.8 µm myotube length, and 35.8 ± 0.1 nuclei per myotube; Controls in RA: 96.5 ± 15.4 µm myotube length, and 18.9 ± 6.0 nuclei per myotube). A two-way ANOVA was used to test the myotube length across the four growth conditions in standard growth media and in RA and the length differed significantly across media conditions (p = 0.000003), between cell types (p = 0.0001) and when cell type and media condition were considered (p = 0.002). A two-way ANOVA was also used to test the number of nuclei per myotube across the four growth conditions in standard growth media and in RA and the nuclear number differed significantly across media conditions (p = 0.00008), and between cell types (p = 0.000009) and when cell type and media condition were considered (p = 0.0005).

Table 7. Data for co-cultures grown in the presence of 1 µg/mL all-trans retinoic acid (RA). C2C12 myoblasts were plated first and allowed two days of growth prior to the addition of neural, cartilage or kidney epithelial cells. Averages (± SD) for total myotube area (Area), area per myotube (Area/MT), myotube length and width, number of nuclei per myotube (Nu/MT), the percentage of branched myotubes, the total number of myotubes (Total MT), and the total number of nuclei found within all myotubes (total Nu within MT) are shown.

C2C12 Plated 1st with 10 µg/mL RA	C2C12 Control	C2C12 with Neural	C2C12 with Cartilage	C2C12 with Kidney
	Average	Average	Average	Average
Area (%)	17.0 ± 3.8	5.1 ± 2.5	25.0 ± 3.5	4.5 ± 1.4
Area/MT ($\mu m^{2)}$	1292.8 ± 498.8	547.9 ± 332.7	2777.4 ± 598.7	352.8 ± 36.4
Length (µm)	96.5 ± 15.4	67.9 ± 3.8	130.9 ± 1.8	51.1 ± 0.4
Width (µm)	16.1 ± 0.6	16.3 ± 2.8	16.7 ± 1.6	16.9 ± 1.3
Nu/MT	18.9 ± 6.0	4.7 ± 1.9	35.8 ± 0.1	7.6 ± 0.5
Branched (%)	2.9 ± 1.2	0.9 ± 1.3	11.0 ± 3.5	1.4 ± 0.6
Total MT	88.0 ± 36.1	59.0 ± 8.5	70.5 ± 17.7	78.0 ± 32.5
Total Nu within MT	1515.3 ± 134	267.0 ± 70.7	1968.5 ± 158.0	352.8 ± 36.4

(Figure 30 continued on next page)

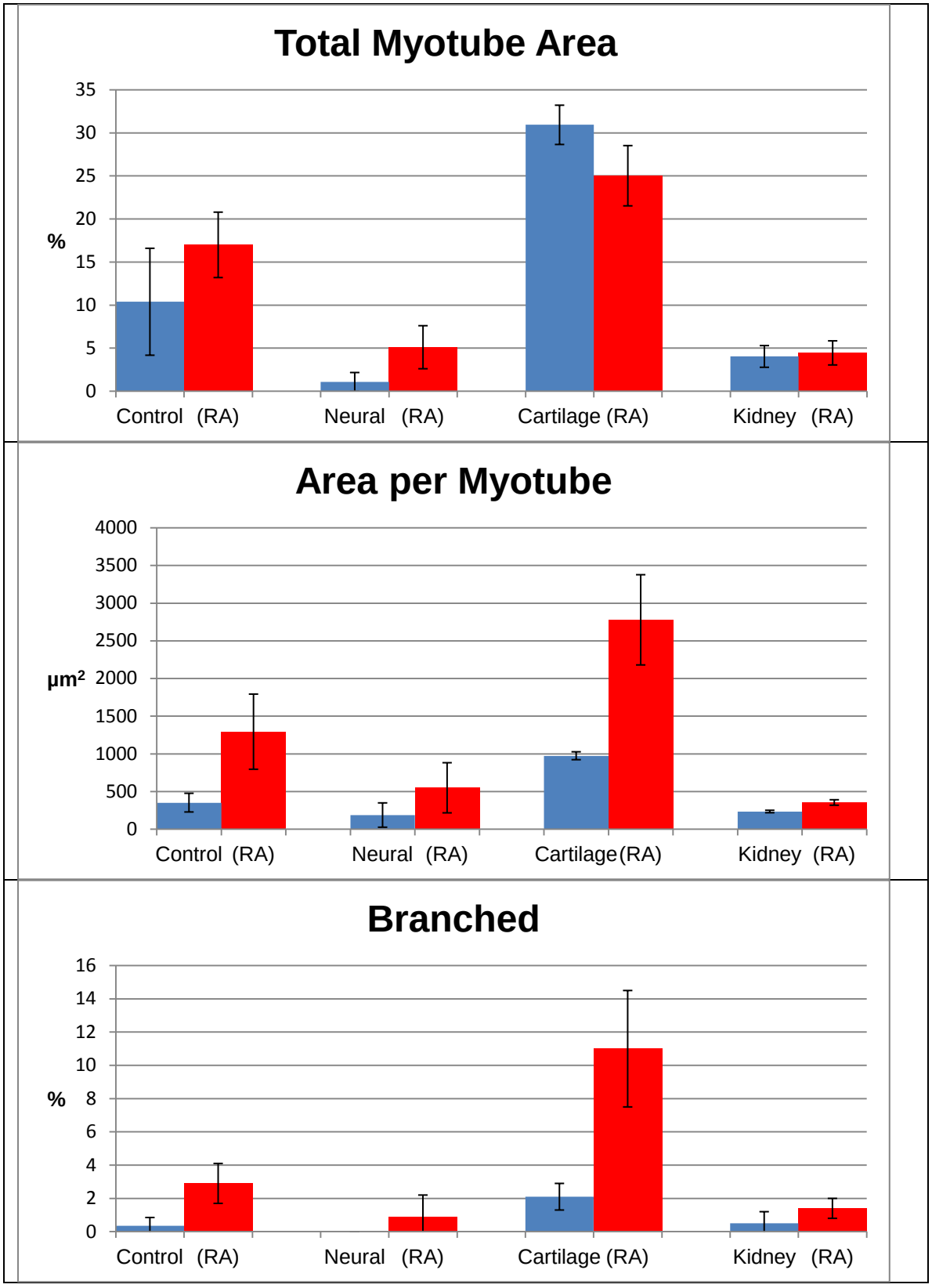

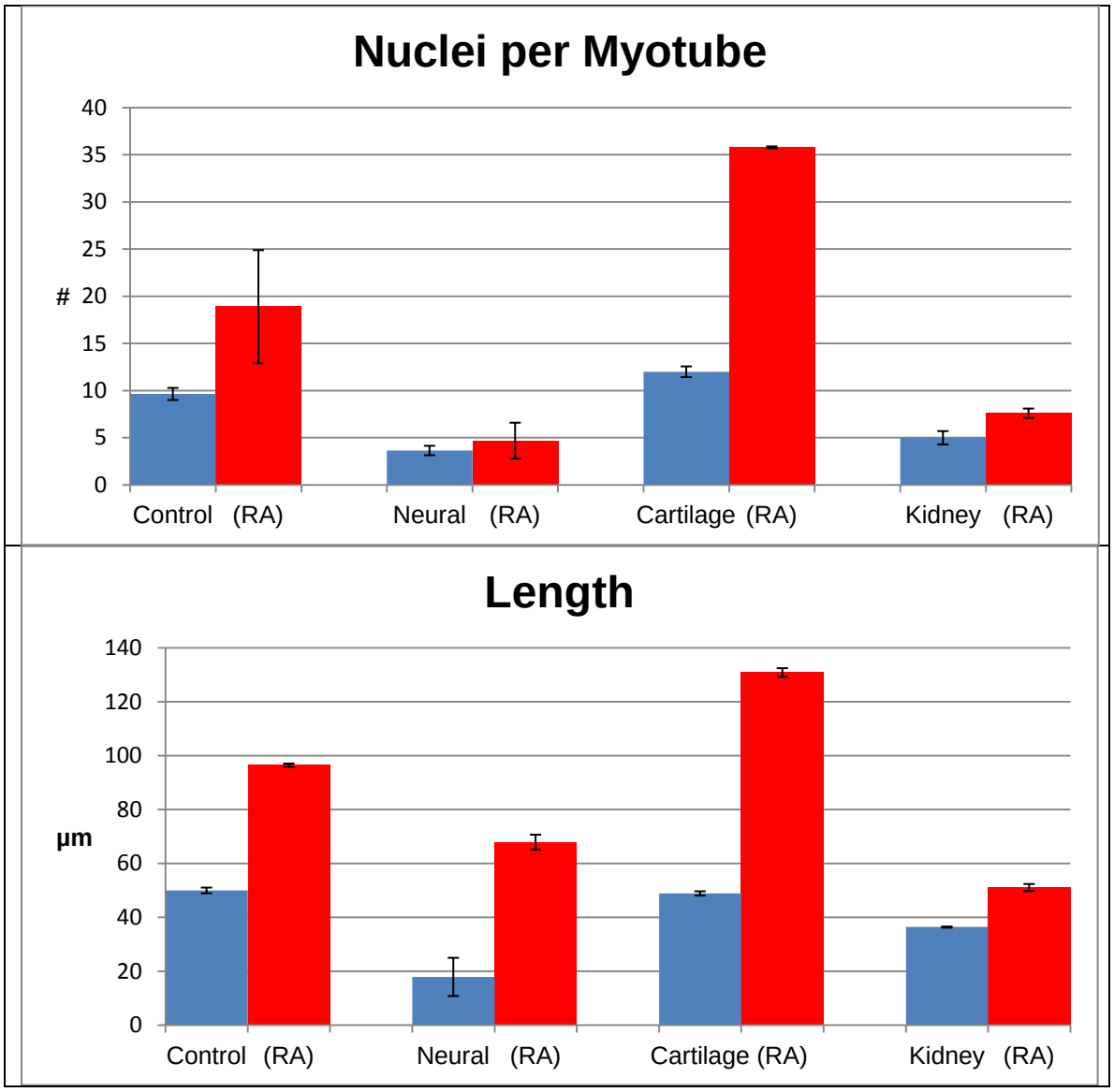

Figure 30. Graphic representation of co-culture conditions with myoblasts grown for two days prior to the addition of a second cell type (neural, cartilage or kidney epithelial) in the presence of 1 µg/mL all-trans retinoic acid (RA). Myoblasts were grown for 11 days total. Blue bars represent growth in standard growth media, red represents RA.

Summary

The most consistent yield of myotubes was found in the C2C12 first co-culture plating strategy. Within this strategy, the highest degree of myotube development was found using C2C12 and cartilage co-cultures. The yield of

large myotubes found in C2C12 and cartilage was further increased when cultured in the presence of all-trans retinoic acid concentrations ranging from 10 ng/mL to 1 µg/mL.

Discussion

Overview

These data indicate that it was possible to improve upon C2C12 myotube bio-engineering by co-culturing with other cell types when compared to controls. The most developed myotubes were consistently found within C2C12 and cartilage co-cultures, followed by C2C12 controls. When C2C12 myoblasts were plated on established, 10 day old neural cultures, they produced myotubes to the same degree of development as the C2C12 control conditions. However, the combination of C2C12 and neural cells exhibited a decrease in myotube size and number when C2C12 myoblasts were plated first for two days or when the two cell types were mixed and plated simultaneously. Combining C2C12 and kidney cells in culture consistently produced fewer myotubes when compared to C2C12 controls. The promoting effects of cartilage on muscle growth, combined with the inhibiting effects of kidney on muscle growth (across all co-culture plating strategies), supports the prediction that developmentally related tissues (i.e. cartilage and neural cells) support and can enhance myotube growth.

What Characterizes Advanced Myotube Development?

Defining the level of myotube development was a crucial first step to interpreting my results since comparisons of muscle bio-engineering co-culture conditions would be impossible without a clear idea of what constitutes myotube development. While it may be assumed that the absolute number of myotubes per experiment would have provided the best measure of myotube development

it does not take into consideration the size of myotubes in culture. For example, if two hypothetical muscle cell cultures were compared, the first of which had 300 myotubes, all containing two nuclei, while the second culture had two large and branched myotubes, which both contained 300 nuclei, the number of myotubes could not be a reliable comparison, as the second dish exhibited a drastically higher degree of myotube development, even though the number of myotubes was lower (Figure 31). Thus, the number of nuclei per myotube provided important data on how many myoblasts were recruited into a myotube.

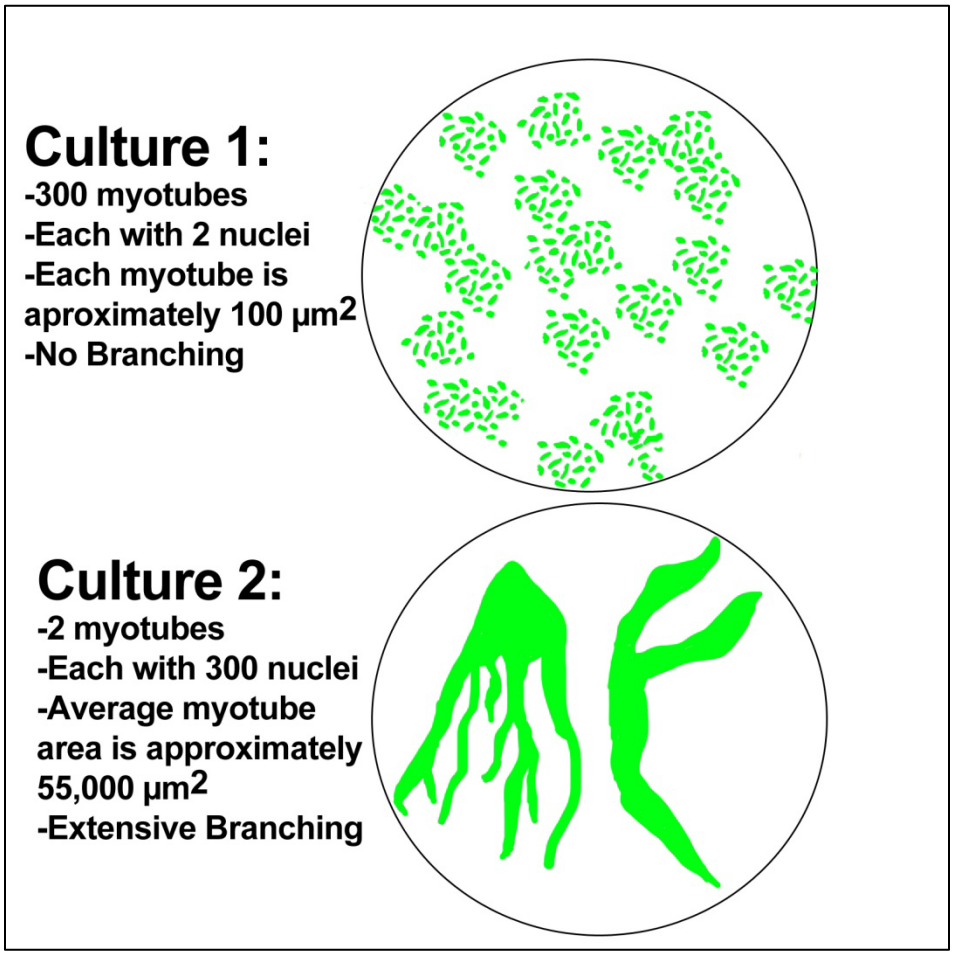

Figure 31. Example of myotube development differences in two hypothetical cultures.

Myotube formation begins with the fusion of two myoblasts, and, as the myotube continues to develop, more myoblasts are incorporated and add their nuclei to the multinucleated syncytium. When compared to the *in vivo* situation, muscle fibers in mature skeletal muscle of mice (35-40 g) have been shown to contain between 200 and 250 nuclei per fiber in the soleus and biceps brachii muscles (Williams and Goldspink, 1971). Thus, a larger number of nuclei within a myotube marked an increased number of fusion events, and approached those numbers in mature skeletal muscle fibers of the body.

A second set of measurements used to ascertain the degree of myotube development was both the overall area of myotubes per field and the average area per myotube. Although coverslips with a high number of small myotubes may have a total myotube area similar to a coverslip with fewer, but larger myotubes, taking the average area per myotube accounted for these differences and provided a better measure of muscle development. Again, this functioned as a reflection of the number of myoblasts that have fused together, as each cell contributes its sarcoplasm and sarcolemma to the myotube upon fusion. Figure 32 shows two graphs, one plotting a crude measurement of myotube area (produced by multiplying the measured myotube width with the length) against the number of nuclei within each myotube, and the other plotting myotube length against the number of nuclei. A regression analysis value of 0.9 for each of these plots denotes a near linear relationship between the number of nuclei within a myotube and the area that the myotube covered and the myotube length. Thus, the average area per myotube corresponded with the number of fusion events,

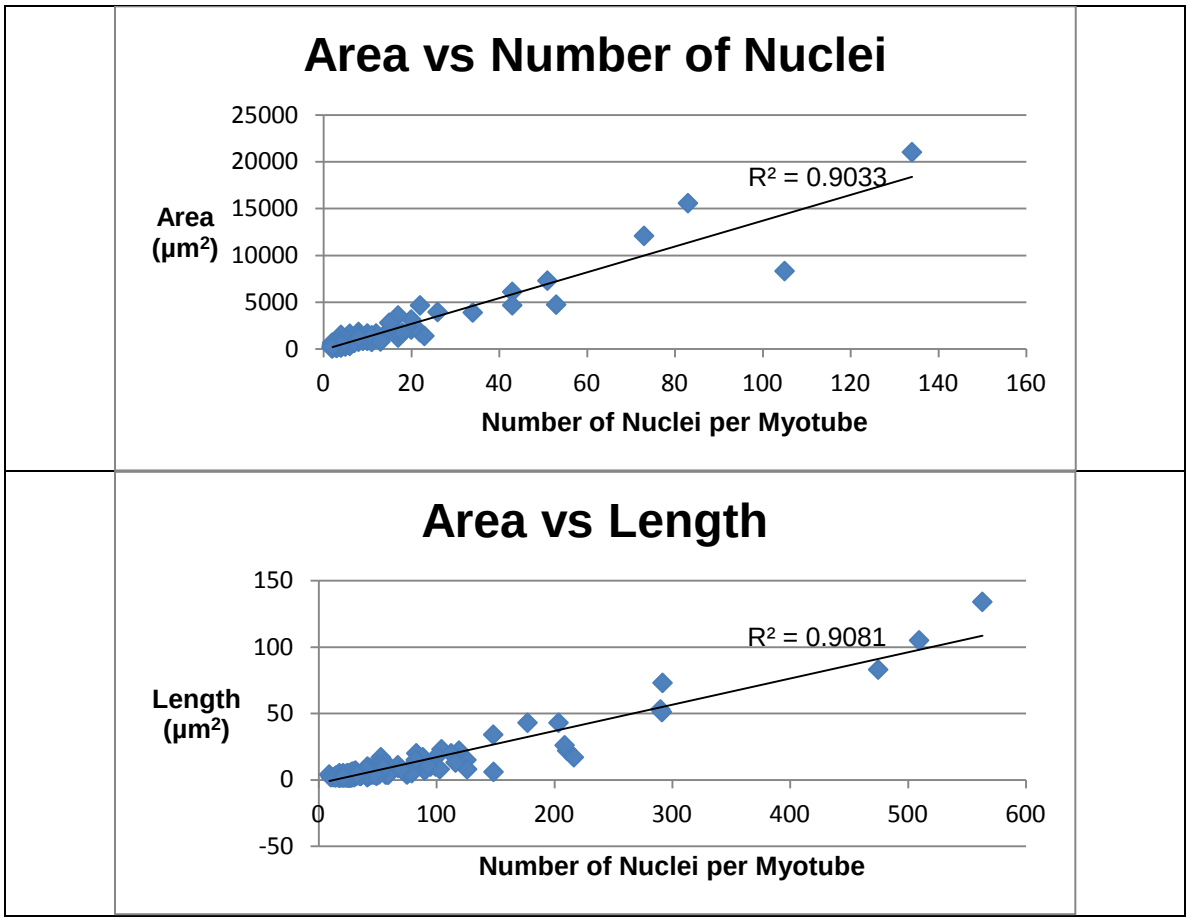

Figure 32. Myotube area and length of plotted against the nuclei count. Myotubes were grown for 11 days.

and could function as a useful cross-reference measurement for myotube development in coverslips.

A third measurement used to assess the degree of muscle development was the number of branched myotubes, which was represented as a percentage of branched myotubes per total number of myotubes. While a branched morphology is not normally seen in mammalian skeletal muscle fibers, it may represent a higher propensity for fusion between myotubes (myotube-to-myotube fusion) in culture. It was not surprising that branched myotubes contained higher nuclear counts as well as larger areas when compared to straight myotubes.

Where possible, a compliment of all three measurements of myotube development (nuclei per myotube, average myotube area in μm^2 and the percent of branched myotubes) were used to compare muscle growth between co-culture conditions.

Co-culture Plating Strategies and the Effects on Muscle Development

Co-culture plating strategies with C2C12 myoblasts plated first for two days before the addition of a second cell type produced the highest degree of myotube development when compared to other co-culture strategies (i.e. mixed or when neural, cartilage, or kidney epithelial cells were plated first and allowed 10 days of growth prior to the addition of myoblasts). The observed increase in myotubes was likely due to availability of substratum space. When C2C12 myoblasts were plated first, there was enough substrate for as many of the plated cells as possible to adhere and begin to proliferate without any competition from other cell types. Allowing the myoblasts two days to divide before the addition of a second cell type permitted the cells to grow, divide and approach confluency. Myoblasts with available substrate nearby will typically continue to divide, whereas those surrounded by other myoblasts will exit the cell cycle in preparation for fusion (Holtzer et al., 1975). However, before fusion, recognition and adhesion must occur in order for the cells to elongate and align into a staggered-parallel arrangement (Bischoff, 1978). Based on my observations, if the myoblasts did not have enough of their own cell type surrounding them, they were unable to align and fuse to form a myotube.

When C2C12 myoblasts and a second cell type were plated at the same time, the myoblasts were interspersed with the co-culture cells. As both cell types divided and increased in number, island clusters of myoblasts were formed. In the mixed culture experiments, it was likely that the second cell type interfered with fusion by reducing the amount of myoblast-to-myoblast contact, and consequently hindered the recognition and adhesion stages required for alignment of myoblasts.

Similarly, when myoblasts were plated on top of a pre-established, 10 day old culture of a second cell type, the substrate available for myoblast adhesion was reduced and, thus, the myoblasts were not able to reach as high of confluency on the substrate. However, Cooper and coworkers showed that when myoblasts were grown on top of an established fibroblast monolayer, they observed an increase in C2C12 myotube development (Cooper et al., 2004). My findings, in combination with those of Cooper and coworkers, suggest that the type of cell grown with muscle plays a significant role in muscle development. If myoblasts formed attachments directly to the pre-established cell layer, rather than competing for the substratum, the effects on myotube development would be significantly different.

C2C12 Myoblasts and Cartilage Cells

Myotube development was significantly increased when C2C12 myoblasts were grown with cartilage cells, across all three co-culture plating strategies, when compared to C2C12 controls, C2C12 and neural, and C2C12 and kidney

epithelial cell co-cultures. A possible mechanism for increased myotube development with cartilage could be that the myoblasts were able to integrate and bind to the secreted extracellular matrix of the cartilage. The proposed linkage between C2C12 myoblasts and the secreted cartilage extracellular matrix likely created a favourable substrate layer for myoblast growth and differentiation, even if chondrocytes were situated below the matrix. Myotubes directly attached to adhered pieces of cartilage supported this prediction.

In addition, the survival of the myotubes attached to pieces of cartilage was greatly increased (up to 74 days). The myotubes exhibited highly organized and aligned sarcomeres when stained with myosin and myomesin, and displayed spontaneous contractions in the elongated myotubes. In contrast, control myotubes would also develop to the point of spontaneous contraction, but they often pulled free and formed myoballs after ~16 days in culture. The ability of myotubes to contract was a notable finding, as Powell and coworkers found mechanically stimulated bio-engineered muscle exhibited increased myofiber diameter and area (Powell et al., 2002). These spontaneous contractions indicated that the myotubes were functionally mature and able to produce force.

Another observation was the increased number of branched myotubes when grown with cartilage. While the overall number of myotubes was often lower, they were consistently larger and showed more branching than myotubes found in C2C12 controls indicating a higher number of fusion events. Secreted proteins by chondrocytes are likely involved in this process and may stimulate

differentiation and fusion pathways either by soluble or physical factors that act on the myoblast membrane.

Myoblasts exhibit a wide array of integral membrane proteins that contribute to substrate adherence and receptor-mediated signaling within the cell. A major integral membrane protein in myoblasts that has been shown to be related to differentiation and fusion is integrin (Schwander et al., 2003). Integrins are heterodimeric proteins that mediate connections of the cytoskeleton to the extracellular matrix (Calderwood et al., 2000) and consist of two subunits, α and β. The heterodimeric nature of integrins enables binding of a variety of extracellular and intracellular ligands that can lead to a wide array of signaling pathways (Tarone et al., 2000; Hynes et al., 2002). For example, it has been shown that myoblasts which lack β1 integrins are unable to form myotubes in culture (Schwander et al., 2003). Further on in development, integrins become concentrated at the myotendinous junction where terminal Z-bands and intermediate desmin filaments anchor to the sarcolemma (Tidball, 1987; Calderwood et al., 2000).

In myoblast and fibroblast cell cultures, integrins are localized to sites of cell adhesion to the substratum (Damsky et al., 1985). The increased adhesion sites provided by the cartilage matrix in my study may have activated integrin-mediated signaling pathways that promoted the formation of myotubes. For example, the connection to the matrix of cartilage may be through myotube integrins binding to laminin molecules, which in turn binds to collagen type IV (Hynes et al., 2002). Collagen type IV can make associations with collagen type

VI which in turn can form associations with collagen type II of the cartilage extracellular matrix (Hynes et al., 2002). A more direct route of myotube adhesion to the cartilage extracellular matrix may be through integrin binding to collagen type VI and then to collagen type II (Hynes et al., 2002). It would be beneficial to study the expression and distribution patterns of integrins in the cartilage-myotube cultures to confirm this prediction.

A variety of secreted molecules has been shown to increase muscle cell growth and development. For example, growth factors and hormones, including insulin-like growth factors (IGF) I and II and growth hormone increase myotube size by promoting myoblast fusion (Florini et al., 1991; Sotiropoulos et al., 2006). IGF-I has also been shown to stimulate chondrocyte extracellular matrix production (Martin et al., 2002). Since IGF-1 is known to be secreted by myoblasts (Yoshiko et al., 2002) and chondrocytes (Bhaumick, 1993) in culture, and IGF-I binding proteins have been identified within cartilage extracellular matrix (Martin et al., 2002), this may create a reservoir of the growth factor and thereby promote myoblast differentiation and myotube growth. It is also possible that this reservoir of growth factors acts to attract other myoblasts to the cartilage extracellular matrix where they fuse with existing myotubes.

The potential mechanisms for the increased myotube size, nuclear count and branching when grown with cartilage could be tested in the following ways. First, the physical presence of the cartilage extracellular matrix may provide support and a three dimensional growth scaffold for muscle could be tested via the removal of the extracellular matrix after cartilage proliferation. By applying a

type II collagenase or matrix metalloproteinase (MMP) the major tensile support of the extracellular matrix would be disrupted and would exclude the potential influences of localized IGF-I reservoirs.

An experiment to test the possibility that chondrocyte-secreted soluble factors are influencing myotube formation would be to grow C2C12 myoblasts in cartilage-conditioned media. This would demonstrate the effects of chondrocyte-secreted signaling molecules on myoblasts and myotubes in the absence of the physical presence of the cells. If a similar increase in myotube formation is observed compared to the cartilage-muscle culture, the physical interaction between the two cell types would be but a minor influence on myotube growth with the secreted agents playing a major role.

The results of my research provide important clues on how cartilage affects muscle development and complements the data presented by Cairns and coworkers who concluded that C2C12 myoblasts were secreting pro-chondrogenic factors (Cairns et al., 2010a). They noted increased alcian blue staining and elevated collagen II and IX expression when chondrocytes were grown in the presence of muscle cell-conditioned medium. In my experiments, C2C12 myoblast differentiation was significantly enhanced by the presence of and/or attachment to the cartilage extracellular matrix. Although cartilage proliferation was not determined in my study, it cannot be ruled out that muscle may have affected chondrocyte growth and production of the matrix in culture.

In addition to the pro-chondrogenic secretion, Cairns and coworkers also found the presence of C2C12 cells, or C2C12 cell-conditioned media, to impart cytokine resistance to cartilage (Cairns et al., 2010b). By exposing chondrocytes to the destructive influence of pro-inflammatory cytokines, Cairns and coworkers found that the physical presence of muscle cells, or the presence of muscle-cell conditioned media, attenuated the expression of cartilage-degrading enzymes. Their results suggested that myoblasts were not only capable of promoting extracellular matrix secretion, but were also capable of providing protection from inflammatory-induced degradation. This form of protection could potentially have occurred in a reciprocal fashion and may explain the increased longevity of myotubes when grown with cartilage.

Effects of All-Trans Retinoic Acid on Muscle Development

A range of all-trans retinoic acid (RA) concentrations from 0.1 µg/mL to 10 µg/mL was found to enhance muscle development, particularly when muscle was grown with cartilage. RA binds to heterodimers of retinoic acid receptors within the nucleus, which act as ligand-inducable transcription factors, and regulate RA-responsive genes (Niederreither and Dolle, 2008). Skeletal muscles are sensitive to RA as they express high levels of RAR and RXR (Mangelsdorf, 1994). RA has been shown to increase expression of the MRFs, MyoD and myogenin, which, in turn, would increase terminal differentiation and number of fusion events (Arnold et al., 1992; Momoi et al., 1992; Albagli-Curiel et al., 1993; Halevy and Lerman, 1993; Froeschle et al., 1998). The presence of RA in the myoblast-cartilage and

control cultures led to larger myotubes and fewer myoblasts and small myotubes, suggesting an increased activation of MyoD and myogenin.

Myotube Development in Co-Culture with Neural or Kidney Epithelial Cells

C2C12 myotube development was significantly reduced in neural and kidney epithelial cultures when compared to C2C12 controls. The observed decrease in myotube formation may be due to the inability of myoblasts to intimately associate with neural or kidney epithelial cells. Although neurons were often found in close proximity to myotubes, it is possible that there were other glial cells from the primary culture which divided rapidly and quickly filled the substrate. The inability of myoblasts to interact with these neural support cells may explain the reduced number of mature myotubes as myoblasts were likely separated into islands. Kidney epithelial cells also appeared to divide rapidly, and, combined with their squamous morphology, occupied the substrate even faster than neural cells. Again, this crowding of myoblasts likely produced separated islands of muscle cells, which were then incapable of the same confluency as those in C2C12 controls.

In addition to limited substrate availability, it may be possible that neurons decreased myotube formation through serum glucose depletion. The cells within the brain (eg. astroglia and neurons) use a disproportionately large amount of glucose *in vitro* (Itoh et al., 2004). Myoblast cell fusion requires a high amount of energy to support cell migration, cytoskeletal rearrangement, sarcolemma coalescence and the fusion event itself (O'Connor et al., 2008), and glucose

restriction has been shown to impair differentiation of skeletal myoblasts (Fulco et al., 2008).

Kidney epithelial cells, as predicted, were not effective in promoting growth of myotubes from C2C12 myoblasts. Kidney epithelial cells *in vivo* are polarized cells with distinct and functionally unique apical and basolateral surfaces, and maintain an asymmetric localization of surface proteins *in vitro* (Louvard, 1980). Kidney epithelial cells are known to form tight connections with gap junctions and desmosomes with neighbouring epithelial cells that helps maintain their functional polarities. Thus, the merging of isolated groups of myoblasts would have been hindered by the tightly bound epithelial cells. This would be different if myoblasts were capable of adhering to the surfaces of the epithelial cells. Myoblasts may have been incapable of adhering directly to the squamous epithelial cells due to the specialized apical surfaces that function in transport and absorption (Louvard, 1980). As these apical surfaces likely lack cell-cell adhesion proteins, they would not be favourable for attachment of myoblasts.

Conclusion

The results of my research indicate that *in vitro* muscle growth can be increased via co-culture with cartilage cells in the presence of low concentrations of retinoic acid (10 ng/mL to 1 µg/mL). When compared to C2C12 controls, myotubes grown with cartilage exhibited increased area, number of nuclei per myotube, branching and lifespan, all of which is predicted to be due to myotubes attaching to the cartilage extracellular matrix. Through this extracellular matrix

attachment, myotubes were able to develop to the point of spontaneous contraction without pulling free of the substratum.

Bibliography

Albagli-Curiel O, Carnac G, Vandromme M, Vincent S, Crepieux P, Bonnieu A. 1993. Serum-induced inhibition of myogenesis is differentially relieved by retinoic acid and triiodothyronine in C2 murine muscle cells. Differentiation 52:201-210.

Arnold HH, Gerharz CD, Gabbert HE, Salminen A. 1992. Retinoic acid induces myogenin synthesis and myogenic differentiation in the rat rhabdomyosarcoma cell line BA-Han-1C. J Cell Biol 118:877-887.

Asakura A, Komaki M, Rudnicki M. 2001. Muscle satellite cells are multipotential stem cells that exhibit myogenic, osteogenic, and adipogenic differentiation. Differentiation 68:245-253.

Atkinson RA, Joseph C, Dal Piaz F, Birolo L, Stier G, Pucci P, Pastore A. 2000. Binding of alpha-actinin to titin: implications for Z-disk assembly. Biochemistry 39:5255-5264.

Bain G, Ray WJ, Yao M, Gottlieb DI. 1996. Retinoic acid promotes neural and represses mesodermal gene expression in mouse embryonic stem cells in culture. Biochem Biophys Res Commun 223:691-694.

Barbero A, Benelli R, Minghelli S, Tosetti F, Dorcaratto A, Ponzetto C, Wernig A, Cullen MJ, Albini A, Noonan DM. 2001. Growth factor supplemented matrigel improves ectopic skeletal muscle formation--a cell therapy approach. J Cell Physiol 186:183-192.

Beier JP, Bitto FF, Lange C, Klumpp D, Arkudas A, Bleiziffer O, Boos A, Horch RE, Kneser U. 2011. Myogenic differentiation of mesenchymal stem cells co-cultured with primary myoblasts. Cell Biol Int.

Berkes CA, Tapscott SJ. 2005. MyoD and the transcriptional control of myogenesis. Semin Cell Dev Biol 16:585-595.

Bhaumick B. 1993. Insulin-like growth factor (IGF) binding proteins and insulin-like growth factor secretion by cultured chondrocyte cells: identification, characterization and ontogeny during cell differentiation. Regul Pept 48:113-122.

Biddulph DM, Dozier MM, Julian NC, Sawyer LM. 1988. Inhibition of chondrogenesis by retinoic acid in limb mesenchymal cells in vitro: effects on PGE2 and cyclic AMP concentrations. Cell Differ Dev 25:65-75.

Bischoff R. 1978. Myoblast fusion. In Membrane Fusion. Cell Surface Reviews 5:128-218.

Blanco-Bose WE, Blau HM. 2001. Laminin-induced change in conformation of preexisting alpha7beta1 integrin signals secondary myofiber formation. Dev Biol 233:148-160.

Blau HM, Chiu CP, Webster C. 1983. Cytoplasmic activation of human nuclear genes in stable heterocaryons. Cell 32:1171-1180.

Block BA, Imagawa T, Campbell KP, Franzini-Armstrong C. 1988. Structural evidence for direct interaction between the molecular components of the transverse tubule/sarcoplasmic reticulum junction in skeletal muscle. J Cell Biol 107:2587-2600.

Blomhoff R, Blomhoff HK. 2006. Overview of retinoid metabolism and function. J Neurobiol 66:606-630.

Boldin S, Jager U, Ruppersberg JP, Pentz S, Rudel R. 1987. Cultivation, morphology, and electrophysiology of contractile rat myoballs. Pflugers Arch 409:462-467.

Braun T, Rudnicki MA, Arnold HH, Jaenisch R. 1992. Targeted inactivation of the muscle regulatory gene Myf-5 results in abnormal rib development and perinatal death. Cell 71:369-382.

Buckingham M. 2006. Myogenic progenitor cells and skeletal myogenesis in vertebrates. Curr Opin Genet Dev 16:525-532.

Buckingham M, Relaix F. 2007. The role of Pax genes in the development of tissues and organs: Pax3 and Pax7 regulate muscle progenitor cell functions. Annu Rev Cell Dev Biol 23:645-673.

Cairns DM, Lee PG, Uchimura T, Seufert CR, Kwon H, Zeng L. 2010a. The role of muscle cells in regulating cartilage matrix production. J Orthop Res 28:529-536.

Cairns DM, Uchimura T, Kwon H, Lee PG, Seufert CR, Matzkin E, Zeng L. 2010b. Muscle cells enhance resistance to pro-inflammatory cytokine-induced cartilage destruction. Biochem Biophys Res Commun 392:22-28.

Calderwood DA, Shattil SJ, Ginsberg MH. 2000. Integrins and actin filaments: reciprocal regulation of cell adhesion and signaling. J Biol Chem 275:22607-22610.

Campbell KP. 1995. Three muscular dystrophies: loss of cytoskeleton-extracellular matrix linkage. Cell 80:675-679.

Canon E, Cosgaya JM, Scsucova S, Aranda A. 2004. Rapid effects of retinoic acid on CREB and ERK phosphorylation in neuronal cells. Mol Biol Cell 15:5583-5592.

Caputo C. 1978. Excitation and contraction processes in muscle. Annu Rev Biophys Bioeng 7:63-83.

Carvalho KA, Oliveira L, Malvezzi M, Simeoni RB, Francisco JC, Olandoski M, Guarita-Souza LC. 2008. Immunophenotypic expression by flow cytometric analysis of cocultured skeletal muscle and bone marrow mesenchymal stem cells for therapy into myocardium. Transplant Proc 40:842-844.

Chambon P. 1996. A decade of molecular biology of retinoic acid receptors. FASEB J 10:940-954.

Choi J, Costa ML, Mermelstein CS, Chagas C, Holtzer S, Holtzer H. 1990. MyoD converts primary dermal fibroblasts, chondroblasts, smooth muscle, and retinal pigmented epithelial cells into striated mononucleated myoblasts and multinucleated myotubes. Proc Natl Acad Sci U S A 87:7988-7992.

Choi JS, Lee SJ, Christ GJ, Atala A, Yoo JJ. 2008. The influence of electrospun aligned poly(epsilon-caprolactone)/collagen nanofiber meshes on the formation of self-aligned skeletal muscle myotubes. Biomaterials 29:2899-2906.

Clark KA, McElhinny AS, Beckerle MC, Gregorio CC. 2002. Striated muscle cytoarchitecture: an intricate web of form and function. Annu Rev Cell Dev Biol 18:637-706.

Conboy IM, Rando TA. 2002. The regulation of Notch signaling controls satellite cell activation and cell fate determination in postnatal myogenesis. Dev Cell 3:397-409.

Cooper ST, Maxwell AL, Kizana E, Ghoddusi M, Hardeman EC, Alexander IE, Allen DG, North KN. 2004. C2C12 co-culture on a fibroblast substratum enables sustained survival of contractile, highly differentiated myotubes with peripheral nuclei and adult fast myosin expression. Cell Motil Cytoskeleton 58:200-211.

Dalkilic I, Schienda J, Thompson TG, Kunkel LM. 2006. Loss of FilaminC (FLNc) results in severe defects in myogenesis and myotube structure. Mol Cell Biol 26:6522-6534.

Damsky CH, Knudsen KA, Bradley D, Buck CA, Horwitz AF. 1985. Distribution of the cell substratum attachment (CSAT) antigen on myogenic and fibroblastic cells in culture. J Cell Biol 100:1528-1539.

Daniels KJ, Sandra A. 1990. Cytoskeletal organization and synthesis in substrate-independent and -dependent myogenesis in chick embryos. Anat Rec 227:254-263.

Das M, Rumsey JW, Bhargava N, Stancescu M, Hickman JJ. 2010. A defined long-term in vitro tissue engineered model of neuromuscular junctions. Biomaterials 31:4880-4888.

Das M, Rumsey JW, Gregory CA, Bhargava N, Kang JF, Molnar P, Riedel L, Guo X, Hickman JJ. 2007. Embryonic motoneuron-skeletal muscle co-culture in a defined system. Neuroscience 146:481-488.

de Meis L, Vianna AL. 1979. Energy interconversion by the Ca2+-dependent ATPase of the sarcoplasmic reticulum. Annu Rev Biochem 48:275-292.

Dutton EK, Uhm CS, Samuelsson SJ, Schaffner AE, Fitzgerald SC, Daniels MP. 1995. Acetylcholine receptor aggregation at nerve-muscle contacts in mammalian cultures: induction by ventral spinal cord neurons is specific to axons. J Neurosci 15:7401-7416.

Dux L, Pikula S, Mullner N, Martonosi A. 1987. Crystallization of Ca2+-ATPase in detergent-solubilized sarcoplasmic reticulum. J Biol Chem 262:6439-6442.

Eagle M, Baudouin SV, Chandler C, Giddings DR, Bullock R, Bushby K. 2002. Survival in Duchenne muscular dystrophy: improvements in life expectancy since 1967 and the impact of home nocturnal ventilation. Neuromuscul Disord 12:926-929.

Ebashi F, Ebashi S. 1962. Removal of calcium and relaxation in actomyosin systems. Nature 194:378-379.

Ebashi S, Lipmann F. 1962. Adenosine Triphosphate-Linked Concentration of Calcium Ions in a Particulate Fraction of Rabbit Muscle. J Cell Biol 14:389-400.

Enomoto M, Pan H, Suzuki F, Takigawa M. 1990. Physiological role of vitamin A in growth cartilage cells: low concentrations of retinoic acid strongly promote the proliferation of rabbit costal growth cartilage cells in culture. J Biochem 107:743-748.

Florini JR, Ewton DZ, Magri KA. 1991. Hormones, growth factors, and myogenic differentiation. Annu Rev Physiol 53:201-216.

Franzini-Armstrong C. 1970. STUDIES OF THE TRIAD : I. Structure of the Junction in Frog Twitch Fibers. J Cell Biol 47:488-499.

Franzini-Armstrong C, Protasi F. 1997. Ryanodine receptors of striated muscles: a complex channel capable of multiple interactions. Physiol Rev 77:699-729.

Froeschle A, Alric S, Kitzmann M, Carnac G, Aurade F, Rochette-Egly C, Bonnieu A. 1998. Retinoic acid receptors and muscle b-HLH proteins: partners in retinoid-induced myogenesis. Oncogene 16:3369-3378.

Fulco M, Cen Y, Zhao P, Hoffman EP, McBurney MW, Sauve AA, Sartorelli V. 2008. Glucose restriction inhibits skeletal myoblast differentiation by activating SIRT1 through AMPK-mediated regulation of Nampt. Dev Cell 14:661-673.

Gentile A, Toietta G, Pazzano V, Tsiopoulos VD, Giglio AF, Crea F, Pompilio G, Capogrossi MC, Di Rocco G. 2011. Human epicardium-derived cells fuse with high efficiency with skeletal myotubes and differentiate toward the skeletal muscle phenotype: a comparison study with stromal and endothelial cells. Mol Biol Cell 22:581-592.

Gros J, Scaal M, Marcelle C. 2004. A two-step mechanism for myotome formation in chick. Dev Cell 6:875-882.

Guo X, Gonzalez M, Stancescu M, Vandenburgh HH, Hickman JJ. 2011. Neuromuscular junction formation between human stem cell-derived motoneurons and human skeletal muscle in a defined system. Biomaterials 32:9602-9611.

Halevy O, Lerman O. 1993. Retinoic acid induces adult muscle cell differentiation mediated by the retinoic acid receptor-alpha. J Cell Physiol 154:566-572.

Henion PD, Weston JA. 1994. Retinoic acid selectively promotes the survival and proliferation of neurogenic precursors in cultured neural crest cell populations. Dev Biol 161:243-250.

Hoffman EP, Brown RH, Jr., Kunkel LM. 1987. Dystrophin: the protein product of the Duchenne muscular dystrophy locus. Cell 51:919-928.

Hollway G, Currie P. 2005. Vertebrate myotome development. Birth Defects Res C Embryo Today 75:172-179.

Holtzer H, Croop J, Dienstman S, Ishikawa H, Somlyo AP. 1975. Effects of cytochaslasin B and colcemide on myogenic cultures. Proc Natl Acad Sci U S A 72:513-517.

Holtzer H, Hijikata T, Lin ZX, Zhang ZQ, Holtzer S, Protasi F, Franzini-Armstrong C, Sweeney HL. 1997. Independent assembly of 1.6 microns long bipolar MHC filaments and I-Z-I bodies. Cell Struct Funct 22:83-93.

Hughes BW, Kusner LL, Kaminski HJ. 2006. Molecular architecture of the neuromuscular junction. Muscle Nerve 33:445-461.

Hume RI, Thomas SA. 1989. A calcium- and voltage-dependent chloride current in developing chick skeletal muscle. J Physiol 417:241-261.

Huxley AF. 2000. Cross-bridge action: present views, prospects, and unknowns. J Biomech 33:1189-1195.

Huxley AF, Niedergerke R. 1954. Structural changes in muscle during contraction; interference microscopy of living muscle fibres. Nature 173:971-973.

Huxley AF, Taylor RE. 1958. Local activation of striated muscle fibres. J Physiol 144:426-441.

Huxley H, Hanson J. 1954. Changes in the cross-striations of muscle during contraction and stretch and their structural interpretation. Nature 173:973-976.

Huxley HE. 1969. The mechanism of muscular contraction. Science 164:1356-1365.

Hynes RO, Lively JC, McCarty JH, Taverna D, Francis SE, Hodivala-Dilke K, Xiao Q. 2002. The diverse roles of integrins and their ligands in angiogenesis. Cold Spring Harb Symp Quant Biol 67:143-153.

Irving M, Piazzesi G, Lucii L, Sun YB, Harford JJ, Dobbie IM, Ferenczi MA, Reconditi M, Lombardi V. 2000. Conformation of the myosin motor during force generation in skeletal muscle. Nat Struct Biol 7:482-485.

Itoh Y, Abe T, Takaoka R, Tanahashi N. 2004. Fluorometric determination of glucose utilization in neurons in vitro and in vivo. J Cereb Blood Flow Metab 24:993-1003.

Jay JC, Barald KF. 1985. Improved culture of individual muscle fibres with and without spinal cord explants in a collagen gel. J Neurosci Methods 15:229-234.

Jiang JX, Choi RC, Siow NL, Lee HH, Wan DC, Tsim KW. 2003. Muscle induces neuronal expression of acetylcholinesterase in neuron-muscle co-culture: transcriptional regulation mediated by cAMP-dependent signaling. J Biol Chem 278:45435-45444.

Kassar-Duchossoy L, Gayraud-Morel B, Gomes D, Rocancourt D, Buckingham M, Shinin V, Tajbakhsh S. 2004. Mrf4 determines skeletal muscle identity in Myf5:Myod double-mutant mice. Nature 431:466-471.

Kennedy KA, Porter T, Mehta V, Ryan SD, Price F, Peshdary V, Karamboulas C, Savage J, Drysdale TA, Li SC, Bennett SA, Skerjanc IS. 2009. Retinoic acid enhances skeletal muscle progenitor formation and bypasses inhibition by bone morphogenetic protein 4 but not dominant negative beta-catenin. BMC Biol 7:67.

Kim HK, Lee YS, Sivaprasad U, Malhotra A, Dutta A. 2006. Muscle-specific microRNA miR-206 promotes muscle differentiation. J Cell Biol 174:677-687.

Kontrogianni-Konstantopoulos A, Ackermann MA, Bowman AL, Yap SV, Bloch RJ. 2009. Muscle giants: molecular scaffolds in sarcomerogenesis. Physiol Rev 89:1217-1267.

Kostrominova TY, Calve S, Arruda EM, Larkin LM. 2009. Ultrastructure of myotendinous junctions in tendon-skeletal muscle constructs engineered in vitro. Histol Histopathol 24:541-550.

Kovalik JP, Slentz D, Stevens RD, Kraus WE, Houmard JA, Nicoll JB, Lea-Currie YR, Everingham K, Kien CL, Buehrer BM, Muoio DM. 2011. Metabolic remodeling of human skeletal myocytes by cocultured adipocytes depends on the lipolytic state of the system. Diabetes 60:1882-1893.

Kreidberg JA, Sariola H, Loring JM, Maeda M, Pelletier J, Housman D, Jaenisch R. 1993. WT-1 is required for early kidney development. Cell 74:679-691.

Kubo T, Randolph MA, Groger A, Winograd JM. 2009. Embryonic stem cell-derived motor neurons form neuromuscular junctions in vitro and enhance motor functional recovery in vivo. Plast Reconstr Surg 123:139S-148S.

Lan MA, Gersbach CA, Michael KE, Keselowsky BG, Garcia AJ. 2005. Myoblast proliferation and differentiation on fibronectin-coated self assembled monolayers presenting different surface chemistries. Biomaterials 26:4523-4531.

Le May M, Mach H, Lacroix N, Hou C, Chen J, Li Q. 2011. Contribution of retinoid x receptor signaling to the specification of skeletal muscle lineage. J Biol Chem 286:26806-26812.

Li L, Zhou J, James G, Heller-Harrison R, Czech MP, Olson EN. 1992. FGF inactivates myogenic helix-loop-helix proteins through phosphorylation of a conserved protein kinase C site in their DNA-binding domains. Cell 71:1181-1194.

Lin Z, Lu MH, Schultheiss T, Choi J, Holtzer S, DiLullo C, Fischman DA, Holtzer H. 1994. Sequential appearance of muscle-specific proteins in myoblasts as a function of time after cell division: evidence for a conserved myoblast differentiation program in skeletal muscle. Cell Motil Cytoskeleton 29:1-19.

Louvard D. 1980. Apical membrane aminopeptidase appears at site of cell-cell contact in cultured kidney epithelial cells. Proc Natl Acad Sci U S A 77:4132-4136.

Lu J, Tan L, Li P, Gao H, Fang B, Ye S, Geng Z, Zheng P, Song H. 2009. All-trans retinoic acid promotes neural lineage entry by pluripotent embryonic stem cells via multiple pathways. BMC Cell Biol 10:57.

Luther PK. 2009. The vertebrate muscle Z-disc: sarcomere anchor for structure and signalling. J Muscle Res Cell Motil 30:171-185.

Mangelsdorf DJ. 1994. Vitamin A receptors. Nutr Rev 52:S32-44.

Mark M, Ghyselinck NB, Chambon P. 2009. Function of retinoic acid receptors during embryonic development. Nucl Recept Signal 7:e002.

Martin JA, Miller BA, Scherb MB, Lembke LA, Buckwalter JA. 2002. Co-localization of insulin-like growth factor binding protein 3 and fibronectin in human articular cartilage. Osteoarthritis Cartilage 10:556-563.

Martinez-Marmol R, David M, Sanches R, Roura-Ferrer M, Villalonga N, Sorianello E, Webb SM, Zorzano A, Guma A, Valenzuela C, Felipe A. 2007. Voltage-dependent Na+ channel phenotype changes in myoblasts. Consequences for cardiac repair. Cardiovasc Res 76:430-441.

Masaki T, Endo M, Ebashi S. 1967. Localization of 6S component of a alpha-actinin at Z-band. J Biochem 62:630-632.

Matsumoto T, Sasaki J, Alsberg E, Egusa H, Yatani H, Sohmura T. 2007. Three-dimensional cell and tissue patterning in a strained fibrin gel system. PLoS One 2:e1211.

Mizuno H. 2010. The potential for treatment of skeletal muscle disorders with adipose-derived stem cells. Curr Stem Cell Res Ther 5:133-136.

Mok GF, Sweetman D. 2011. Many routes to the same destination: lessons from skeletal muscle development. Reproduction 141:301-312.

Molnar P, Wang W, Natarajan A, Rumsey JW, Hickman JJ. 2007. Photolithographic patterning of C2C12 myotubes using vitronectin as growth substrate in serum-free medium. Biotechnol Prog 23:265-268.

Momoi T, Miyagawa-Tomita S, Nakamura S, Kimura I, Momoi M. 1992. Retinoic acid ambivalently regulates the expression of MyoD1 in the myogenic cells in the limb buds of the early developmental stages. Biochem Biophys Res Commun 187:245-253.

Montarras D, Morgan J, Collins C, Relaix F, Zaffran S, Cumano A, Partridge T, Buckingham M. 2005. Direct isolation of satellite cells for skeletal muscle regeneration. Science 309:2064-2067.

Myer A, Olson EN, Klein WH. 2001. MyoD cannot compensate for the absence of myogenin during skeletal muscle differentiation in murine embryonic stem cells. Dev Biol 229:340-350.

Nave R, Furst DO, Weber K. 1990. Interaction of alpha-actinin and nebulin in vitro. Support for the existence of a fourth filament system in skeletal muscle. FEBS Lett 269:163-166.

Niederreither K, Dolle P. 2008. Retinoic acid in development: towards an integrated view. Nat Rev Genet 9:541-553.

O'Connor RS, Steeds CM, Wiseman RW, Pavlath GK. 2008. Phosphocreatine as an energy source for actin cytoskeletal rearrangements during myoblast fusion. J Physiol 586:2841-2853.

Ottenheijm CA, Granzier H. 2010. New insights into the structural roles of nebulin in skeletal muscle. J Biomed Biotechnol 2010:968139.

Oustanina S, Hause G, Braun T. 2004. Pax7 directs postnatal renewal and propagation of myogenic satellite cells but not their specification. EMBO J 23:3430-3439.

Peterson ER. 1978. Coculture of adult skeletal muscle with fetal mouse spinal cord complex. Tissue Culture Association 4:921-924.

Powell CA, Smiley BL, Mills J, Vandenburgh HH. 2002. Mechanical stimulation improves tissue-engineered human skeletal muscle. Am J Physiol Cell Physiol 283:C1557-1565.

Reddy KB, Fox JE, Price MG, Kulkarni S, Gupta S, Das B, Smith DM. 2008. Nuclear localization of Myomesin-1: possible functions. J Muscle Res Cell Motil 29:1-8.

Relaix F, Montarras D, Zaffran S, Gayraud-Morel B, Rocancourt D, Tajbakhsh S, Mansouri A, Cumano A, Buckingham M. 2006. Pax3 and Pax7 have distinct and overlapping functions in adult muscle progenitor cells. J Cell Biol 172:91-102.

Relaix F, Rocancourt D, Mansouri A, Buckingham M. 2005. A Pax3/Pax7-dependent population of skeletal muscle progenitor cells. Nature 435:948-953.

Rios E, Ma JJ, Gonzalez A. 1991. The mechanical hypothesis of excitation-contraction (EC) coupling in skeletal muscle. J Muscle Res Cell Motil 12:127-135.

Rudnicki MA, Braun T, Hinuma S, Jaenisch R. 1992. Inactivation of MyoD in mice leads to up-regulation of the myogenic HLH gene Myf-5 and results in apparently normal muscle development. Cell 71:383-390.

Rudnicki MA, Schnegelsberg PN, Stead RH, Braun T, Arnold HH, Jaenisch R. 1993. MyoD or Myf-5 is required for the formation of skeletal muscle. Cell 75:1351-1359.

Ryan T, Liu J, Chu A, Wang L, Blais A, Skerjanc IS. 2011. Retinoic Acid Enhances Skeletal Myogenesis in Human Embryonic Stem Cells by Expanding the Premyogenic Progenitor Population. Stem Cell Rev.

Sato M, Ito A, Kawabe Y, Nagamori E, Kamihira M. 2011. Enhanced contractile force generation by artificial skeletal muscle tissues using IGF-I gene-engineered myoblast cells. J Biosci Bioeng 112:273-278.

Schiaffino S, Reggiani C. 2011. Fiber types in mammalian skeletal muscles. Physiol Rev 91:1447-1531.

Schwander M, Leu M, Stumm M, Dorchies OM, Ruegg UT, Schittny J, Muller U. 2003. Beta1 integrins regulate myoblast fusion and sarcomere assembly. Dev Cell 4:673-685.

Sekiya I, Tsuji K, Koopman P, Watanabe H, Yamada Y, Shinomiya K, Nifuji A, Noda M. 2000. SOX9 enhances aggrecan gene promoter/enhancer activity and is up-regulated by retinoic acid in a cartilage-derived cell line, TC6. J Biol Chem 275:10738-10744.

Sharples AP, Al-Shanti N, Stewart CE. 2010. C2 and C2C12 murine skeletal myoblast models of atrophic and hypertrophic potential: relevance to disease and ageing? J Cell Physiol 225:240-250.

Skuk D, Tremblay JP. 2011. Intramuscular cell transplantation as a potential treatment of myopathies: clinical and preclinical relevant data. Expert Opin Biol Ther 11:359-374.

Smith DS. 1966. The organization and function of the sarcoplasmic reticulum and T-system of muscle cells. Prog Biophys Mol Biol 16:107-142.

Sotiropoulos A, Ohanna M, Kedzia C, Menon RK, Kopchick JJ, Kelly PA, Pende M. 2006. Growth hormone promotes skeletal muscle cell fusion independent of insulin-like growth factor 1 up-regulation. Proc Natl Acad Sci U S A 103:7315-7320.

Sugiyama Y, Suzuki A, Kishikawa M, Akutsu R, Hirose T, Waye MM, Tsui SK, Yoshida S, Ohno S. 2000. Muscle develops a specific form of small heat shock protein complex composed of MKBP/HSPB2 and HSPB3 during myogenic differentiation. J Biol Chem 275:1095-1104.

Sumariwalla VM, Klein WH. 2001. Similar myogenic functions for myogenin and MRF4 but not MyoD in differentiated murine embryonic stem cells. Genesis 30:239-249.

Tajbakhsh S, Rocancourt D, Cossu G, Buckingham M. 1997. Redefining the genetic hierarchies controlling skeletal myogenesis: Pax-3 and Myf-5 act upstream of MyoD. Cell 89:127-138.

Tarone G, Hirsch E, Brancaccio M, De Acetis M, Barberis L, Balzac F, Retta SF, Botta C, Altruda F, Silengo L. 2000. Integrin function and regulation in development. Int J Dev Biol 44:725-731.

Tidball JG. 1987. Alpha-actinin is absent from the terminal segments of myofibrils and from subsarcolemmal densities in frog skeletal muscle. Exp Cell Res 170:469-482.

Treves S, Vukcevic M, Maj M, Thurnheer R, Mosca B, Zorzato F. 2009. Minor sarcoplasmic reticulum membrane components that modulate excitation-contraction coupling in striated muscles. J Physiol 587:3071-3079.

Wang K. 1982. Purification of titin and nebulin. Methods Enzymol 85 Pt B:264-274.

Wang K, McClure J, Tu A. 1979. Titin: major myofibrillar components of striated muscle. Proc Natl Acad Sci U S A 76:3698-3702.

Weintraub H, Tapscott SJ, Davis RL, Thayer MJ, Adam MA, Lassar AB, Miller AD. 1989. Activation of muscle-specific genes in pigment, nerve, fat, liver, and fibroblast cell lines by forced expression of MyoD. Proc Natl Acad Sci U S A 86:5434-5438.

Williams PE, Goldspink G. 1971. Longitudinal growth of striated muscle fibres. J Cell Sci 9:751-767.

Xiao Y, Grieshammer U, Rosenthal N. 1995. Regulation of a muscle-specific transgene by retinoic acid. J Cell Biol 129:1345-1354.

Yaffe D, Saxel O. 1977. Serial passaging and differentiation of myogenic cells isolated from dystrophic mouse muscle. Nature 270:725-727.

Yoshiko Y, Hirao K, Maeda N. 2002. Differentiation in C(2)C(12) myoblasts depends on the expression of endogenous IGFs and not serum depletion. Am J Physiol Cell Physiol 283:C1278-1286.

Zammit PS, Relaix F, Nagata Y, Ruiz AP, Collins CA, Partridge TA, Beauchamp JR. 2006. Pax7 and myogenic progression in skeletal muscle satellite cells. J Cell Sci 119:1824-1832.

Zebedin E, Mille M, Speiser M, Zarrabi T, Sandtner W, Latzenhofer B, Todt H, Hilber K. 2007. C2C12 skeletal muscle cells adopt cardiac-like sodium current properties in a cardiac cell environment. Am J Physiol Heart Circ Physiol 292:H439-450.

Zebedin E, Sandtner W, Galler S, Szendroedi J, Just H, Todt H, Hilber K. 2004. Fiber type conversion alters inactivation of voltage-dependent sodium currents in murine C2C12 skeletal muscle cells. Am J Physiol Cell Physiol 287:C270-280.